

学位論文（要約）

Iron-Based Aromatic C–H Bond Functionalization with Electrophiles

（鉄と求電子剤を用いた芳香族炭素－水素結合の官能基化）

平成 25 年 12 月博士（理学）申請

東京大学大学院理学系研究科

化学専攻

浅子 壮美

Abstract

With numerous urgent issues such as the energy crisis, resource depletion, and environmental problems to address, modern organic synthesis should aim toward maximizing efficiency and sustainability. To this end, transition metal-catalyzed C–H bond functionalization has recently received much attention as a potential strategy for solving these problems. This thesis describes the development of an efficient iron-based system for aromatic C–H bond activation followed by reaction with electrophiles.

Chapter 1 describes the significance of sustainability concepts for transition metal-catalyzed C–H bond functionalization reactions, with a focus on those under iron catalysis, together with current challenges in this field and the goal of this study.

Chapter 2 describes an initial attempt for iron-mediated C–H bond functionalization with electrophiles using metallacyclic iron intermediate derived from 2-phenylpyridine.

In Chapter 3, iron-catalyzed *ortho*-allylation of arylpyrazoles using allyl phenyl ether as an electrophilic coupling partner is described. In the presence of a catalytic amount of an iron salt, 4,4'-di-*t*-butyl-2-2'-bipyridine, and diphenylzinc reagent as an organometallic base, *ortho*-allylation of arylpyrazoles with allyl phenyl ether took place smoothly at 0 °C.

In Chapter 4, iron-catalyzed *ortho*-allylation of carboxamides with allyl phenyl ether is described. In the presence of a catalytic amount of iron salt, *cis*-1,2-bis(diphenylphosphino)ethylene, and dineopentylzinc reagent as an organometallic base, the reaction of *N*-(quinlin-8-yl)benzamide and congeners with allyl phenyl ether proceeded smoothly under mild conditions. *N*-(quinlin-8-yl) amide bidentate directing group and dineopentylzinc reagent were utilized to stabilize the metallacyclic iron intermediate and suppress the competing reaction between the substrate and the neopentyl reagent.

Chapter 5 describes further attempts for iron-mediated C–H bond functionalization with electrophiles. The metallacyclic iron intermediate derived from *N*-(quinlin-8-yl)benzamide was

reacted with various electrophiles. These results demonstrated that this iron intermediate is an excellent and general tool for C–H bond functionalization with electrophiles.

Finally, Chapter 6 summarizes the present studies and gives a future outlook.

Acknowledgment

I would like to express my deepest gratitude for the guidance from my research mentor, Professor Eiichi Nakamura. All his valuable advice and insightful suggestions greatly elevated the significance of my research.

I am indebted to Dr. Laurean Ilies for his daily support in my research project as well as continuous encouragement. I am also indebted to Dr. Naohiko Yoshikai and Dr. Etienne Derat for their guidance in computational and organometallic chemistry.

I am grateful to Dr. Hayato Tsuji, Dr. Koji Harano, Dr. Hideyuki Tanaka, and Dr. Shunsuke Furukawa for their valuable discussions and kind instructions.

I appreciate all the members in the Laboratory, especially former and present members in room 2503, Dr. Jakob Norinder, Dr. Xiaoming Zeng, Dr. Adam Mieczkowski, Dr. Arimasa Matsumoto, Dr. Yuki Nakamura, Dr. Masaki Sekine, Mr. Takeshi Yamakawa, Mr. Chen Quan, Mr. Rui Shang, Mr. Motoaki Kobayashi, Mr. Shinichi Yamauchi, Mr. Tatsuaki Matsubara, Mr. Eita Konno, Mr. Takumi Yoshida, Mr. Hiroki Sato, Mr. Yuki Itabashi, Ms. Saki Ichikawa, Ms. Mayuko Isomura, Ms. Pritha Verma, Ms. Rou Hua Chua, and Ph.D. colleagues, Mr. Yasuyuki Ueda and Mr. Junpei Sukegawa.

Financial supports from the Global COE program “Chemistry Innovation through Cooperation of Science and Engineering” and Japan Society for the Promotion of Science (JSPS) are greatly appreciated.

Finally, I would like to thank my parents, Kazumi and Atsuko for their continuous encouragement and support during this study.

Sobi Asako

Hongo

December 2013

CHAPTER 1

GENERAL INTRODUCTION 1

1.1. TRANSITION METAL-CATALYZED C–H BOND FUNCTIONALIZATION	2
1.2. IRON-CATALYSIS FOR SUSTAINABLE C–H BOND FUNCTIONALIZATION	3
1.3. IRON-CATALYZED DIRECTED AROMATIC C–H BOND FUNCTIONALIZATION WITH NUCLEOPHILE.....	7
1.4. IRON-CATALYZED DIRECTED AROMATIC C–H BOND FUNCTIONALIZATION WITH ELECTROPHILE ENABLED BY MECHANISTIC UNDERSTANDING	7
1.5. THESIS OUTLINE	9

CHAPTER 2

IRON-MEDIATED C–H BOND FUNCTIONALIZATION OF 2-PHENYLPYRIDINE WITH ELECTROPHILES 15

2.1. INTRODUCTION	16
2.2. METALLACYCLIC IRON INTERMEDIATE	18
2.3. REACTION OF METALLACYCLIC IRON INTERMEDIATE WITH ELECTROPHILES	20
2.4. SUMMARY	22
2.5. EXPERIMENTAL PART	23

CHAPTER 3

IRON-CATALYZED *ORTHO*-ALLYLATION OF ARYLPYRAZOLES WITH ALLYL PHENYL ETHER 27

3.1. INTRODUCTION	28
3.2. INITIAL FINDING	29
3.3. EFFECT OF LIGAND AND ORGANOZINC REAGENT	30
3.4. EFFECT OF ALLYLIC ELECTROPHILES	32
3.5. OPTIMIZATION OF AMOUNT OF CATALYST AND REAGENTS	34
3.6. POSSIBLE CATALYST DEACTIVATION BY PHENOXIDE	36
3.7. SCOPE OF THE REACTION.....	39
3.8. MECHANISTIC CONSIDERATIONS	41
3.9. A POSSIBLE CATALYTIC CYCLE	42

3.10. SUMMARY	43
3.11. EXPERIMENTAL PART	44

CHAPTER 4

IRON-CATALYZED ORHTO-ALLYLATION OF AROMATIC CARBOXAMIDES WITH ALLYL ETHERS 59

4.1. INTRODUCTION	60
4.2. REACTION DESIGN	60
4.3. EFFECT OF ORGANOMETALLIC REAGNET	63
4.4. EFFECT OF LIGAND	65
4.5. EFFECT OF ALLYLIC ELECTROPHILE	66
4.6. SCOPE OF SUBSTRATE	68
4.7. γ -SELECTIVE ALLYLATION WITH α -SUBSTITUTED ALLY PHENYL ETHER	70
4.8. MECHANISTIC INSIGHT	71
4.9. METALLACYCLIC IRON INTERMEDIATE	73
4.10. A POSSIBLE CATALYTIC CYCLE	74
4.11. SUMMARY	75
4.12. EXPERIMENTAL PART	76

CHAPTER 6

SUMMARY AND OUTLOOK 109

List of publications

- [1] “Iron-Catalyzed C–H Bond Activation for the *ortho*-Arylation of Aryl Pyridines and Imines with Grignard Reagents”, Yoshikai, N.; Asako, S.; Yamakawa, T.; Ilies, L.; Nakamura, E. *Chem. Asian J.* **2011**, 6, 3059–3065. (Chapter 2)
- [2] “*ortho*-Allylation of 1-Arylpyrazoles with Allyl Phenyl Ether via Iron-Catalyzed C–H Bond Activation under Mild Conditions”, Asako, S.; Norinder, J.; Yoshikai, N.; Ilies, L.; Nakamura, E. *Adv. Synth. Catal.* **2014** (DOI: 10.1002/adsc.201400063). (Chapter 3)
- [3] “Iron-Catalyzed *Ortho*-Allylation of Aromatic Carboxamides with Allyl Ethers”, Asako, S.; Ilies, L.; Nakamura, E. *J. Am. Chem. Soc.* **2013**, 135, 17755–17757. (Chapter 4)

Publications not included in this thesis

- [1] “Iron-Catalyzed Stereospecific Activation of Olefinic C–H Bonds with Grignard Reagent for Synthesis of Substituted Olefins”, Ilies, L.; Asako, S.; Nakamura, E. *J. Am. Chem. Soc.* **2011**, 133, 7672–7675.
- [2] “Synthesis of Anthranilic Acid Derivatives through Iron-Catalyzed *Ortho* Amination of Aromatic Carboxamides with *N*-Chloroamines”, Matsubara, T; Asako, S.; Ilies, L.; Nakamura, E. *J. Am. Chem. Soc.* **2014**, 136, 646–649.
- [3] “Theoretical Study on Alkoxydiphosphine Ligand for Bimetallic Cooperation in Nickel-Catalyzed Monosubstitution of C–F Bond”, Asako, S.; Ilies, L.; Verma, P.; Ichikawa, S.; Nakamura, E. *Chem. Lett.* **2014** (DOI: 10.1246/cl.131205).

Abbreviations

Ac: Acetyl

APCI: Atmospheric Pressure Chemical Ionization

Ar: Aryl

bpy: 2,2'-bipyridine

Bu: Butyl

Cy: Cyclohexyl

dppbz: 1,2-bis(diphenylphosphino)benzene

dppe: 1,2-bis(diphenylphosphino)ethane

dppen: *cis*-1,2-bis(diphenylphosphino)ethylene

dtbpy: 4,4'-di-*t*-butyl-2,2'-bipyridine

GC: Gas Chromatography

GC–MS: Gas Chromatography–Mass Spectrometry

GPC: Gel Permeation Chromatography

h: hour(s)

HRMS: High-Resolution Mass Spectrometry

Hz: Hertz

KIE: Kinetic Isotope Effect

Me: Methyl

Mes: Mesityl

MHz: MegaHertz

min: minute(s)

NMR: Nuclear Magnetic Resonance

Ph: Phenyl

phen: 1,10-phenanthroline

ppm: parts per million

rt: room temperature

THF: Tetrahydrofuran

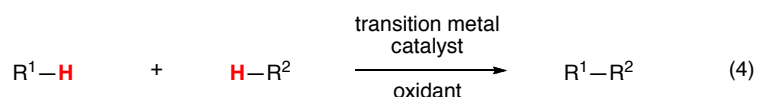
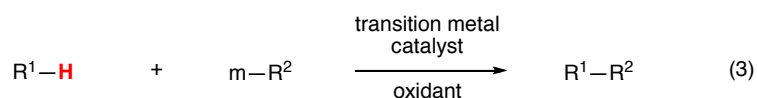
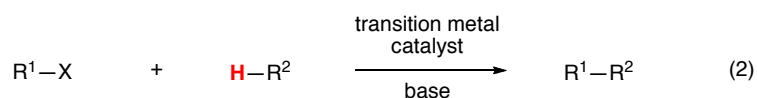
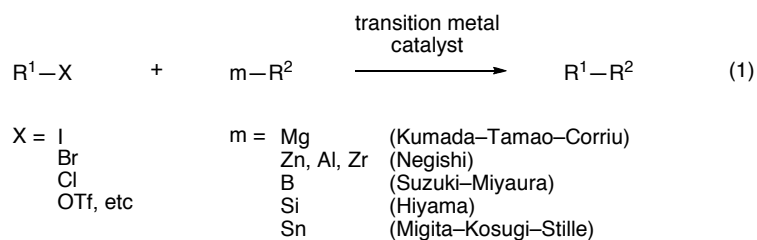
TMEDA: *N,N,N',N'*-Tetramethylethylenediamine

CHAPTER 1

General Introduction

1.1. Transition Metal-Catalyzed C–H Bond Functionalization

The transition metal-catalyzed cross-coupling reaction between an electrophilic reagent and a nucleophilic reagent has matured into one of the most important C–C bond forming reactions, due to high versatility, practicality, and reliability (eq. 1).¹ It has found numerous applications both in the field of academia and chemical industry for the construction of complex natural products, bioactive compounds, functional materials, and so on. However, these reactions require preactivation of both of the coupling partners, which have to be functionalized in advance as an organic (pseudo)halide and an organometallic reagent, resulting in consumption of a large amount of chemicals, energy, and time resources. On the other hand, transition metal-catalyzed direct functionalization of a ubiquitous C–H bond has recently emerged as a more efficient and straightforward method, because it avoids the requirement for preactivation of the organic (pseudo)halide, of the organometallic reagent, or even of both (eqs. 2–4).² Although a great number of C–H bond functionalization reactions have been developed, in which various types of C–H bonds such as sp , sp^2 , and even sp^3 C–H bonds can be employed as “reactive” sites, most of these reactions require rare and toxic second or third-row transition metals such as ruthenium, rhodium, and palladium, and typically harsh reaction conditions, which is incompatible with the concept of sustainability. Therefore, the development of direct C–H bond functionalization reactions that are sustainable still remain a major challenge.³

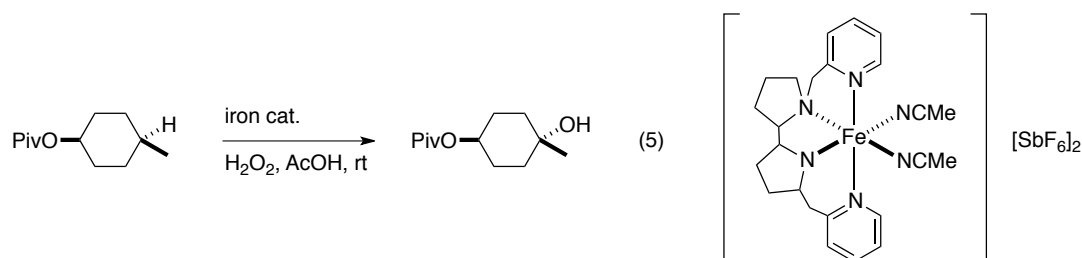


1.2. Iron-Catalysis for Sustainable C–H Bond Functionalization

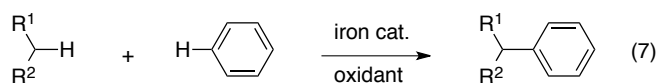
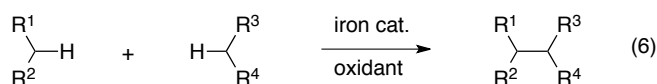
On the other hand, iron is one of the first metals that human started to exploit and has been the most valuable metal for human society since ancient times. Because iron is abundant, inexpensive, non-toxic, and environmentally benign, it is currently recognized as an indispensable metal for sustainable catalysis.⁴ Therefore, it is not surprising that iron-catalyzed C–H bond functionalization reactions, which combine the advantages of iron catalysis and C–H bond transformation, have recently attracted much attention.^{4h}

C–H bond oxidation catalyzed by natural enzymes containing high valent iron center is a well-known process.⁵ Inspired by these natural systems, synthetic iron complexes have been investigated for their application in iron-catalyzed C–H bond oxidation reactions. Following the seminal studies by Que et al.,⁶ a number of non-heme iron complexes have been designed, among which a cationic Fe(II) complex

possessing a tetradentate nitrogen ligand developed by White et al. performed well for the oxidation of unactivated sp^3 C–H bonds under mild conditions (eq. 5).⁷

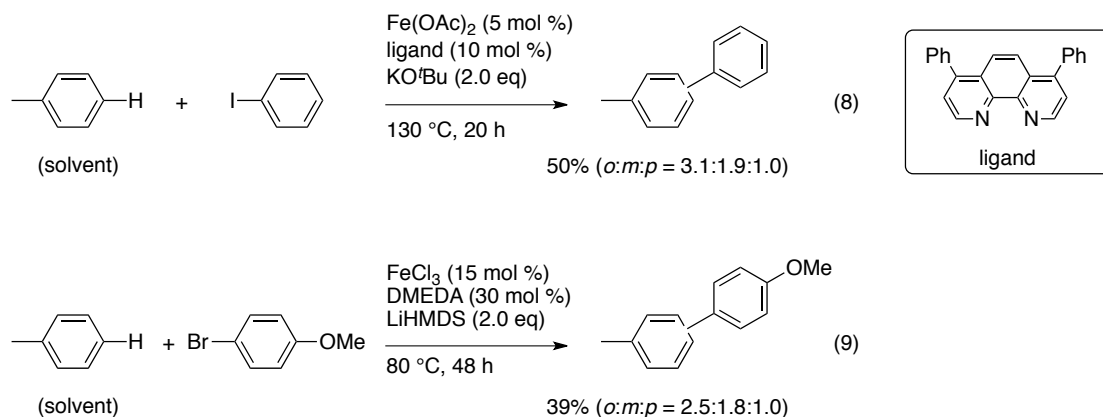


Iron-catalyzed cross-dehydrogenative coupling is one of the C–C bond forming reactions via iron-catalyzed C–H bond activation, which connects two sp^3 C–H bonds (eq. 6)⁸ or sp^3 and sp^2 C–H bond (eq. 7).⁹ Typically, sp^3 C–H bonds of active methylene compounds or those adjacent to heteroatoms, and sp^2 C–H bonds of electron-rich arenes participate in these reactions.

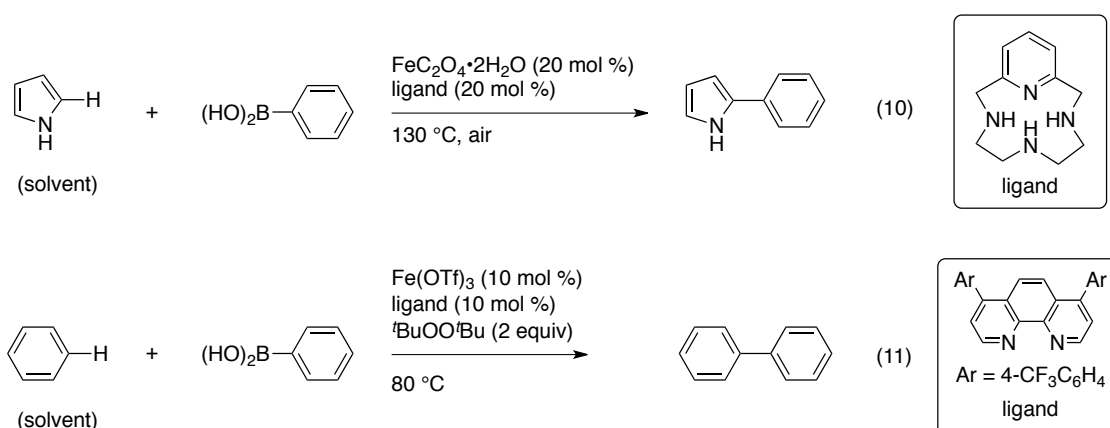


Except for the classical Lewis-acid-promoted Friedel–Crafts reactions,¹⁰ a few reports have appeared on iron-catalyzed aromatic C–H bond functionalization reactions. Charette et al. and Lei et al. independently reported iron-catalyzed C–H bond arylation of simple arenes with aryl halides (eqs. 8 and 9).¹¹ Arenes are used as a solvent and a mixture of regioisomers was obtained due to a radical pathway, which was proposed

based on mechanistic studies.

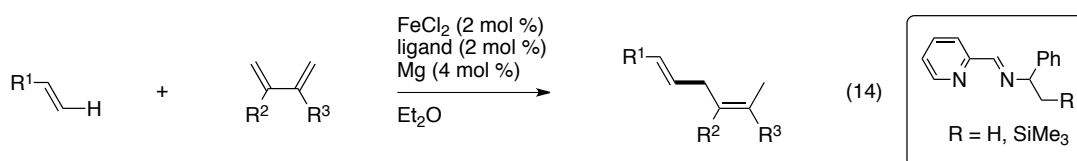
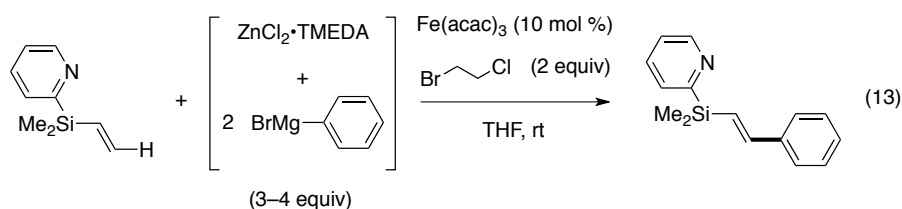
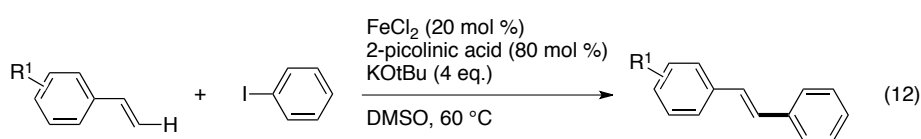


Hu, Yu et al. and Shirakawa, Hayashi et al. developed iron-catalyzed C–H bond arylation of pyrroles, pyridines, and simple arenes with arylboronic acids (eqs. 10 and 11).¹² A non-radical mechanism was proposed for the former reaction based on DFT calculations, while a radical pathway was proposed for the latter reaction.



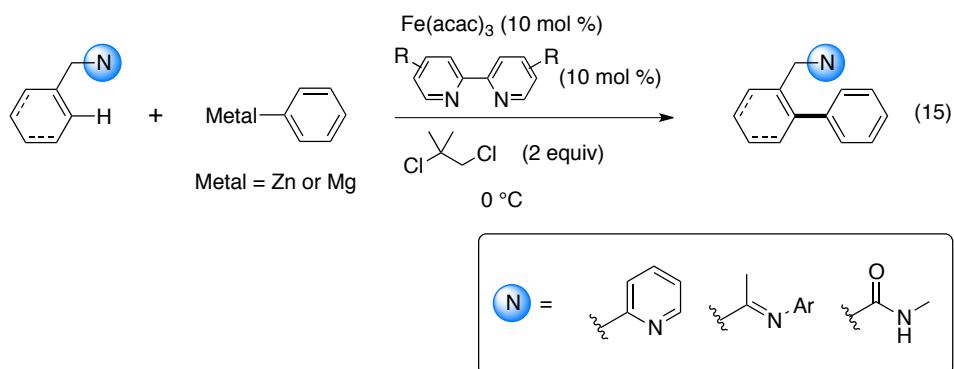
The similar reaction conditions for the direct arylation with aryl halides can be applied to formal iron-catalyzed olefinic C–H bond arylation reaction. Vogel et al.

reported an iron-catalyzed Mizoroki–Heck reaction of aryl iodides with styrenes (eq. 12).¹³ Nakamura et al. developed a chelation-assisted iron-catalyzed oxidative Mizoroki–Heck reaction using arylzinc reagents (eq. 13). The reaction proceeds via chelation-assisted carbometallation to form a stable five-membered iron intermediate. Another example for iron-catalyzed olefinic C–H bond functionalization is an intermolecular iron-catalyzed 1,4-addition of terminal olefins to 1,3-dienes reported by Ritter et al. (eq. 14).¹⁴ An active species generated upon reduction of FeCl_2 with Mg in the presence of a diamine ligand is assumed to trigger an oxidative coupling of the two substrates, followed by *syn* β -hydride elimination and reductive elimination to give 1,4-dienes with high regio- and (*E*)-stereoselectivity.



1.3. Iron-Catalyzed Directed Aromatic C–H Bond Functionalization with Nucleophile

As a part of our continuous efforts towards sustainable synthetic methodologies using iron as a ubiquitous and benign catalyst,¹⁵ the author's group has reported a series of iron-catalyzed C–H bond arylation reactions with a nucleophilic coupling partner (eq. 15).¹⁶ In contrast to the aromatic C–H bond arylation of simple arenes (eqs. 8–11), the reaction is completely regioselective due to the presence of a nitrogen directing group. While these reactions are the first and still the only catalytic examples of iron-catalyzed directed sp^2 C–H bond functionalization,^{17,18} the coupling partner was always limited to nucleophilic aryl groups such as arylzinc reagents and aryl Grignard reagents.



1.4. Iron-Catalyzed Directed Aromatic C–H Bond Functionalization with Electrophile Enabled by Mechanistic Understanding

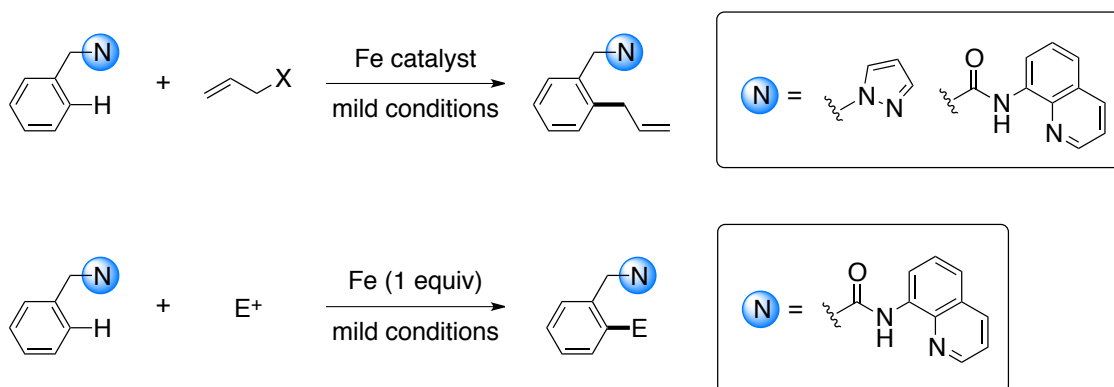
Although iron has many attractive features as sustainable catalyst, iron chemistry is not yet as reliable and practical as palladium chemistry. One of the reasons is the lack of understanding of the “crucial factors” governing the iron-catalyzed reactions, resulting in sporadic and nondirectional research. To date, mechanistic

studies on iron catalysis are in their infancy, and even for the long-studied iron-catalyzed cross-coupling reactions, there is no agreement between various different mechanisms.¹⁹ Naturally, the situation is far more serious for iron-catalyzed C–H bond activation reactions.

Considering the rapid growth in the second- and third-row transition-metal-catalyzed C–H bond functionalization reactions, which now enable introduction of almost every type of coupling partner and find practical applications, the introduction of various types of functional groups using iron and electrophiles would be highly desirable and further expand the utility of iron as a sustainable catalyst for the functionalization of C–H bonds. This should be enabled by understanding important factors controlling the iron-catalyzed C–H bond activation reactions.

1.5. Thesis Outline

In this thesis, the author developed iron-based aromatic C–H bond functionalization reactions with electrophilic coupling partners. This unprecedented reaction type was first attempted by the investigation of stoichiometric reactions using 2-phenylpyridine and electrophiles (Chapter 2), and was indeed demonstrated by iron-catalyzed *ortho*-allylation of arylpyrazole and *N*-(quinlin-8-yl)benzamide derivatives with allyl phenyl ether for the regioselective synthesis of allylbenzene derivatives (Chapters 3 and 4). The careful control of reaction parameters such as directing group and organometallic base was crucial for achieving the selective allylation reactions. Furthermore, iron-mediated C–H bond functionalization with electrophiles were developed by the reaction of a chelated iron intermediate generated via stoichiometric C–H bond activation of *N*-(quinlin-8-yl)benzamide with various electrophiles (Chapter 5). These examples demonstrated for the first time that the iron-based C–H bond activation could be followed by reaction with electrophiles. These newly established reaction modes will greatly expand the utility of iron-based C–H bond activation.



References

- ¹ (a) *Cross-Coupling reactions: A Practical Guide* (Ed.: N. Miyaura), Springer, Berlin, **2002**. (b) *Metal-Catalyzed Cross-Coupling Reactions*, 2nd ed. (Eds.: A. de Meijere, F. Diederich), Wiley-VCH, Weinheim, **2004**.
- ² (a) Ritleng, V.; Sirlin, C.; Pfeffer, M. *Chem. Rev.* **2002**, *102*, 1731–1769. (b) *Handbook of C–H Transformations*; Dyker, G., Ed.; Wiley-VCH: Weinheim, Germany, **2005**. (c) Alberico, D.; Scott, M. E.; Lautens, M. *Chem. Rev.* **2007**, *107*, 174–238.
- ³ Nakamura, E.; Sato, K. *Nat. Mater.* **2011**, *10*, 158–161.
- ⁴ (a) Bolm, C.; Legros, J.; Paih, J. L.; Zani, L. *Chem. Rev.* **2004**, *104*, 6217–6254. (b) *Iron Catalysis in Organic Chemistry: Reactions and Applications*, (Ed.: B. Plietker), Wiley-VCH, Weinheim, **2008**. (c) Fürstner, A. *Angew. Chem. Int. Ed.* **2009**, *48*, 1364–1367. (d) Sherry, B. D.; Fürstner, A. *Acc. Chem. Res.* **2008**, *41*, 1500–1511. (e) Correa, A.; Mancheno, O. G.; Bolm, C. *Chem. Soc. Rev.* **2008**, *37*, 1108–1117. (f) Enthaler, S.; Junge, K.; Beller, M. *Angew. Chem., Int. Ed.* **2008**, *47*, 3317–3321. (g) Czaplik, W. M.; Mayer, M.; Cvengros, J.; Jacobi von Wangelin, A. *ChemSusChem* **2009**, *2*, 396–417. (h) Sun, C.-L.; Li, B.-J.; Shi, Z.-J. *Chem. Rev.* **2011**, *111*, 1293–1314.
- ⁵ (a) Fridovich, I. *Science* **1978**, *201*, 875–880. (b) Ford, P. C.; Fernandez, B. O.; Lim, M. D. *Chem. Rev.* **2005**, *105*, 2439–2456. (c) Shaik, S.; Cohen, S.; Wang, Y.; Chen, H.; Kumar, D.; Thiel, W. *Chem. Rev.* **2010**, *110*, 949–1017.
- ⁶ (a) Kim, C.; Chen, K.; Kim, J.; Que, L., Jr.; *J. Am. Chem. Soc.* **1997**, *119*, 5964–5965. (b) Chen, K.; Que, L., Jr.; *J. Am. Chem. Soc.* **2001**, *123*, 6327–6337.
- ⁷ Chen, M. S.; White, M. C. *Science* **2007**, *318*, 783–787.

⁸ (a) Li, Z.; Li, C.-J. *J. Am. Chem. Soc.* **2005**, *127*, 6968–6969. (b) Zhang, Y.; Li, C.-J. *Angew. Chem., Int. Ed.* **2006**, *45*, 1949–1952. (c) Li, Z.; Cao, L.; Li, C.-J. *Angew. Chem., Int. Ed.* **2007**, *46*, 6505–6507. (d) Zhang, Y.; Li, C.-J. *Eur. J. Org. Chem.* **2007**, 4654–4657. (e) Li, Z.; Yu, R.; Li, H. *Angew. Chem., Int. Ed.* **2008**, *47*, 7497–7500. (f) Li, H.; He, Z.; Guo, X.; Li, W.; Zhao, X.; Li, Z. *Org. Lett.* **2009**, *11*, 4176–4179. (g) Richter, H.; Mancheño, O. G. *Eur. J. Org. Chem.* **2010**, 4460–4467. (h) Zeng, T.; Song, G.; Moores, A.; Li, C.-J. *Synlett* **2010**, 2002–2008. (i) Xie, Y.; Yu, M.; Zhang, Y. *Synthesis* **2011**, 2803–2809.

⁹ (a) Guo, X.; Yu, R.; Li, H.; Li, Z. *J. Am. Chem. Soc.* **2009**, *131*, 17387–17393. (b) Li, Y.-Z.; Li, B.-J.; Lu, X.-Y.; Lin, S.; Shi, Z.-J. *Angew. Chem., Int. Ed.* **2009**, *48*, 3817–3820. (c) Guo, X.; Pan, S.; Liu, J.; Li, Z. *J. Org. Chem.* **2009**, *74*, 8848–8851. (d) Ohta, M.; Quick, M. P.; Yamaguchi, J.; Wunsch, B.; Itami, K. *Chem. Asian J.* **2009**, *4*, 1416–1419. (e) Guo, X.; Li, W.; Li, Z. *Eur. J. Org. Chem.* **2010**, 5787–5790. (f) Ghobrial, M.; Harhammer, K.; Mihovilovic, M. D.; Schnürch, M. *Chem. Commun.* **2010**, *46*, 8836–8838. (g) Wu, W.; Su, W. *J. Am. Chem. Soc.* **2011**, *133*, 11924–11927. (h) Shirakawa, E.; Uchiyama, N.; Hayashi, T. *J. Org. Chem.* **2011**, *76*, 25–34. (i) Ghobrial, M.; Schnürch, M.; Mihovilovic, M. D. *J. Org. Chem.* **2011**, *76*, 8781–8793.

¹⁰ (a) *Electrophilic Aromatic Substitution*; Taylor, R., Ed.; Wiley: Chichester, 1990. (b) *Friedel–Crafts and Related Reactions*; Olah, G. A., Ed.; Wiley-Interscience: New York, 1963–1965; Vols. I–IV.

¹¹ (a) Vallée, F.; Mousseau, J. J.; Charette, A. B. *J. Am. Chem. Soc.* **2010**, *132*, 1514–1516. (b) Liu, W.; Cao, H.; Lei, A. *Angew. Chem., Int. Ed.* **2010**, *49*, 2004–2008.

¹² (a) Wen, J.; Qin, S.; Ma, L.-F.; Dong, L.; Zhang, J.; Liu, S.-S.; Duan, Y.-S.; Chen,

S.-Y.; Hu, C.-W.; Yu, X.-Q. *Org. Lett.* **2010**, *12*, 2694–2697. (b) Uchiyama, N.; Shirakawa, E.; Nishikawa, R.; Hayashi, T. *Chem. Commun.* **2011**, *47*, 11671–11673.

¹³ Loska, R.; Volla, C. M. R.; Vogel, P. *Adv. Synth. Catal.* **2008**, *350*, 2859–2864.

¹⁴ Moreau, B.; Wu, J. Y.; Ritter, T. *Org. Lett.* **2009**, *11*, 337–339.

¹⁵ (a) Nakamura, M.; Hirai, A.; Nakamura, E. *J. Am. Chem. Soc.* **2000**, *122*, 978–979.

(b) Nakamura, M.; Matsuo, K.; Ito, S.; Nakamura, E. *J. Am. Chem. Soc.* **2004**, *126*, 3686–3687. (c) Nakamura, E.; Yoshikai, N. *J. Org. Chem.* **2010**, *75*, 6061–6067.

¹⁶ (a) Norinder, J.; Matsumoto, A.; Yoshikai, N.; Nakamura, E. *J. Am. Chem. Soc.* **2008**, *130*, 5858–5859. (b) Yoshikai, N.; Matsumoto, A.; Norinder, J.; Nakamura, E. *Angew. Chem. Int. Ed.* **2009**, *48*, 2925–2928. (c) Ilies, L.; Asako, S.; Nakamura, E. *J. Am. Chem. Soc.* **2011**, *133*, 7672–7675. (d) Yoshikai, N.; Asako, S.; Yamakawa, T.; Ilies, L.; Nakamura, E. *Chem. Asian J.* **2011**, *6*, 3059–3065. (e) Ilies, L.; Kobayashi, M.; Matsumoto, A.; Yoshikai, N.; Nakamura, E. *Adv. Synth. Catal.* **2012**, *354*, 593–596. (f) Ilies, L.; Konno, E.; Chen, Q.; Nakamura, E. *Asian J. Org. Chem.* **2012**, *1*, 142–145. (g) Shang, R.; Ilies, L.; Matsumoto, A.; Nakamura, E. *J. Am. Chem. Soc.* **2013**, *135*, 6030–6032.

¹⁷ Jones, W. D.; Foster, G. P.; Putinas, J. M. *J. Am. Chem. Soc.* **1987**, *109*, 5047–5048.

¹⁸ Stoichiometric cyclometalation: (a) Bagga, M. M.; Pauson, P. L.; Preston, F. J.; Reed, R. I. *Chem. Commun.* **1965**, 543–544. (b) Hata, G.; Kondo, H.; Miyake, A. *J. Am. Chem. Soc.* **1968**, *90*, 2278–2281. (c) Karsch, H. H.; Klien, H.-F.; Schmidbaur, H. *Angew. Chem. Int. Ed. Engl.* **1975**, *14*, 637–638. (d) Rathke, J. W.; Muetterties, E. L. *J. Am. Chem. Soc.* **1975**, *97*, 3272–3273. (e) Tolman, C. A.; English, A. D.; Ittel, S. D.; Jesson, J. P. *Inorg. Chem.* **1978**, *17*, 2374–2378. (f) Ittel, S. D.; Tolman, C. A.; Krusic,

P. J.; English, A. D.; Jesson, J. P. *Inorg. Chem.* **1978**, *17*, 3432–3438. (g) Imhof, W.; Göbel, A.; Ohlmann, D.; Flemming, J.; Fritzsche, H. *J. Organomet. Chem.* **1999**, *584*, 33–43. (h) Klein, H.-F.; Camadanli, S.; Beck, R.; Leukel, D.; Flörke, U. *Angew. Chem. Int. Ed.* **2005**, *44*, 975–977. (i) Klein, H.-F.; Camadanli, S.; Beck, R.; Flörke, U. *Chem. Commun.* **2005**, 381–382. (j) Beck, R.; Sun, H.; Li, X.; Camadanli, S.; Klien, H.-F. *Eur. J. Inorg. Chem.* **2008**, 3253–3257. (k) Beck, R.; Zheng, T.; Sun, H.; Li, X.; Flörke, U.; Klien, H.-F. *J. Organomet. Chem.* **2008**, *693*, 3471–3478. (l) Camadanli, S.; Beck, R.; Flörke, U.; Klein, H.-F. *Organometallics* **2009**, *28*, 2300–2310. (m) Xu, G.; Sun, H.; Li, X. *Organometallics* **2009**, *28*, 6090–6095. (n) Liu, N.; Li, X.; Sun, H. *J. Organomet. Chem.* **2011**, *696*, 2537–2542.

¹⁹ For example: (a) Fürstner, A.; Martin, R.; Krause, H.; Seidel, G.; Goddard, R.; Lehmann, C. W. *J. Am. Chem. Soc.* **2008**, *130*, 8773–8787. (b) Noda, D.; Sunada, Y.; Hatakeyama, T.; Nakamura, M.; Nagashima, H. *J. Am. Chem. Soc.* **2009**, *131*, 6078–6079. (c) Kleimark, J.; Hedström, A.; Larsson, P.-F.; Johansson, C.; Norrby, P.-O. *ChemCatChem*, **2009**, *1*, 152–161. (d) Adams, C. J.; Bedford, R. B.; Carter, E.; Gower, N. J.; Haddow, M. F.; Harvey, J. N.; Huwe, M.; Cartes, M. A.; Mansell, S. M.; Mendoza, C.; Murphy, D. M.; Neeve, E. C.; Nunn, J. *J. Am. Chem. Soc.* **2012**, *134*, 10333–10336.

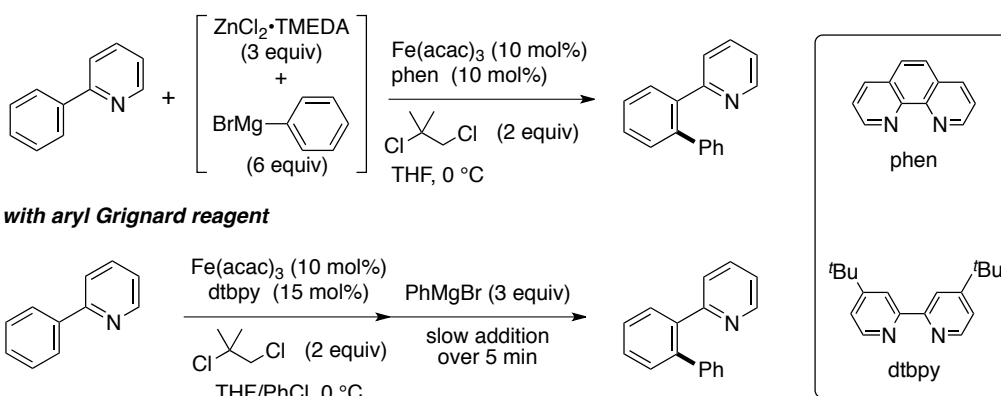
Chapter 1

CHAPTER 2

Iron-Mediated C–H Bond Functionalization of 2-Phenylpyridine with Electrophiles

2.1. Introduction

The research project for iron-catalyzed aromatic C–H bond functionalization with electrophiles commenced with considering the mechanism of the iron-catalyzed aromatic C–H bond functionalization with aryl nucleophiles, which was developed previously (Scheme 1).¹

Scheme 1.**with arylzinc reagent**

A possible catalytic cycle for the iron-catalyzed oxidative aromatic C–H bond arylation is shown in Figure 1. Reversible coordination of the pyridyl group of the substrate to the iron center of an aryliron species (**A**) is followed by irreversible metalation of the *ortho* position with concomitant elimination of an arene molecule. It has been previously confirmed in the iron-catalyzed oxidative arylation using deuterated substrate that 1 equiv of arylzinc reagent was used for the abstraction of the *ortho* C–H bond (eq. 1).^{1a} The *ortho*-metalated intermediate **B** undergoes reductive elimination upon interaction with 1,2-dichloro-2-methylpropane to afford the *ortho*-arylation product, isobutene, and dichloroiron species. Transmetalation with the

Grignard reagent regenerates the active species **A**.

With the background described in the previous chapter as well as the proposed mechanism in Figure 1, it was envisioned that the metallacyclic iron intermediate **B** could be trapped with electrophiles.

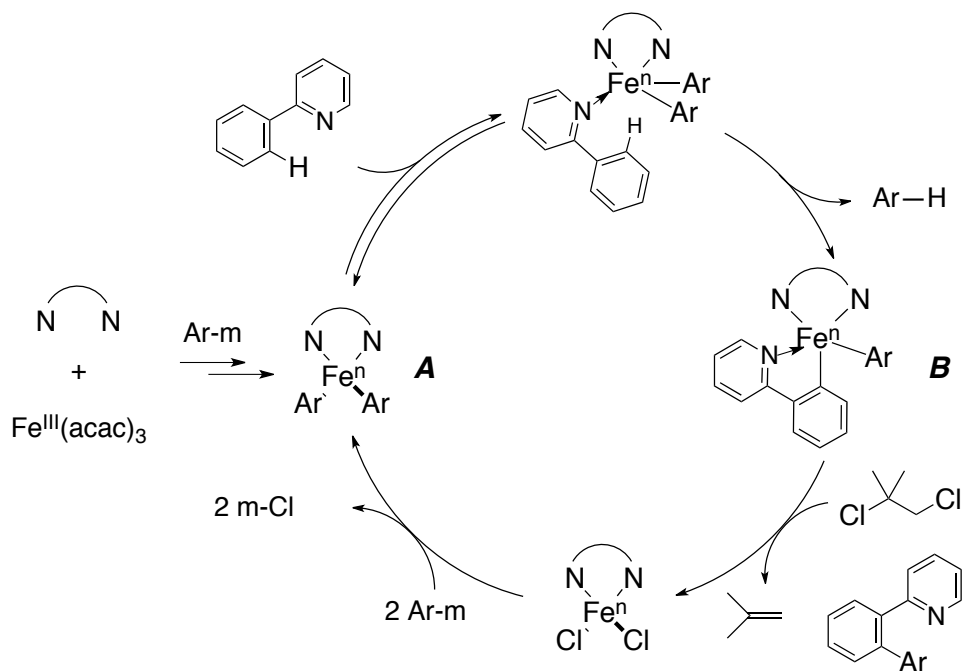
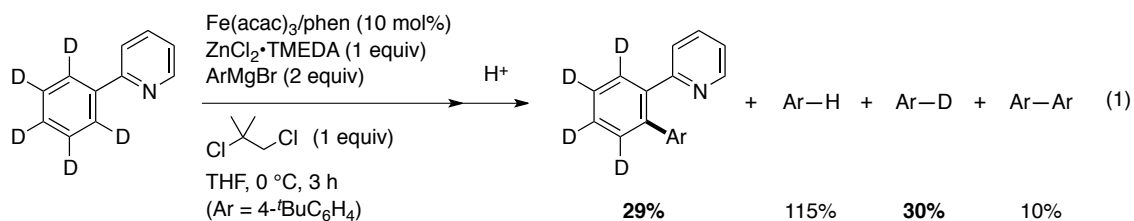


Figure 1. A Possible Catalytic Cycle for Iron-Catalyzed Directed Arylation under Oxidative Conditions



2.2. Metallacyclic Iron Intermediate

In order to probe the putative metallacyclic iron intermediate, a series of stoichiometric reactions were initially performed. First, PhMgBr (4 equiv) was added to a mixture of 2-phenylpyridine (**1**), Fe(acac)₃ (1 equiv), and 4,4'-di-*t*-butyl-2,2'-bipyridine (dtbpy, 2 equiv) in PhCl over a period of 3 minutes. After stirring for 10 seconds, the reaction was immediately quenched with the addition of D₂O to afford recovered **1**, phenylated product (**2**), and biphenyl in 82%, 6%, and 90% yields, respectively (Table 1, entry 1). A deuterium atom was incorporated into the ortho position of **1** in 59%. When the same reaction was stirred for 1 h before the addition of D₂O, the D incorporation increased to 86%, while the yields of the products did not change (entry 2). On the other hand, when 1,2-dichloro-2-methylpropane was added before quenching with D₂O, the recovery of **1** decreased to 27% with the increased yield of **2** in 59% (entry 3). In the absence of dtbpy, oxidative homocoupling reaction took place to give biphenyl, and neither phenylation nor deuterium incorporation occurred (entry 4). The reaction of **1** with PhMgBr without any catalyst resulted in quantitative recovery of **1** without deuterium incorporation (entry 5).

Table 1.

entry	x	y	t_1	oxidant	t_2	yield (%) ^a		
						1 (%D) ^b	2	Ph-Ph
1	1	2	3 min	none	10 s	82 (59)	6	90
2	1	2	3 min	none	1 h	80 (86)	6	92
3	1	2	3 min		40 s ^c	27 (20)	59	114
4	1	0	5 min	none	30 s	86 (0)	0	138
5	0	0	5 min	none	30 s	> 95 (0)	0	0

^a Determined by GC using *n*-tridecane as an internal standard.^b Determined by ¹H NMR analysis.^c Stirring for 10 s, addition of 1,2-dichloro-2-methylpropane, and additional stirring for 30 s were followed by the addition of D₂O.

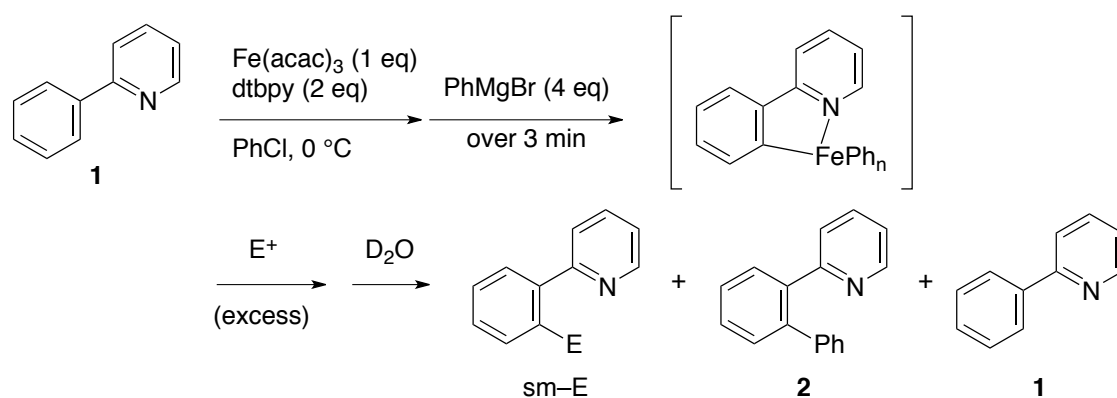
The above stoichiometric experiments indicate the presence of a stable metallacyclic interintermediate that bears an *ortho* C–metal bond. Because the intermediate forms only when the iron salt and the dtbpy ligand are present, the intermediate seems to be a metallacyclic iron intermediate bearing 2-(2-pyridyl)phenyl group. The iron intermediate is stable enough at 0 °C at least for 1 h in the absence of an oxidant. However, it quickly decomposes to give the *ortho*-phenylated product **2** upon addition of 1,2-dichloro-2-methylpropane as an oxidant.

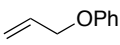
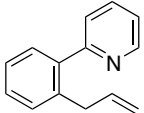
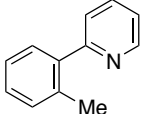
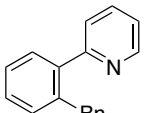
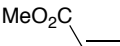
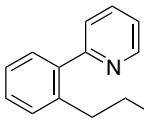
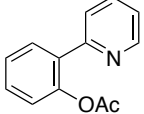
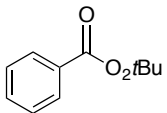
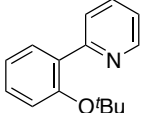
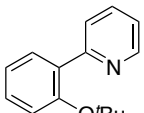
2.3. Reaction of Metallacyclic Iron Intermediate with Electrophiles

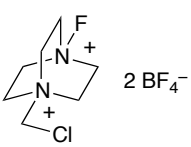
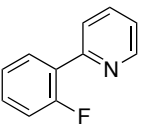
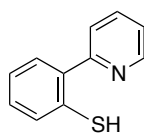
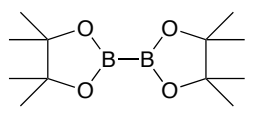
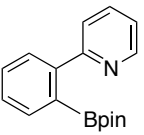
The stability of the metallacyclic iron intermediate in the absence of an oxidant suggests a possibility to investigate its reactivity towards various electrophiles for introducing various functional groups. The possibility of this unprecedented iron-catalyzed directed functionalization of aromatic C–H bond with an electrophile was encouraged by a recent mechanistic study on iron-catalyzed cross coupling reaction between alkyl halides and aryl Grignard reagents reported by Nakamura and Nagashima et al.,² describing that $\text{Ar}_2\text{Fe}\cdot\text{TMEDA}$ species could react with alkyl halide to produce an Ar–alkyl product.

The reactions of the stoichiometrically generated metallacyclic iron intermediate with various electrophiles were attempted using 2-phenylpyridine as a substrate (Table 2). The results when using carbon electrophiles are summarized in entries 1–4. While allyl phenyl ether and iodomethane gave the corresponding products in about 10% yield (entries 1 and 2), benzyl bromide, which also has sp^3 carbon afforded no benzylated product (entry 3). In these cases, the reactions yielded a large amount of phenylated product **2**. The use of methyl acrylate as a Michael acceptor gave no product, again with the exclusive formation of **2** (entry 4). Entries 5–10 describe attempts toward carbon–heteroatom bond formation. However, all the attempts to incorporate O, F, S, and B atoms were unsuccessful and either phenylated product **2** was formed or the starting material was recovered.

Table 2.



entry	E^+	yield ^a			
		SM-E	2	1	Ph-Ph
1		 8%	27%	50% (51% D)	87%
2 ^b	MeI	 9%	21%	26%	108%
3	BnBr	 0%	80%	12%	100%
4		 0%	56%	13%	90%
5	PhI(OAc) ₂	 0%	73%	21%	99%
6		 0%	80%	23%	102%
7	<i>t</i> Bu-O-O- <i>t</i> Bu	 0%	7%	84% (76% D)	84%

8			0%	69%	23%	89%
9	S		0%	60%	18%	95%
10			0%	6%	65%	93%

^a Determined by GC using *n*-tridecane as an internal standard.

^b Benzene was used instead of PhCl.

2.4. Summary

The properties and reactivity of a metallacyclic iron intermediate derived from 2-phenylpyridine were investigated. The iron intermediate was found to be stable at 0 °C when no oxidant was present, suggesting a possibility of introducing various functional groups by electrophilic trapping of the intermediate. However, the reaction of the intermediate with various electrophiles was found to be difficult. Thus, the attempts to form carbon–carbon and carbon–heteroatom bonds using electrophiles were hampered by the undesired coupling with the Ph group from PhMgBr used for the generation of the iron intermediate.

2.5. Experimental Part

General. All reactions dealing with air- or moisture-sensitive compounds were carried out in a dry reaction vessel under nitrogen or argon. The water content of the solvent was confirmed with a Karl-Fischer Moisture Titrator (MKC-210, Kyoto Electronics Company) to be less than 30 ppm. Analytical thin-layer chromatography was performed on glass plates coated with 0.25 mm 230–400 mesh silica gel containing a fluorescent indicator (Merck). Gas-liquid chromatographic (GLC) analysis was performed on a Shimadzu 14A or 14B machine equipped with glass capillary column HR-1 (0.25-mm i.d. x 25 m). Flash silica gel column chromatography was performed on silica gel 60N (Kanto, spherical and neutral, 140–325 mesh) as described by Still.³ NMR spectra were measured on a JEOL ECA-500 spectrometer and reported in parts per million from tetramethylsilane. ¹H NMR spectra in CDCl₃ were referenced internally to tetramethylsilane as a standard, and ¹³C NMR spectra to the solvent resonance. Methyl, methylene, and methyne signals in ¹³C NMR spectra were assigned by DEPT spectra.

Materials. Unless otherwise noted, materials were purchased from Tokyo Kasei Co., Aldrich Inc., and other commercial suppliers and used after appropriate purification before use. Anhydrous ethereal solvents (stabilizer-free) were purchased from WAKO Pure Chemical and purified by a solvent purification system (GlassContour) equipped with columns of activated alumina and supported copper catalyst (Q-5) prior to use.⁴ Chlorobenzene was purified by distillation over CaH₂ and stored over molecular sieves 4Å. Fe(acac)₃ and 4,4'-di-*tert*-butyl-2,2'-bipyridyl were purchased from Aldrich Inc. and 1,2-dichloroisobutane was purchased from Tokyo Kasei Co, respectively, and used as received. Grignard reagents were purchased from Aldrich Inc. or prepared from the

corresponding halides and magnesium turnings in anhydrous THF, and titrated prior to use.

Trapping of Metallacyclic Iron Intermediate with D₂O

To a solution of 2-phenylpyridine (31.0 mg, 0.2 mmol), Fe(acac)₃ (70.5 mg, 0.2 mmol), and 4,4'-di-*t*-butyl-2,2'-bipyridine (107 mg, 0.4 mmol) in PhCl (3.0 mL) was added a THF solution of PhMgBr (0.76 M, 1.05 mL, 1.6 mmol) over 3 min at 0 °C. After a certain time, the reaction was quenched with D₂O followed by the addition of saturated aqueous solution of potassium sodium tartrate and water. The organic layer was collected and analyzed by GC using *n*-tridecane as an internal standard to determine the yield, and by ¹H NMR to determine D incorporation of recovered substrate.

Trapping of Metallacyclic Iron Intermediate with Electrophiles

To a solution of 2-phenylpyridine (31.0 mg, 0.2 mmol), Fe(acac)₃ (70.5 mg, 0.2 mmol), and 4,4'-di-*t*-butyl-2,2'-bipyridine (107 mg, 0.4 mmol) in PhCl (3.0 mL) was added a THF solution of PhMgBr (0.76 M, 1.05 mL, 1.6 mmol) over 3 min at 0 °C. The reaction was quenched with electrophiles followed by addition of D₂O, saturated aqueous solution of potassium sodium tartrate, and water. The organic layer was collected and analyzed by GC and GC–MS using *n*-tridecane as an internal standard.

References

- ¹ (a) Norinder, J.; Matsumoto, A.; Yoshikai, N.; Nakamura, E. *J. Am. Chem. Soc.* **2008**, *130*, 5858–5859. (b) Yoshikai, N.; Asako, S.; Yamakawa, T.; Ilies, L.; Nakamura, E. *Chem. Asian J.* **2011**, *6*, 3059–3065.
- ² Noda, D.; Sunada, Y.; Hatakeyama, T.; Nakamura, M.; Nagashima, H. *J. Am. Chem. Soc.* **2009**, *131*, 6078–6079.
- ³ Still, W. C.; Kahn, M.; Mitra, A. *J. Org. Chem.* **1978**, *43*, 2923–2925.
- ⁴ Pangborn, A. B.; Giardello, M. A.; Grubbs, R. H.; Rosen R. K.; Timmers, F. J. *Organometallics* **1996**, *15*, 1518–1520.

Chapter 2

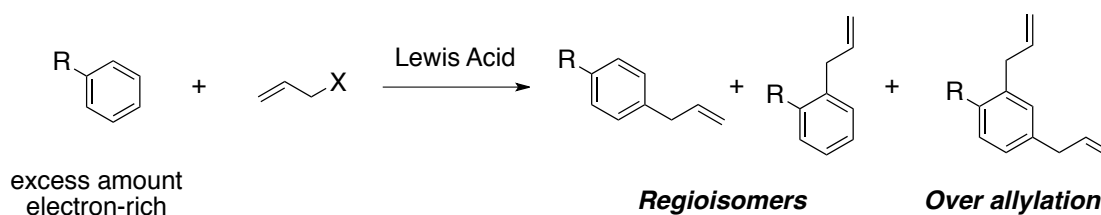
CHAPTER 3

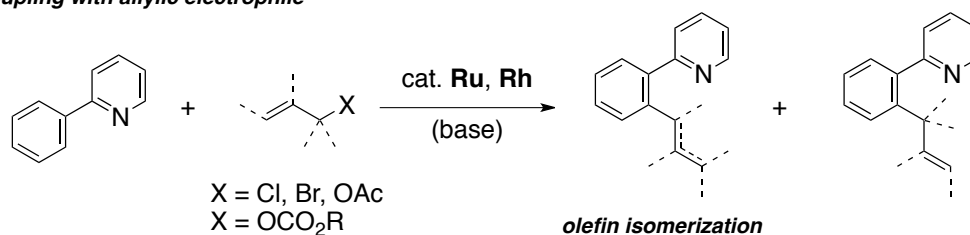
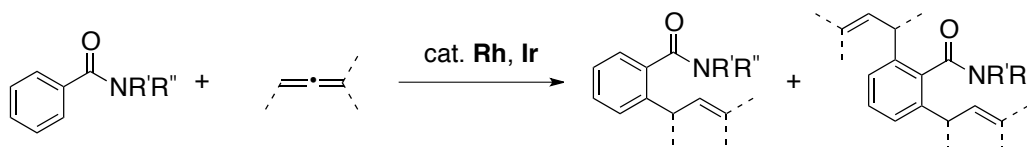
Iron-Catalyzed *Ortho*-Allylation of Arylpyrazoles with Allyl Phenyl Ether

3.1. Introduction

Derivatives of allylbenzene, a structural motif in numerous natural products and biologically active compounds,¹ which serve as versatile intermediates in synthesis are typically synthesized via the reaction of an aryl donor with an allylic fragment.² The Lewis acid-promoted Friedel–Crafts-type allylation of a simple arene is a classical and straightforward method to synthesize allylarenes (Scheme 1).³ However, the reaction is limited to electron-rich arenes and it often produces a mixture of regioisomers and overallylated products. Transition-metal-catalyzed directed C–H bond allylation has been recently developed to achieve broader scope and superior regioselectivity, in which C–H bond activation is followed by either coupling with allylic electrophiles or addition to allenes (Scheme 2).^{4,5,6,7,8} However, these reactions require a precious metal catalyst and/or typically harsh reaction conditions, which sometimes lead to product isomerization from the terminal olefin to styrene compounds.

Scheme 1. Lewis Acid-Promoted Friedel–Crafts-Type Allylation



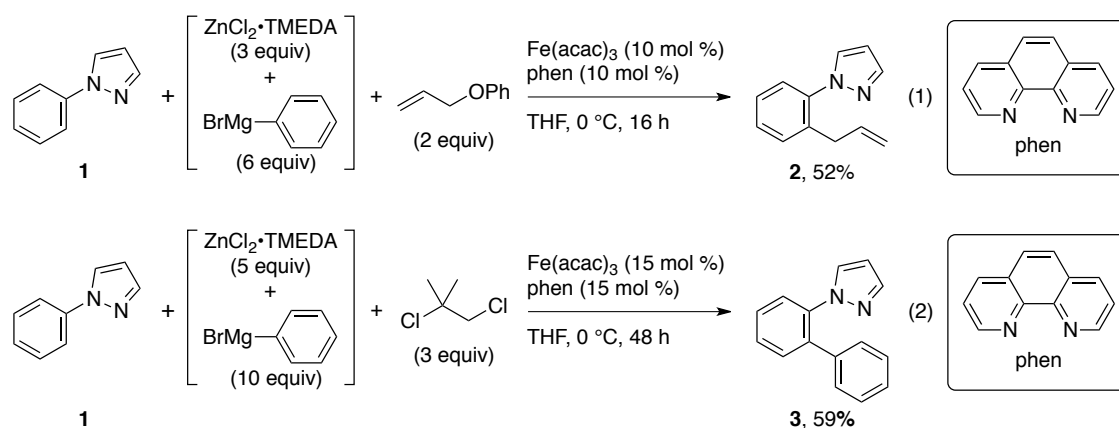
Scheme 2. Transition-Metal-Catalyzed Directed C–H Bond Allylation**coupling with allylic electrophile****addition to allene**

On the other hand, the author's group has been interested in sustainable synthetic methodologies using iron as a ubiquitous and benign catalyst and have reported a series of iron-catalyzed sp^2 and sp^3 C–H bond arylation reactions with a nucleophilic coupling partner.⁹ With these backgrounds, in this Chapter, an unprecedented iron-catalyzed *ortho*-allylation of arenes with allylic electrophile that takes place in γ -selective manner under mild conditions was developed.

3.2. Initial Finding

The investigation of this project started with unexpected discovery in the author's group when allyl phenyl ether was used instead of 1,2-dichloro-2-methylpropane for the iron-catalyzed reaction of 1-phenylpyrazole under the standard conditions which were optimized for iron-catalyzed *N*-directed aromatic C–H bond arylation with diphenylzinc reagent (eqs. 1 and 2).^{9a,10} Thus, the *ortho* C–H bond of 1-phenylpyrazole was allylated in the presence of catalytic amount of $\text{Fe}(\text{acac})_3/1,10\text{-phenanthroline}$, diphenylzinc reagent prepared from $\text{ZnCl}_2 \cdot \text{TMEDA}$ and

PhMgBr, and allyl phenyl ether (eq 1). Surprisingly, the phenylated product produced by the reaction with diphenylzinc reagent was not observed under these conditions, which is in stark contrast to the result observed when 2-phenylpyridine was used as a substrate as described in Chapter 2. In order to improve the efficiency of this allylation reaction as well as to understand the factors which control the selectivity of the reaction, i.e., allylation vs. phenylation, the model reaction in eq 1 was further investigated.

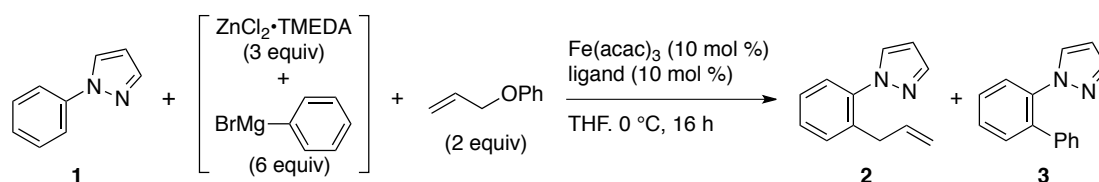


3.3. Effect of Ligand and Organozinc Reagent

The effect of ligand on the allylation reaction was initially investigated using 10 mol % of $\text{Fe}(\text{acac})_3/\text{ligand}$, 3 equiv of diphenylzinc reagent, and 2 equiv of allyl phenyl ether (Table 1). In the absence of any ligand, the *ortho*-allylation reaction did not proceed at all and the starting material was completely recovered, while a small amount of allylbenzene was formed by cross-coupling between allyl phenyl ether and diphenylzinc reagent (entry 1). The *ortho*-allylated product **2** was obtained when 2,2'-bipyridine and congeners were used, among which 4,4'-di-*t*-butyl-2,2'-bipyridine (dtbpy) showed the best performance to afford **2** in 70% at 0 °C after 16 h (entry 4).

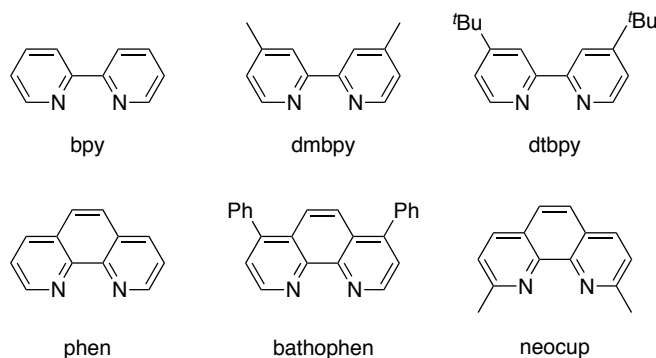
The reaction was sensitive to the substituents on the ligand as illustrated by much decreased yields obtained with 2,2'-bipyridine (bpy) and 4,4'-dimethyl-2,2'-bipyridine (dmbpy) compared with dtbpy (entries 2 and 3). While 1,10-phenanthroline afforded the product in moderate yield, bathophenanthroline and neocuproine greatly reduced the yields of the allylated product **2** (entries 5–7).

Table 1. Investigation of Ligands for the Iron-Catalyzed Allylation of 1-Phenylpyrazole with Allyl Phenyl Ether



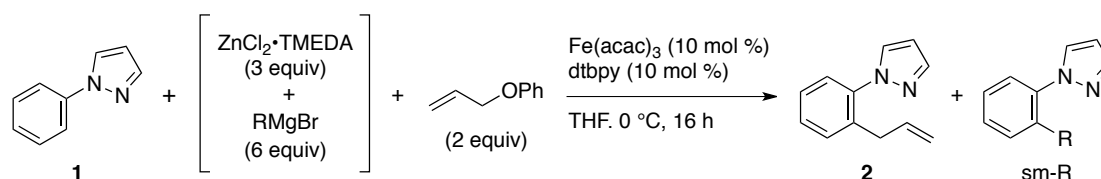
entry	ligand	yield (%) ^a						
		2	3	1	allyl-OPh	allyl-Ph	PhOH	Ph-Ph
1	none	0	0	106	217	5	19	7
2	bpy	31	0	62	127	30	80	26
3	dmbpy	26	1	65	132	21	62	19
4	dtbpy	70	3	15	85	29	136	34
5	phen	52	0	39	58	41	132	39
6	bathophen	12	0	83	27	43	161	81
7	neocup	0	0	99	189	9	18	17

^a GC yield using *n*-tridecane as an internal standard.



With identifying dtbpy as the best ligand, the effect of organozinc reagent was investigated to find that the choice of the zinc reagent largely affected the efficiency of the allylation reaction (Table 2). Thus, both the diarylzinc reagents possessing either an electron-donating or electron-withdrawing substituent dramatically decreased the yield of the allylated product **2** (entries 2–4). The use of dimesitylzinc reagent and dimethylzinc reagent completely shut off the reaction and the starting material was recovered (entries 5 and 6).

Table 2. Investigation of Organozinc Reagents for the Iron-Catalyzed Allylation of 1-Phenylpyrazole with Allyl Phenyl Ether



entry	RMgBr	yield (%) ^a						
		2	sm-R	1	allyl-OPh	allyl-R	PhOH	R-R
1	PhMgBr	70	3	15	85	29	136	34
2	4-MeOC ₆ H ₄ MgBr	19	0	77	144	79	55	8
3	4-FC ₆ H ₄ MgBr	49	0	43	49	46	68	12
4	C ₆ F ₅ MgBr	0	0	103	196	ND	8	ND
5	MesMgBr	0	0	102	193	11	ND	1
6	MeMgBr	0	0	96	171	–	21	–

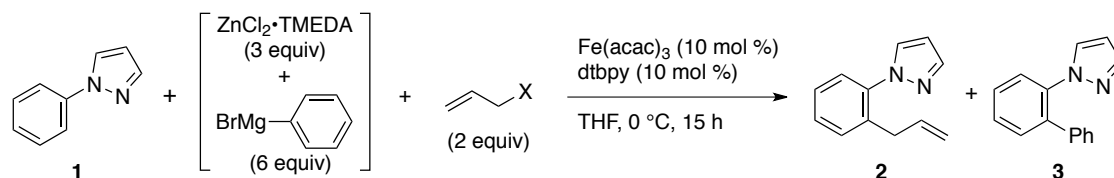
^a GC yield using *n*-tridecane as an internal standard.

3.4. Effect of Allylic Electrophiles

Significant dependence of the allylating reagent on the reaction efficiency was also found (Table 3). Thus, other allylic electrophiles than allyl phenyl ether, bearing a

poor leaving group such as thiolate, amide, and siloxy decreased the yield of allylated product and the starting material was largely recovered (entries 2–4). Allylic substrates bearing a better leaving group such as acetate, benzoate, carbonate, and chloride also lowered the reaction efficiency largely due to the competing iron-catalyzed cross-coupling between those allylic electrophiles with diphenylzinc reagent which gave allylbenzene in a large amount (entries 5–8).

Table 3. Iron-Catalyzed Allylation of *N*-(quinolin-8-yl)benzamide with Allylic Electrophiles

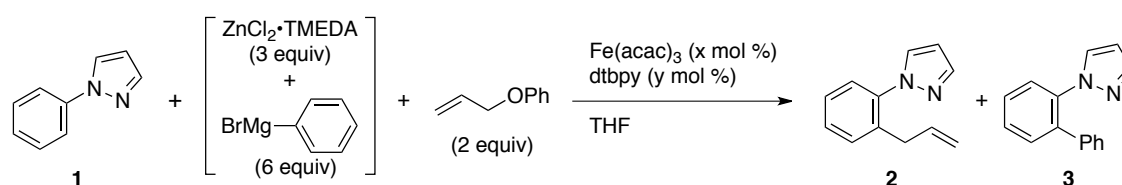


entry	electrophile	yield (%) ^a				
		2	3	1	allyl-Ph	Ph-Ph
1		65	2	27	17	13
2		20	3	73	3	14
3		2	2	77	1	7
4		14	2	67	2	15
5		19	1	78	155	19
6		6	1	74	104	24
7		1	1	106	177	10
8		1	0	95	138	26

^a GC yield using *n*-tridecane as an internal standard.

3.5. Optimization of Amount of Catalyst and Reagents

With allyl phenyl ether as the best allylating reagent, the reaction with 10 mol % of Fe(acac)₃/dtbpy was monitored (Table 4). Although the yield of the allylated product **2** increased to 80% after 48 h, the reaction stopped at this stage and the yield was not further increased (81% yield after 88 h) (entry 1). The reaction did not further proceed even by the addition of extra 10 mol % of Fe(acac)₃/dtbpy. Neither increased ligand ratio nor catalyst loading improved the reaction yield (entries 2 and 3). The reaction at rt was much less effective (entry 4).

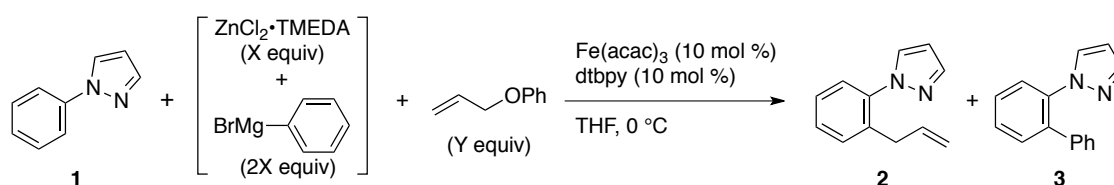
Table 4.

entry	temp	x/y	time	yield (%) ^a						
				2	3	1	allyl-OPh	allyl-Ph	Ph-OH	Ph-Ph
1	0 °C	10/10	15 h	65	2	27	97	17	67	13
			48 h	80	3	12	46	43	115	16
			88 h	81	3	11	46	43	116	15
		+ 10/10	+ 10 h	80	3	7	2	77	202	21
2	0 °C	10/20	15 h	59	2	23	83	28	97	14
			48 h	70	2	11	23	64	128	18
			96 h	77	2	14	7	90	219	20
3	0 °C	20/20	15 h	67	2	19	52	37	110	28
			24 h	70	2	15	34	47	136	29
4	25 °C	10/10	15 h	27	3	50	74	36	73	24
			48 h	25	3	39	21	62	137	30

^a GC yield using *n*-tridecane as an internal standard.

A brief examination of the amount of diphenylzinc reagent and allyl phenyl ether revealed that the use of 3 equiv of diphenylzinc reagent and 2 equiv of allyl phenyl ether was optimal (Table 5, entries 1–6). The use of monophenylzinc reagent instead of diphenylzinc reagent completely shut off the reaction (entry 7).

Table 5. Iron-Catalyzed Allylation of 1-Phenylpyrazole with Allyl Phenyl Ether and Phenylzinc reagent



entry	X	Y	time	yield (%) ^a						
				2	3	1	allyl–OPh	allyl–Ph	Ph–OH	Ph–Ph
1	2	2	15 h	56	2	33	104	16	89	10
			48 h	69	2	23	63	42	135	10
2	3	2	15 h	65	2	26	96	16	88	11
			48 h	80	2	10	41	46	159	13
3	5	2	15 h	58	2	35	112	12	52	16
			48 h	74	3	11	53	34	110	22
			96 h	77	3	6	8	68	208	31
4	3	1.2	15 h	64	3	27	29	9	72	13
			48 h	62	3	11	2	16	110	17
			96 h	58	3	10	1	17	137	20
5	3	1.5	15 h	58	2	28	56	13	68	12
			48 h	66	3	16	12	35	113	15
			96 h	63	3	13	1	40	149	16
6	3	3	15 h	65	2	34	202	23	99	13
			48 h	71	2	16	116	78	182	19
			96 h	80	2	20	114	108	232	22
7 ^b	3	2	15 h	0	0	106	229	0	12	4

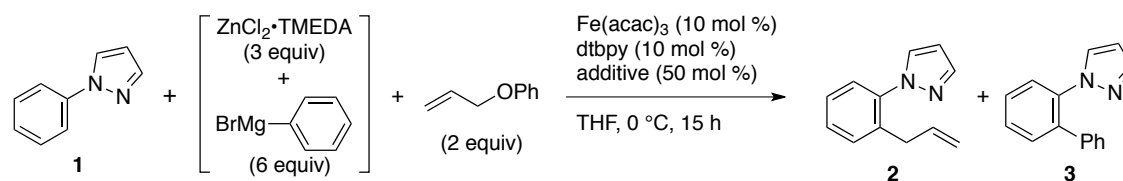
^a GC yield using *n*-tridecane as an internal standard.

^b PhZnCl·TMEDA was used instead of Ph₂Zn·TMEDA

3.6. Possible Catalyst Deactivation by Phenoxide

The fact that the reaction stopped after 48 h in Table 4 suggested a possibility of catalyst deactivation caused by phenoxide ion because the amount of phenol increased gradually with time, which should be generated by the allylation reaction as well as the cross-coupling between allyl phenyl ether and diphenylzinc reagent. With the assumption of catalyst deactivation by phenoxide, the effect of Lewis acids or oxophilic reagents which would capture it was examined (Table 6). However, All the reagents examined such as aluminum, boron, scandium, and silicon failed to improve the yield of the allylated product **2**.

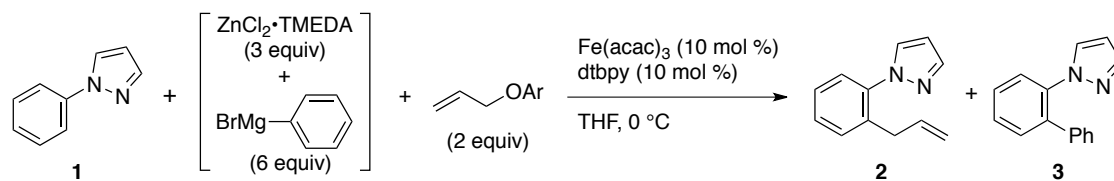
Table 6. Effect of Additive on Iron-Catalyzed Allylation of 1-Phenylpyrazole with Allyl Phenyl Ether



entry	additive	yield (%) ^a						
		2	3	1	allyl-OPh	allyl-Ph	PhOH	Ph-Ph
1	none	65	2	27	97	17	67	13
2	AlF_3	61	2	31	108	20	103	10
3	$\text{Al(O}^i\text{Pr)}_3$	2	6	86	191	18	108	55
4	B(OEt)_3	49	1	38	134	11	81	10
5	$\text{B(O}^i\text{Pr)}_3$	57	2	35	111	16	93	10
6	$\text{B(C}_6\text{F}_5)_3$	45	2	46	135	11	74	9
7	B_2O_3	54	2	40	121	16	93	10
8	Sc(OTf)_3	33	1	67	162	12	62	8
9	$\text{-(Si(CH}_3\text{)}_2\text{-O-)}_4$	42	3	46	53	62	113	25

^a GC yield using *n*-tridecane as an internal standard.

Allyl aryl ethers bearing bulky substituents which might prevent their coordination to the iron center were next examined (Table 7, entries 1–5). As expected, the reaction rate increased at the early stage of the reaction in some cases. However, after 48 h all the allylating reagents showed similar yields around 80%. Allyl trichlorophenyl ether, which was expected to have less coordinating ability, was much less effective due to the fast cross coupling with diphenylzinc reagent (entry 6). No significant effect was observed with allyl aryl ethers having a methoxy and trifluoromethyl substituent (entries 7 and 8).

Table 7. Iron-Catalyzed Allylation of 1-Phenylpyrazole with Allyl Aryl Ethers

entry	Ar	time	yield (%) ^a				
			2	3	1	allyl-Ph	Ph-Ph
1	Ph	15 h	65	2	27	17	13
		24 h	72	2	18	26	14
		48 h	80	3	12	43	16
2		15 h	77	2	24	22	14
		24 h	79	2	16	32	15
		48 h	82	2	9	59	15
3		15 h	79	1	19	20	20
		24 h	82	2	12	30	19
		48 h	83	1	6	54	18
4		15 h	67	1	22	16	13
		24 h	76	1	15	25	15
		48 h	84	1	9	45	17
5		15 h	69	1	21	14	14
		24 h	80	2	15	23	15
		42 h	78	1	9	38	12
6		15 h	46	2	46	118	19
		24 h	46	2	42	133	17
7		16 h	62	2	23	16	20
8		16 h	59	2	29	29	18

^a GC yield using *n*-tridecane as an internal standard.

3.7. Scope of the Reaction

Various 1-arylpyrazoles and congeners could be allylated with allyl phenyl ether under the optimized conditions (Table 8). All the reactions gave the monoallylated product selectively, and the diallylated product was observed in a trace amount (< 2%). This selectivity agrees with the poor reactivity of an *ortho*-substituted substrate (entry 7), probably due to steric interactions disturbing the formation of a planar metallacycle. Isomerization of the allylated product to the more thermodynamically stable styrene derivative, was largely suppressed (< 5%), while prolonged reaction time led to an increase in the amount of the styrene derivative for some cases. The phenylated product was obtained in a trace amount, except for electron-deficient substrates and 2-naphthylpyrazole (entries 5, 8, and 10) where it was obtained in 5–7%.

While the reaction of substrates bearing an electron-donating group at the para position proceeded smoothly (entries 2–4), para-substituted substrates bearing an electron-withdrawing group were less reactive (entry 5). The allylation of meta-substituted substrates took place selectively at the less hindered position with good yields (entries 6 and 8). A substrate where the pyrazole is substituted with a methyl group reacted more efficiently than the one substituted with an ester group (entries 9 and 10). The ester group was tolerated under the reaction conditions, and the unreacted substrate was recovered (entry 10). An indazolyl group also acted as an excellent directing group (entry 11).

Table 8. Iron-Catalyzed Allylation of 1-Arylpyrazoles with Allyl Phenyl Ether^a

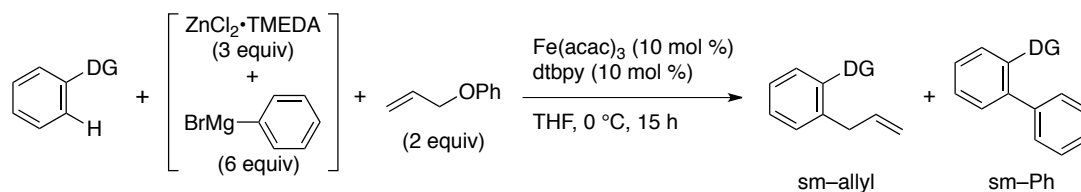
entry	substrate	product	time	yield (%) ^b
1 ^c			48 h	80 (X = H)
2			36 h	67 (X = Me)
3			18 h	60 (X = OMe)
4			48 h	64 (X = NMe ₂)
5			15 h	23 (X = F) ^d
6 ^e			48 h	65
7			48 h	9 ^f
8			24 h	54
9			24 h	71 (X = Me)
10			48 h	32 (X = CO ₂ Et) ^d
11			36 h	72

^a Conditions: substrate (0.4 mmol), Fe(acac)₃/dtbpy (10 mol %), allyl phenyl ether (2 equiv), and Ph₂Zn•TMEDA (3 equiv). ^b Isolated yield. ^c 0.8 mmol scale.

^d Containing a trace amount of phenylated product.

^e ZnBr₂•TMEDA was used instead of ZnCl₂•TMEDA. ^f Determined by ¹H NMR.

Other directing groups such as triazole, pyridine, imine, and *N*-methanamide were less effective for the *ortho*-allylation, and resulted in the recovery of the starting material or afforded mainly the phenylated product (Table 9). The results highlight the importance of the choice of directing group for the selective allylation. Under these conditions, substituted allyl ethers did not participate in the allylation reaction and the arylpyrazole substrate was either recovered or partially phenylated.

Table 9. Iron-Catalyzed Allylation of Arenes Possessing Various Directing Groups

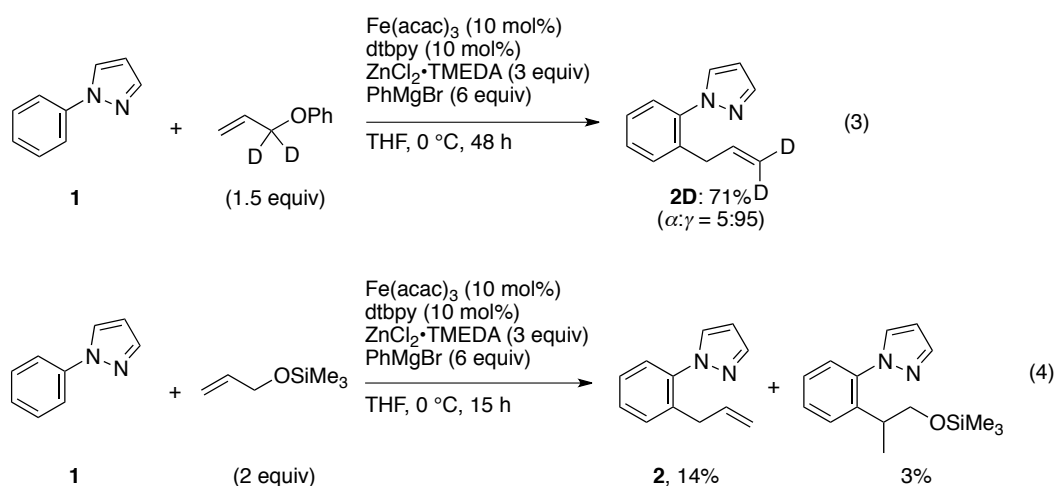
entry	substrate	yield (%)		
		sm-allyl	sm-Ph	recov.
1 ^a		65	2	27
2 ^b		0	0	99
3 ^b		17	42 + 4 (mono + di)	22
4 ^b	 Ar = 4-MeOC ₆ H ₄	8	80 (<i>E</i> : <i>Z</i> = 3:1)	9
5 ^b		13	18	64

^a GC yield using *n*-tridecane as an internal standard.^b ¹H NMR yield using 1,1,2,2-tetrachloroethane as an internal standard.

3.8. Mechanistic Considerations

In order to gain mechanistic insight into the allylation step, 1-phenylpyrazole was reacted with 1,1-dideuterioallyl phenyl ether (eq. 3). The two deuterium atoms were found selectively at the terminal vinylic positions, which suggests that the allylation took place with high γ selectivity and excludes the involvement of π -allyl iron intermediate during the catalytic cycle. When allyloxytrimethylsilane was used as an

allylating reagent, a small amount of alkylation product was observed suggesting that the reaction proceeds through the insertion of the alkene with the necessary presence of a β leaving group (eq. 4). This conjecture is supported by the complete lack of reactivity of benzyl phenyl ether and homoallyl phenyl ether.



3.9. A Possible Catalytic Cycle

A possible catalytic cycle of the allylation reaction is shown in Figure 1. Active iron species is first generated from the catalyst precursor and organozinc reagent. The ortho C–H bond cleavage takes place to form the iron metallacyclic intermediate together with elimination of benzene. A sequence of olefin insertion of allyl phenyl ether and β -phenoxy elimination affords the allylated product. The subsequent transmetallation completes the catalytic cycle.

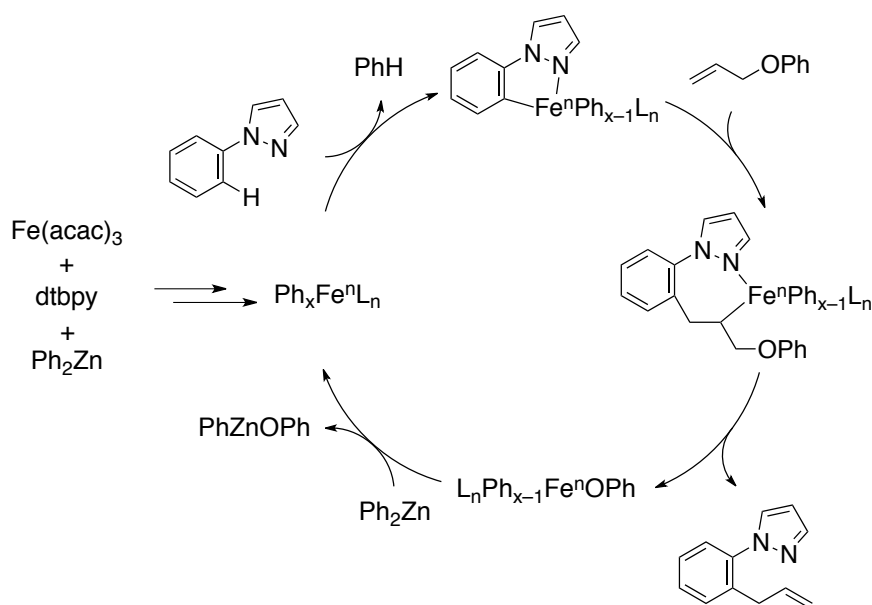


Figure 1. A Possible Catalytic Cycle

3.10. Summary

In conclusion, an iron-catalyzed *ortho*-allylation of 1-arylpyrazole and congeners with allyl phenyl ether under mild reaction conditions was developed. The reaction proceeds smoothly at 0 °C to afford allylated pyrazole derivatives with high γ selectivity and without overallylation and isomerization of the double bond to styrene derivatives. Notably, the reaction for the first time demonstrated that iron-catalyzed directed C-H bond activation can be followed by coupling with an electrophile.

3.11. Experimental Part

General. All reactions dealing with air- or moisture-sensitive compounds were carried out in a flame-dried, sealed Schlenk reaction tube under an atmosphere of nitrogen or argon. The water content of the solvent was confirmed with a Karl-Fischer Moisture Titrator (CA-21, Mitsubishi Chemical Analytech Company) to be less than 30 ppm. Analytical thin-layer chromatography was performed on glass plates coated with 0.25 mm 230–400 mesh silica gel containing a fluorescent indicator (Merck). Flash silica gel column chromatography was performed on silica gel 60N (Kanto, spherical and neutral, 140–325 mesh) as described by Still.¹¹ Gas-liquid chromatographic (GLC) analysis was performed on a Shimadzu GC-14B or CG-2025 machine equipped with glass capillary column HR-1 (0.25-mm i.d. x 25 m). Gel permeation column chromatography was performed on a Japan Analytical Industry LC-908 (eluent: chloroform or toluene) with JAIGEL 1H and 2H polystyrene columns. NMR spectra were measured on a JEOL ECA-500 or ECX-400 spectrometer and reported in parts per million from an internal standard, tetramethylsilane (0.0 ppm) and CDCl₃ (77.0 ppm), respectively. Methyl, methylene, and methyne signals in ¹³C NMR spectra were assigned by DEPT spectra. Mass spectra were acquired by Shimadzu Parvum 2 gas chromatograph mass spectrometer (GC-MS) or by atmospheric pressure ionization (APCI) or electrospray ionization (ESI) using a time-of-flight mass analyzer on JEOL JMS-T100LC (AccuTOF) spectrometer with a calibration standard of polyethylene glycol (MW 400).

Materials. Unless otherwise noted, materials were purchased from Tokyo Kasei Co., Aldrich Inc., and other commercial suppliers and used as received. Anhydrous THF and diethyl ether (stabilizer-free) were purchased from WAKO Pure Chemical and purified

by a solvent purification system (GlassContour) equipped with columns of activated alumina and supported copper catalyst (Q-5) prior to use.¹² Fe(acac)₃ (99.9% metal basis) and 4,4'-di-*tert*-butyl-2,2'-bipyridyl were purchased from Aldrich Inc. and 1-phenylpyrazole and allyl phenyl ether were purchased from Tokyo Kasei Co., respectively, and used as received. Grignard reagents were purchased from Aldrich Inc. or prepared from the corresponding halides and magnesium turnings in anhydrous THF, and titrated prior to use. ZnCl₂•TMEDA was prepared according to the literature.¹³

Preparation of Substrates

The following compounds were prepared according to the literature procedures, and purified by column chromatography.

1-(4-Methylphenyl)-1*H*-pyrazole¹⁴

1-(4-Methoxyphenyl)-1*H*-pyrazole¹⁴

N,N-Dimethyl-4-(1*H*-pyrazol-1-yl)aniline¹⁴

1-(4-Fluorophenyl)-1*H*-pyrazole¹⁴

1-(3-Methylphenyl)-1*H*-pyrazole¹⁴

1-(Naphthalen-2-yl)-1*H*-pyrazole¹⁴

1-(2-Methylphenyl)-1*H*-pyrazole¹⁵

4-Methyl-1-phenyl-1*H*-pyrazole¹⁴

Ethyl 1-phenyl-1*H*-pyrazole-4-carboxylate¹⁴

1-Phenyl-1*H*-indazole¹⁶

((1,1-Dideuterioallyl)oxy)benzene¹⁷

Spectral data for the following compounds showed good agreement with the literature

data:

1-(4-Methylphenyl)-1*H*-pyrazole¹⁸

1-(4-Methoxyphenyl)-1*H*-pyrazole¹⁹

N,N-Dimethyl-4-(1*H*-pyrazol-1-yl)aniline²⁰

1-(4-Fluorophenyl)-1*H*-pyrazole¹⁹

1-(3-Methylphenyl)-1*H*-pyrazole¹⁹

1-(Naphthalen-2-yl)-1*H*-pyrazole²¹

1-(2-Methylphenyl)-1*H*-pyrazole²⁰

4-Methyl-1-phenyl-1*H*-pyrazole²²

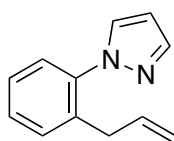
Ethyl 1-phenyl-1*H*-pyrazole-4-carboxylate²³

1-Phenyl-1*H*-indazole¹⁶

((1,1-Dideuterioallyl)oxy)benzene¹⁷

General Procedure for Iron-Catalyzed *ortho*-Allylation with Allyl Phenyl Ether

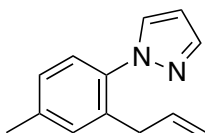
1-(2-Allylphenyl)-1*H*-pyrazole (Table 1, entry 1):



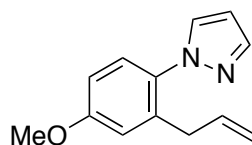
1-Phenyl-1*H*-pyrazole (116 mg, 0.8 mmol) and ZnCl₂•TMEDA (606 mg, 2.4 mmol) were placed in an oven-dried Schlenk flask under argon. A solution of PhMgBr in THF (1.09 M, 4.40 mL, 4.8 mmol) was added dropwise to this mixture at 0 °C. After stirring for 3 min, allyl phenyl ether (220 μL, 1.6 mmol) and a solution of Fe(acac)₃/4,4'-di-*tert*-butyl-2,2'-bipyridyl in THF (1.0 mL, 0.08 M, 80 μmol) were sequentially added. The reaction mixture was stirred at 0 °C for 48 h, and was diluted with Et₂O followed

by the addition of a saturated aqueous solution of Rochelle's salt. After extraction with ethyl acetate, the combined organic layers were filtered through a pad of Florisil, and concentrated under reduced pressure. The crude product was purified by column chromatography on silica gel (hexane/AcOEt/NEt₃ = 99/0.5/0.5) and GPC using toluene as an eluent to afford the title compound as a colorless oil (118 mg, 80%). The spectral data were in accordance with those reported in the literature.²⁴

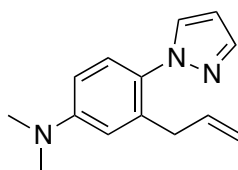
1-(2-Allyl-4-methylphenyl)-1*H*-pyrazole (Table 1, entry 2):



The general procedure was applied to 1-(4-methylphenyl)-1*H*-pyrazole (63.2 mg, 0.40 mmol) using PhMgBr in THF (0.96 M, 2.49 mL, 2.4 mmol), and the reaction mixture was stirred at 0 °C for 36 h. The crude product was purified by column chromatography on silica gel (hexane/AcOEt/NEt₃ = 98/1/1) and GPC using toluene as an eluent to afford the title compound as a colorless oil (53.0 mg, 67%); ¹H NMR (500 MHz, CDCl₃): δ 7.70 (d, 1.7 Hz, 1H), 7.56 (d, 2.3 Hz, 1H), 7.21 (d, 8.1 Hz, 1H), 7.13–7.09 (m, 2H), 6.40 (t, 1.7 Hz, 1H), 5.87–5.79 (m, 1H), 5.00 (dd, *J* = 9.7, 1.2 Hz, 1H), 4.93 (dd, *J* = 16.9, 1.4 Hz, 1H), 3.27 (d, *J* = 6.3 Hz, 2H), 2.39 (s, 3H); ¹³C NMR (125 MHz, CDCl₃): δ 140.2, 138.5, 137.3, 136.6, 135.4, 131.1, 130.8, 127.6, 126.3, 116.1, 106.0, 35.5, 21.1; GC-MS (EI) *m/z* (relative intensity): 198 (M⁺, 12), 183 (100), 168 (19), 144 (19), 130 (41), 115 (19); HRMS (APCI) Calcd for C₁₃H₁₅N₂⁺ [M+H]⁺ 199.1235, found, 199.1241.

1-(2-Allyl-4-methoxyphenyl)-1*H*-pyrazole (Table 1, entry 3):

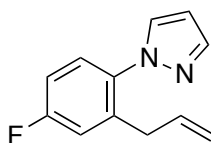
The general procedure was applied to 1-(4-methoxyphenyl)-1*H*-pyrazole (69.7 mg, 0.40 mmol) using PhMgBr in THF (0.75 M, 3.20 mL, 2.4 mmol), and the reaction mixture was stirred at 0 °C for 18 h. The crude product was purified by column chromatography on silica gel (hexane/AcOEt/NEt₃ = 90.5/9/0.5) and GPC using toluene as an eluent to afford the title compound as a colorless oil (51.1 mg, 60%); ¹H NMR (500 MHz, CDCl₃): δ 7.69 (d, 1.2 Hz, 1H), 7.53 (d, 2.3 Hz, 1H), 7.24 (d, 8.6 Hz, 1H), 6.84–6.80 (m, 2H), 6.39 (t, 2.0 Hz, 1H), 5.86–5.77 (m, 1H), 5.01 (dd, *J* = 9.8, 1.2 Hz, 1H), 4.94 (dd, *J* = 17.2, 1.7 Hz, 1H), 3.83 (s, 3H), 3.24 (d, *J* = 6.3 Hz, 2H); ¹³C NMR (125 MHz, CDCl₃): δ 159.5, 140.1, 137.6, 136.2, 133.0, 131.0, 127.8, 116.4, 115.4, 111.9, 105.9, 55.5, 35.6; GC-MS (EI) *m/z* (relative intensity): 214 (*M*⁺, 16), 199 (100), 146 (47); HRMS (APCI) Calcd for C₁₃H₁₅N₂O⁺ [*M*+H]⁺ 215.1184, found, 215.1175.

3-Allyl-*N,N*-dimethyl-4-(1*H*-pyrazol-1-yl)aniline (Table 1, entry 4):

The general procedure was applied to *N,N*-Dimethyl-4-(1*H*-pyrazol-1-yl)aniline (74.7 mg, 0.40 mmol) using PhMgBr in THF (1.01 M, 2.38 mL, 2.4 mmol), and the reaction mixture was stirred at 0 °C for 48 h. The crude product was purified by column chromatography on silica gel (hexane/AcOEt/NEt₃ = 90.5/9/0.5) and GPC using toluene

as an eluent to afford the title compound as a pale yellow oil (58.2 mg, 64%); ^1H NMR (500 MHz, CDCl_3): δ 7.67 (d, 1.7 Hz, 1H), 7.51 (d, 2.3 Hz, 1H), 7.18 (d, 8.1 Hz, 1H), 6.62–6.59 (m, 2H), 6.37 (t, 2.0 Hz, 1H), 5.86–5.80 (m, 1H), 4.98 (dd, J = 10.3, 1.2 Hz, 1H), 4.93 (dd, J = 17.2, 1.7 Hz, 1H), 3.22 (d, J = 6.3 Hz, 2H), 2.99 (s, 6H); ^{13}C NMR (125 MHz, CDCl_3): δ 150.6, 139.8, 136.9, 136.7, 131.2, 129.4, 127.4, 115.9, 113.2, 110.3, 105.5, 40.5, 35.9; GC-MS (EI) m/z (relative intensity): 227 (M^+ , 48), 212 (100), 199 (29), 173 (17), 159 (33); HRMS (APCI) Calcd for $\text{C}_{14}\text{H}_{18}\text{N}_3^+$ [$\text{M}+\text{H}$] $^+$ 228.1501, found, 228.1505.

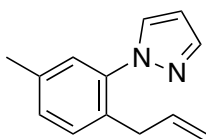
1-(2-Allyl-4-fluorophenyl)-1H-pyrazole (Table 1, entry 5):



The general procedure was applied to 1-(4-fluorophenyl)-1H-pyrazole (65.1 mg, 0.40 mmol) using PhMgBr in THF (1.01 M, 2.38 mL, 2.4 mmol) and the reaction mixture was stirred at 0 °C for 15 h. The crude product was purified by column chromatography on silica gel (hexane/ $\text{AcOEt}/\text{NEt}_3$ = 98/1/1) and GPC using toluene as an eluent to afford the title compound as a colorless oil (19.7 mg, 23%). A phenylated product was obtained in 1% yield as an inseparable mixture with the desired product; ^1H NMR (500 MHz, CDCl_3): δ 7.71 (d, 1.7 Hz, 1H), 7.56 (d, 2.3 Hz, 1H), 7.31 (dd, 8.6, 5.2 Hz, 1H), 7.04 (dd, 9.2, 2.9 Hz, 1H), 6.99 (td, 8.1, 2.9 Hz, 1H), 6.42 (t, 2.0 Hz, 1H), 5.85–5.77 (m, 1H), 5.06 (dd, J = 10.0, 1.4 Hz, 1H), 4.97 (dd, J = 17.2, 1.7 Hz, 1H), 3.27 (d, J = 6.9 Hz, 2H); ^{13}C NMR (125 MHz, CDCl_3): δ 162.3 ($^1J_{\text{C-F}}$ = 246.8 Hz), 140.5, 138.6 ($^3J_{\text{C-F}}$ = 8.3 Hz), 135.8, 135.6, 130.9, 128.3 ($^3J_{\text{C-F}}$ = 9.5 Hz), 117.02, 116.98 ($^2J_{\text{C-F}}$ = 22.6 Hz), 113.8

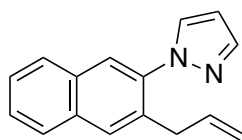
($^2J_{\text{C-F}} = 22.7$ Hz), 106.3, 35.4; GC-MS (EI) m/z (relative intensity): 202 (M^+ , 13), 187 (100), 148 (29), 134 (55); HRMS (APCI) Calcd for $\text{C}_{12}\text{H}_{12}\text{FN}_2^+$ [$M+H$] $^+$ 203.0985, found, 203.0986.

1-(2-Allyl-5-methylphenyl)-1*H*-pyrazole (Table 1, entry 6):



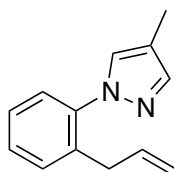
The general procedure was applied to 1-(3-methylphenyl)-1*H*-pyrazole (63.4 mg, 0.40 mmol) using PhMgBr in THF (1.01 M, 2.38 mL, 2.4 mmol) and $\text{ZnBr}_2 \cdot \text{TMEDA}$ (410 mg, 1.20 mmol), and the reaction mixture was stirred at 0 °C for 48 h. The crude product was purified by column chromatography on silica gel (hexane/AcOEt/ NEt_3 = 98/1/1) and GPC using toluene as an eluent to afford the title compound as a pale yellow oil (51.7 mg, 65%); ^1H NMR (400 MHz, CDCl_3): δ 7.70 (d, 1.4 Hz, 1H), 7.59 (d, 2.3 Hz, 1H), 7.21 (d, 8.1 Hz, 1H), 7.22–7.16 (m, 3H), 6.41 (t, 2.5 Hz, 1H), 5.88–5.78 (m, 1H), 5.00 (ddd, $J = 10.1, 3.0, 1.6$ Hz, 1H), 4.93 (ddd, $J = 17.0, 3.6, 1.7$ Hz, 1H), 3.28 (d, $J = 6.4$ Hz, 2H), 2.36 (s, 3H); ^{13}C NMR (100 MHz, CDCl_3): δ 140.2, 139.4, 136.9, 136.8, 132.3, 130.7, 130.4, 129.3, 127.1, 116.0, 106.0, 35.2, 20.7; GC-MS (EI) m/z (relative intensity): 198 (M^+ , 9), 183 (100), 168 (18), 144 (17), 128 (21), 115 (35), 91 (19), 77 (30); HRMS (APCI) Calcd for $\text{C}_{13}\text{H}_{15}\text{N}_2^+$ [$M+H$] $^+$ 199.1235, found, 199.1238.

1-(3-Allylnaphthalen-2-yl)-1*H*-pyrazole (Table 1, entry 8):



The general procedure was applied to 1-(naphthalen-2-yl)-1*H*-pyrazole (77.7 mg, 0.40 mmol) using PhMgBr in THF (1.15 M, 2.09 mL, 2.4 mmol), and the reaction mixture was stirred at 0 °C for 24 h. The crude product was purified by column chromatography on silica gel (hexane/AcOEt/NEt₃ = 98/1/1) and GPC using toluene as an eluent to afford the title compound as a pale yellow oil (50.3 mg, 54%); ¹H NMR (400 MHz, CDCl₃): δ 7.85–7.76 (m, 5H), 7.68 (d, 2.3 Hz, 1H), 7.54–7.46 (m, 2H), 6.46 (t, 2.3 Hz, 1H), 5.93–5.82 (m, 1H), 5.03 (ddd, *J* = 10.1, 2.7, 1.4 Hz, 1H), 4.96 (ddd, *J* = 17.2, 3.2, 1.7 Hz, 1H), 3.50 (d, *J* = 6.4 Hz, 2H); ¹³C NMR (100 MHz, CDCl₃): δ 140.5, 138.2, 136.3, 134.0, 133.1, 131.9, 131.2, 129.3, 127.7, 127.3, 126.8, 126.3, 125.1, 116.4, 106.2, 35.9; GC-MS (EI) *m/z* (relative intensity): 235 (M⁺, 2), 234 (13), 220 (17), 166 (37); HRMS (APCI) Calcd for C₁₆H₁₅N₂⁺ [M+H]⁺ 235.1235, found, 235.1229.

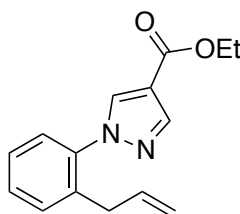
1-(2-Allylphenyl)-4-methyl-1*H*-pyrazole (Table 1, entry 9):



The general procedure was applied to 4-methyl-1-phenyl-1*H*-pyrazole (62.8 mg, 0.40 mmol) using PhMgBr in THF (0.96 M, 2.50 mL, 2.4 mmol), and the reaction mixture was stirred at 0 °C for 24 h. The crude product was purified by column chromatography on silica gel (hexane/AcOEt/NEt₃ = 98/1/1) and GPC using toluene as an eluent to afford the title compound as a colorless oil (56.2 mg, 71%); ¹H NMR (500 MHz,

CDCl₃): δ 7.52 (s, 1H), 7.37 (s, 1H), 7.36–7.26 (m, 5H), 5.90–5.81 (m, 1H), 5.03 (dd, J = 10.3, 1.7 Hz, 1H), 4.95 (ddd, J = 17.2, 3.4, 1.7 Hz, 1H), 3.35 (d, J = 6.3 Hz, 2H), 2.16 (s, 3H); ¹³C NMR (125 MHz, CDCl₃): δ 141.0, 139.8, 136.6, 135.4, 130.5, 129.4, 128.2, 126.9, 126.3, 116.6, 116.2, 35.5, 8.8; GC-MS (EI) m/z (relative intensity): 198 (M⁺, 15), 183 (100), 130 (20), 116 (43); HRMS (APCI) Calcd for C₁₃H₁₅N₂⁺ [M+H]⁺ 199.1235, found, 199.1227.

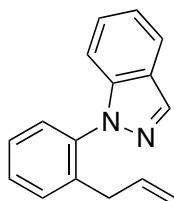
Ethyl 1-(2-allylphenyl)-1*H*-pyrazole-4-carboxylate (Table 1, entry 10):



The general procedure was applied to ethyl 1-phenyl-1*H*-pyrazole-4-carboxylate (86.5 mg, 0.40 mmol) using PhMgBr in THF (1.01 M, 2.38 mL, 2.4 mmol), and the reaction mixture was stirred at 0 °C for 48 h. The crude product was purified by column chromatography on silica gel (hexane/AcOEt/NEt₃ = 90.5/9/0.5) and GPC using CHCl₃ as an eluent to afford the title compound as a pale yellow oil (36.5 mg, 32%). A phenylated product was obtained in 3% yield as an inseparable mixture with the desired product; ¹H NMR (400 MHz, CDCl₃): δ 8.10 (s, 1H), 8.09 (s, 1H), 7.43–7.28 (m, 4H), 5.88–5.77 (m, 1H), 5.03 (dd, J = 10.1, 1.4 Hz, 1H), 4.92 (ddd, J = 17.0, 1.8 Hz, 1H), 4.33 (q, J = 7.0 Hz, 2H), 3.33 (d, J = 6.4 Hz, 2H), 1.37 (t, 7.1 Hz, 3H); ¹³C NMR (100 MHz, CDCl₃): δ 163.0, 141.6, 138.8, 136.0, 135.7, 134.2, 130.8, 129.4, 127.2, 126.4, 116.5, 115.9, 60.3, 35.5, 14.4; GC-MS (EI) m/z (relative intensity): 256 (M⁺, 10), 241 (82), 227 (22), 213 (62), 154 (25), 130 (36), 116 (100), 91 (20), 77 (24); HRMS (APCI)

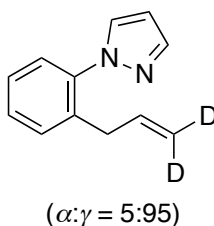
Calcd for $C_{15}H_{17}N_2O_2^+$ $[M+H]^+$ 257.1290, found, 257.1299.

1-(2-Allylphenyl)-1*H*-indazole (Table 1, entry 11):



The general procedure was applied to 1-phenyl-1*H*-indazole (77.6 mg, 0.40 mmol) using PhMgBr in THF (0.96 M, 2.49 mL, 2.4 mmol), and the reaction mixture was stirred at 0 °C for 36 h. The crude product was purified by column chromatography on silica gel (hexane/AcOEt/NEt₃ = 98/1/1) and GPC using toluene as an eluent to afford the title compound as a pale yellow oil (67.0 mg, 72%); ¹H NMR (500 MHz, CDCl₃): δ 8.20 (s, 1H), 7.80 (d, 8.0 Hz, 1H), 7.46–7.43 (m, 2H), 7.39–7.34 (m, 3H), 7.25–7.219 (m, 2H), 5.76–5.68 (m, 1H), 4.89–4.81 (m, 2H), 3.24 (d, *J* = 6.9 Hz, 2H); ¹³C NMR (125 MHz, CDCl₃): δ 140.6, 137.9, 137.8, 136.1, 134.5, 130.7, 129.0, 127.7, 127.1, 126.8, 124.0, 121.05, 120.95, 116.2, 110.1, 35.6; GC-MS (EI) *m/z* (relative intensity): 234 (*M*⁺, 25), 219 (100), 204 (16), 180 (14), 130 (22), 116 (28), 104 (19), 89 (13), 77 (22); HRMS (APCI) Calcd for $C_{16}H_{15}N_2^+$ $[M+H]^+$ 235.1235, found, 235.1237.

1-(2-(3,3-Dideuterioallyl)phenyl)-1*H*-pyrazole (eq 3):



The general procedure was applied to 1-phenyl-1*H*-pyrazole (58.2 mg, 0.40 mmol) and

Chapter 3

((1,1-dideuterioallyl)oxy)benzene (82 mg, 0.60 mmol) using PhMgBr in THF (1.01 M, 2.38 mL, 2.4 mmol), and the reaction mixture was stirred at 0 °C for 48 h. The crude mixture was analyzed by GC using *n*-tridecane as an internal standard to determine the yield and was analyzed by ^1H NMR to determine the D ratio.

References

- ¹ (a) Williams, R. M.; Stocking, E. M.; Sanz-Cervera, J. F. *Top. Curr. Chem.* **2000**, *209*, 97–173. (b) Koeduka, T.; Fridman, E.; Gang, D. R.; Vassão, D. G.; Jackson, B. L.; Kishi, C. M.; Orlova, I.; Spassova, S. M.; Lewis, N. G.; Noel, J. P.; Baiga, T. J.; Dudareva, N.; Pichersky, E. *Proc. Natl. Acad. Sci. USA* **2006**, *103*, 10128–10133. (c) Davin, L. B.; Jourdes, M.; Patten, A. M.; Kim, K.-W.; Vassão, D. G.; Lewis, N. G. *Nat. Prod. Rep.* **2008**, *25*, 1015–1090.
- ² (a) Magid, R. M. *Tetrahedron* **1980**, *36*, 1901–1930. (b) Ohmiya, H.; Makida, Y.; Tanaka, T.; Sawamura, M. *J. Am. Chem. Soc.* **2008**, *130*, 17276–17277. (c) Li, D.; Tanaka, T.; Ohmiya, H.; Sawamura, M. *Org. Lett.* **2010**, *12*, 2438–2440.
- ³ (a) Rueping, M.; Nachtsheim, B. J. *Beilstein J. Org. Chem.* **2010**, *6* (6), DOI: 10.3762/bjoc.6.6. (b) Poulsen, T. B.; Jørgensen, K. A. *Chem. Rev.* **2008**, *108*, 2903–2915. (c) Kodomari, M.; Nawa, S.; Miyoshi, T. *J. Chem. Soc., Chem. Commun.* **1995**, 1895–1896.
- ⁴ Dyker, G. (Ed.). *Handbook of C–H Transformations: Applications in Organic Synthesis*; Wiley-VCH: Weinheim, 2005.
- ⁵ (a) Oi, S.; Tanaka, Y.; Inoue, Y. *Organometallics* **2006**, *25*, 4773–4778. (b) Cheng, K.; Yao, B.; Zhao, J.; Zhang, Y. *Org. Lett.* **2008**, *10*, 5309–5312. (c) Kuninobu, Y.; Yu, P.; Takai, K. *Chem. Commun.* **2011**, *47*, 10791–10793. (d) Wang, H.; Schröder, N.; Glorius, F. *Angew. Chem. Int. Ed.* **2013**, *52*, 5386–5389. (e) Aihara, Y.; Chatani, N. *J. Am. Chem. Soc.* **2013**, *135*, 5308–5311.
- ⁶ (a) Zhang, Y. J.; Skucas, E.; Krische, M. J. *Org. Lett.* **2009**, *11*, 4248–4250. (b) Zeng, R.; Fu, C.; Ma, S. *J. Am. Chem. Soc.* **2012**, *134*, 9597–9600. (c) Ye, B.; Cramer, N. J.

Am. Chem. Soc. **2013**, *135*, 636–639.

⁷ (a) Yao, T.; Hirano, K.; Satoh, T.; Miura, M. *Angew. Chem. Int. Ed.* **2011**, *50*, 2990–2994. (b) Fan, S.; Chen, F.; Zhang, X. *Angew. Chem. Int. Ed.* **2011**, *50*, 5918–5923. (c) Makida, Y.; Ohmiya, H.; Sawamura, M. *Angew. Chem. Int. Ed.* **2012**, *51*, 4122–4127.

⁸ Usui, S.; Hashimoto, Y.; Morey, J. V.; Wheatley, A. E. H.; Uchiyama, M. *J. Am. Chem. Soc.* **2007**, *129*, 15102–15103.

⁹ (a) Norinder, J.; Matsumoto, A.; Yoshikai, N.; Nakamura, E. *J. Am. Chem. Soc.* **2008**, *130*, 5858–5859. (b) Yoshikai, N.; Matsumoto, A.; Norinder, J.; Nakamura, E. *Angew. Chem. Int. Ed.* **2009**, *48*, 2925–2928. (c) Ilies, L.; Asako, S.; Nakamura, E. *J. Am. Chem. Soc.* **2011**, *133*, 7672–7675. (d) Yoshikai, N.; Asako, S.; Yamakawa, T.; Ilies, L.; Nakamura, E. *Chem. Asian J.* **2011**, *6*, 3059–3065. (e) Ilies, L.; Kobayashi, M.; Matsumoto, A.; Yoshikai, N.; Nakamura, E. *Adv. Synth. Catal.* **2012**, *354*, 593–596. (f) Ilies, L.; Konno, E.; Chen, Q.; Nakamura, E. *Asian J. Org. Chem.* **2012**, *1*, 142–145. (g) Shang, R.; Ilies, L.; Matsumoto, A.; Nakamura, E. *J. Am. Chem. Soc.* **2013**, *135*, 6030–6032.

¹⁰ Norinder, J.; Yoshikai, N.; Nakamura, E. *unpublished results*.

¹¹ Still, W. C.; Kahn, M.; Mitra, A. *J. Org. Chem.* **1978**, *43*, 2923–2925.

¹² Pangborn, A. B.; Giardello, M. A.; Grubbs, R. H.; Rosen R. K.; Timmers, F. J. *Organometallics* **1996**, *15*, 1518–1520.

¹³ Isobe, M.; Kondo, S.; Nagasawa, N.; Goto, T. *Chem. Lett.* **1977**, 679–682.

¹⁴ Teo, Y.-C.; Yong, F.-F.; Lim, G. S. *Tetrahedron Lett.* **2011**, *52*, 7171–7174.

¹⁵ Correa, A.; Bolm, C. *Adv. Synth. Catal.* **2007**, *349*, 2673–2676.

¹⁶ Yong, F.-F.; Teo, Y.-C.; Tay, S.-H.; Tan, B. Y.-H.; Lim, K.-H. *Tetrahedron Lett.*

2011, 52, 1161–1164.

¹⁷ (a) Tsang, D. S.; Yang, S.; Alphonse, F.-A.; Yudin, A. K. *Chem. Eur. J.* **2008**, 14, 886–894. (b) Dimmel, D. R.; Gharpure, S. B. *J. Am. Chem. Soc.* **1971**, 93, 3991–3996.

¹⁸ Yang, K.; Qiu, Y.; Li, Z.; Wang, Z.; Jiang, S. *J. Org. Chem.* **2011**, 76, 3151–3159.

¹⁹ Correa, A.; Bolm, C. *Angew. Chem. Int. Ed.* **2007**, 46, 8862–8865.

²⁰ Asaumi, T.; Matsuo, T.; Fukuyama, T.; Ie, Y.; Kakiuchi, F.; Chatani, N. *J. Org. Chem.* **2004**, 69, 4433–4440.

²¹ Barbero, N.; Martin, R. *Org. Lett.* **2012**, 14, 796–799.

²² Cristau, H.-J.; Cellier, P. P.; Spindler, J.-F.; Taillefer, M. *Eur. J. Org. Chem.* **2004**, 695–709.

²³ Noguchi, M.; Matsumoto, S.; Shirai, M.; Yamamoto, H. *Tetrahedron* **2003**, 59, 4123–4133.

²⁴ Wang, H.; Schröder, N.; Glorius, F. *Angew. Chem. Int. Ed.* **2013**, 52, 5386–5389.

Chapter 3

CHAPTER 4

Iron-Catalyzed *Ortho*-Allylation of Aromatic Carboxamides with Allyl Ethers

4.1. Introduction

In the previous chapter, unprecedented iron-catalyzed directed C–H bond activation with an electrophile was demonstrated using 1-arylpyrazole as a substrate and allyl phenyl ether as an electrophile. While the selective allylation proceeded under mild conditions for various arylpyrazole and indazole derivatives, a large amount of diphenylzinc reagent and the allylic electrophile were necessary and the scope of allylic electrophile was limited to the nonsubstituted allyl ether. In this chapter, *N*-(quinolin-8-yl)benzamides were found to undergo the selective iron-catalyzed *ortho*-allylation reaction much more efficiently. Notably, the reaction features the improved atom economy with reduced amount of reagents as well as the broader scope of the substrate and the allylic electrophile.

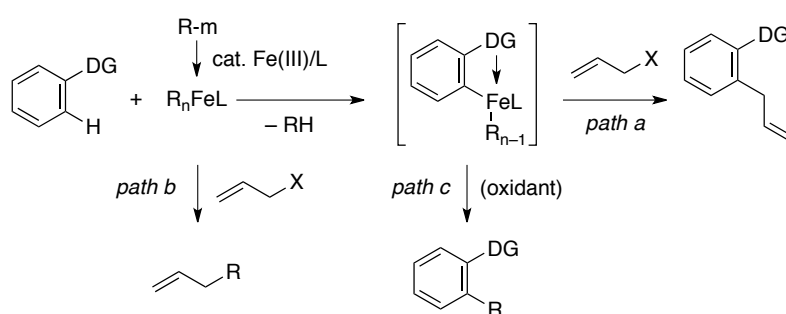
4.2. Reaction Design

Many of the reaction parameters such as directing group, organozinc base, and allylating reagent were found to significantly affect the selectivity and reactivity of the *ortho*-allylation reaction in Chapter 3, in which the reasons for the low yield of the allylated product could be often ascribed to the competing side reactions such as the phenylation and the cross-coupling of allylic reagent. With these observations, the *ortho*-allylation reaction was reconsidered in order to improve the efficiency and selectivity in a rational way.

The reaction was designed based on the following two considerations (Scheme 1, path a): 1) an organoiron species cleaves the *ortho* C–H bond of an arene possessing a directing group under mild conditions,^{1,2} and 2) the resulting metallacyclic iron intermediate may react with an allylic electrophile. In order to achieve this scenario,

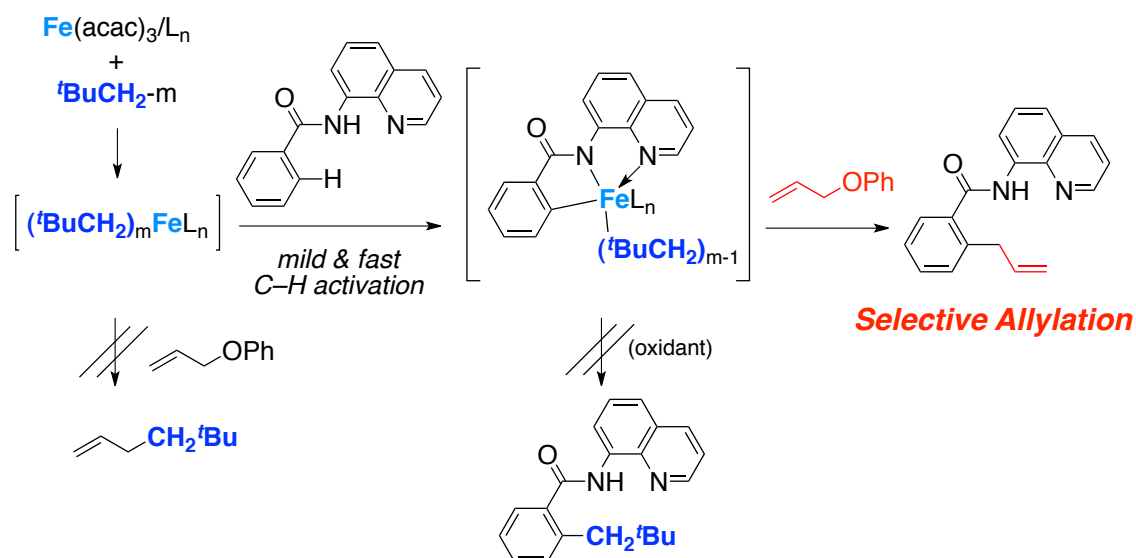
two potential competing reactions must be overcome: the cross-coupling of the organometallic reagent (R-m) with the allyl electrophile (path b),³ and the decomposition of the iron intermediate through oxidant-induced reductive elimination (path c).²

Scheme 1.

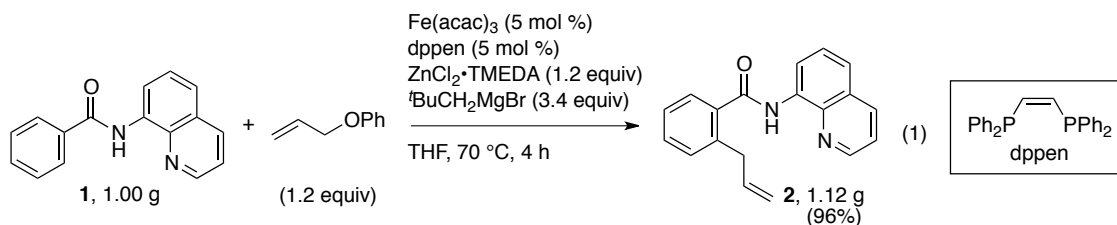


For this purpose, the following two key parameters, i.e., directing group and organometallic base, were reconsidered (Scheme 2). First, a bidentate directing group such as *N*-quinolinyll amide should be used, instead of a monodentate directing group to stabilize the chelated iron intermediate against reductive elimination which gives the undesired product. This bidentate directing group has been recently shown to be beneficial for C–H bond activation.⁴ Second, bulky sp^3 metal species such as neopentyl group should be used instead of Ph group because the competing reductive elimination and the cross-coupling reaction should be slower for neopentyl group than Ph group.

Scheme 2.



After extensive experimentation with the above hypothesis, the choice of directing group and organometallic reagent was found indeed crucial to selectively promote the allylation reaction (path a). Thus, *N*-(quinolin-8-yl)benzamide (**1**, 1.00 g, 4.03 mmol) reacted with allyl phenyl ether (1.2 equiv) in the presence of $\text{Fe}(\text{acac})_3$ (5 mol %), *cis*-1,2-bis(diphenylphosphino)ethylene (dppen, 5 mol %), $\text{ZnCl}_2 \cdot \text{TMEDA}$ (1.2 equiv), and *t*- BuCH_2MgBr (3.4 equiv) to give the *ortho*-allylated product **2** in 96% yield after 4 h at 70 °C (eq 1).

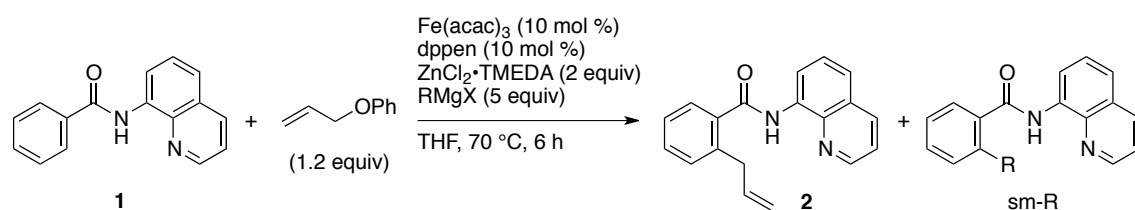


Ortho-neopentylated product (path c) was obtained in a trace amount (1%). Among 3.4 equiv of *t*- BuCH_2MgBr , 1 equiv is consumed to deprotonate the amide proton and the other 2.4 equiv forms 1.2 equiv of $(t\text{-BuCH}_2)_2\text{Zn}$. Arenes possessing a

monodentate directing group such as *N*-methylbenzamide, 2-phenylpyridine, arylimine, and 1-phenylpyrazole gave no product under these conditions. When organozinc reagents such as Ph_2Zn or Me_2Zn were used instead of the neopentyl reagent, **2** was obtained in a trace amount and paths b and c were dominant. Details of the investigation of reaction conditions are described in the following sections.

4.3. Effect of Organometallic Reagent

The choice of organometallic reagent affected the reaction greatly (Table 1). Diorganozinc reagents derived from PhMgBr and MeMgBr afforded the corresponding phenylated and methylated product in larger amount than the allylated product (entries 1 and 2). $\text{Me}_3\text{SiCH}_2\text{MgCl}$ was ineffective both for the allylation and alkylation reactions (entry 3). The reaction with a diorganozinc reagent prepared from CyMgBr , which also has a bulky alkyl group, was comparable to that with *t*- BuCH_2MgBr (entry 4).

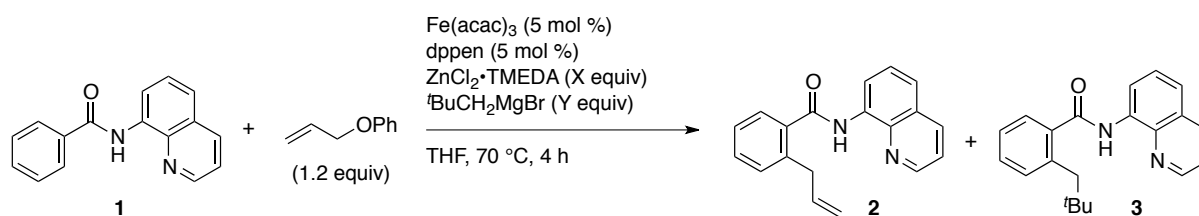
Table 1. Iron-Catalyzed Allylation of *N*-(quinolin-8-yl)benzamide with Diorganozinc*Reagents*

entry	RMgX	yield (%) ^a		
		2	sm-R	1
1	PhMgBr	3	28	66
2	MeMgBr	trace	33	51
3	Me ₃ SiCH ₂ MgCl	trace	trace	90
4	CyMgBr	88	trace	trace
5 ^b	^t BuCH ₂ MgBr	98	1	0

^a ¹H NMR yield using 1,1,2,2-tetrachloroethane as an internal standard.^b Fe(acac)₃ (5 mol %), dppen (5 mol %), ZnCl₂·TMEDA (1.2 equiv), ^tBuCH₂MgBr (3.4 equiv), 4 h.

When the amount of (*t*-BuCH₂)₂Zn•TMEDA was decreased from 1.2 equiv to 0.5 equiv, the yield of the allylated product decreased (Table 2, entries 1 and 2). The use of the monoalkylzinc reagent *t*-BuCH₂ZnCl•TMEDA instead of the dialkylzinc reagent dramatically decreased the product yield (entry 3). While the presence of TMEDA was not important for the allylation (entry 4), the presence of zinc was crucial and the use of *t*-BuCH₂MgBr resulted in low yield (entry 5).

Table 2. Iron-Catalyzed Allylation of *N*-(quinolin-8-yl)benzamide with Various Organometallic Reagents



entry	organometallic reagent	X	Y	yield (%) ^a		
				2	3	1
1	(^t BuCH ₂) ₂ Zn·TMEDA + 2 MgBrCl	1.2	3.4	98	1	0
2	(^t BuCH ₂) ₂ Zn·TMEDA + 2 MgBrCl	0.5	2.0	45	0	55
3	(^t BuCH ₂)ZnCl·TMEDA + MgBrCl	1.2	2.2	13	0	87
4 ^{b,c}	(^t BuCH ₂) ₂ Zn + 2 MgBrCl	3.0	7.0	87	3	7
5 ^b	^t BuCH ₂ MgBr	0	2.5	7	3	88

^a ¹H NMR yield using 1,1,2,2-tetrachloroethane as an internal standard.

^b Fe(acac)₃ (10 mol %), dppbz (10 mol %), allyl phenyl ether (2 equiv), 70 °C for 15 h.

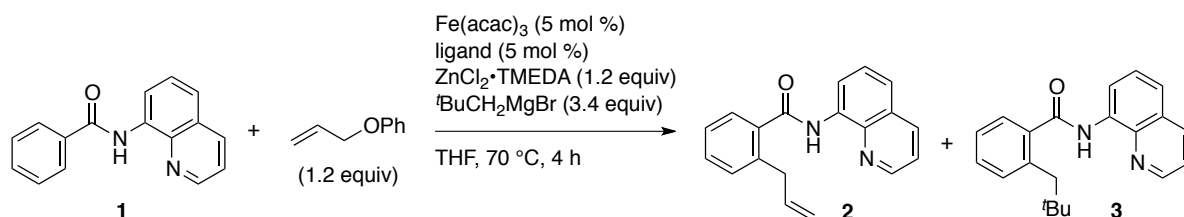
^c ZnCl₂ was used instead of ZnCl₂·TMEDA.

4.4. Effect of Ligand

The effect of ligand was investigated (Table 3). While no reaction took place in the absence of any ligand (entry 11), 1,2-bis(diphenylphosphino)benzene (dppbz) and congeners were found to be efficient for the allylation reaction, in which an electron-rich ligand performed better (entries 1–3). *cis*-1,2-Bis(diphenylphosphino)ethylene (dppen) showed the highest reactivity affording the allylated product **2** in 98% yield at 70 °C after 4 h. The reaction also proceeded under milder conditions at 50 °C when longer reaction time was applied (entries 5 and 6). In the presence of a diphosphine having a flexible backbone (dppe, entry 7), monodentate PPh₃ (entry 8), a bipyridine-type ligand (entries 9 and 10), the

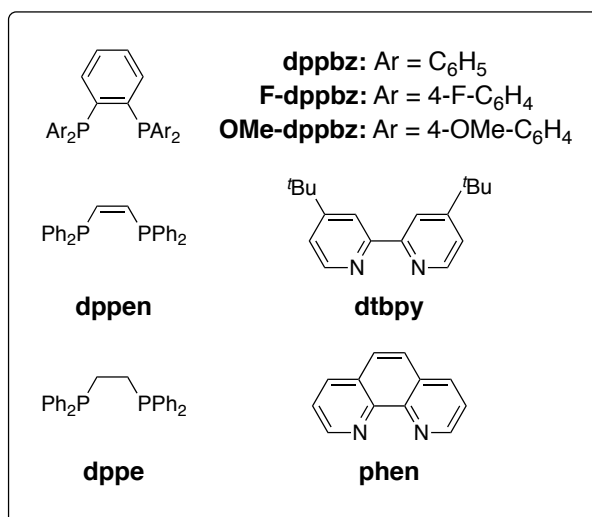
substrate was largely recovered.

Table 3. Investigation of Ligands for the Iron-Catalyzed Allylation of *N*-(quinolin-8-yl)benzamide with Allyl Phenyl Ether



entry	ligand	yield (%) ^a		
		2	3	1
1	F-dppbz	9	3	88
2	dppbz	61	3	39
3	OMe-dppbz	85	1	16
4	dppen	98	1	0
5	dppen (50 °C, 4 h)	73	trace	25
6	dppen (50 °C, 12 h)	99	trace	0
7	dppe	13	1	84
8	PPh ₃ (10 mol %)	0	0	100
9	dtbpy	5	0	95
10	phen	5	0	98
11	none	0	0	100

^a ¹H NMR yield using 1,1,2,2-tetrachloroethane as an internal standard.

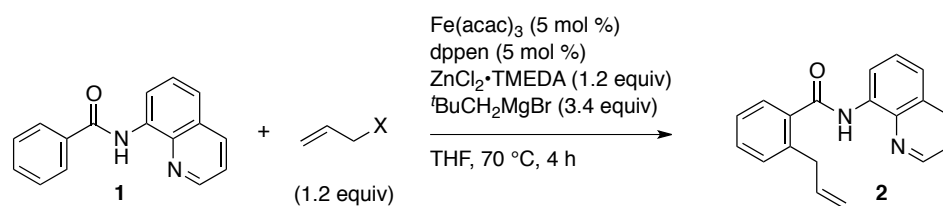


4.5. Effect of Allylic Electrophile

Compared with the reaction using 1-arylpyrazoles as a substrate, where only allyl phenyl ether performed well as an allylic electrophile, the reaction with *N*-(quinolin-8-yl)benzamide was less sensitive to the choice of electrophiles (Table 4). While allyl phenyl ether still showed the best performance, other allylic substrates having a different directing group, such as allyl acetate, allyl phenyl carbonate, allyl

propyl ether, allyloxytrimethylsilane, and allyl phenyl sulfide gave the allylated product **2** in moderate to good yields (entries 2–6). Even highly reactive allyl chloride could be used to afford the product in 24% yield (entry 7).

Table 4. Iron-Catalyzed Allylation of *N*-(quinolin-8-yl)benzamide with Allylic Electrophiles



entry	allylX	yield (%) ^a	
		2	1
1		98	0
2		82	20
3		47	52
4		71	25
5		65	27
6		40	60
7		24	69

^a ¹H NMR yield using 1,1,2,2-tetrachloroethane as an internal standard.

4.6. Scope of Substrate

The scope of the allylation reaction is illustrated in Table 5. The reaction with carboxamides bearing an electron-donating or electron-withdrawing substituent at the para position proceeded smoothly to afford the corresponding *ortho*-allylated product in good yields, while the latter needed longer reaction time (entries 1–8). Functional groups such as chloride, bromide, trifluoromethyl, and ester are tolerated. Meta-substituted carboxamides reacted smoothly at the less hindered *ortho* position (entries 9 and 10). The allylation of *ortho*-substituted substrate (entry 11) on the opposite *ortho* position proceeded slowly but still in good yield if higher catalyst loading and longer reaction time were employed. This slow reaction accounts for the selective mono allylation. The C–H bond of naphthalene, pyrene, and heteroarenes such as indole and thiophene could also be allylated in a regioselective manner (entries 12–15). Isomeric styrene compounds were not observed, despite the known reports on double bond isomerization of terminal olefins in the presence of an iron catalyst and an organometallic reagent.⁵

Table 5. Iron-Catalyzed Allylation of *N*-(Quinolin-8-yl)benzamides^a

entry	substrate	product	time (h)	yield (%)
1 ^b			4	96 (X = H)
2			4	97 (X = Me)
3			4	96 (X = OMe)
4 ^{c,d,f,h}			24	93 (X = F)
5			15	93 (X = Cl)
6 ^{c,d,f,h}			24	92 (X = Br)
7			36	90 (X = CF ₃)
8			6	74 (X = CO ₂ Me)
9			4	95 (X = Me)
10			4	98 (X = OMe)
11 ^{e,g,h}			160	74
12			4	98
13 ^{e,g,i}			135	68
14			18	91
15 ^c			40	61

^a The reaction was performed under the conditions in eq 1 on a 0.4 mmol scale.Qn = quinolin-8-yl ^b 1 g scale. ^c 50 °C. ^d 10 mol % catalyst. ^e 20 mol % catalyst.^f 1.5 equiv of ZnCl₂•TMEDA and 4.0 equiv of *t*-BuCH₂MgBr.^g 2.0 equiv of ZnCl₂•TMEDA and 5.0 equiv of *t*-BuCH₂MgBr.^h 1.5 equiv of allylOPh. ⁱ 2.0 equiv of allylOPh.

4.7. γ -Selective Allylation with α -Substituted Allyl Phenyl Ether

The reaction with allyl phenyl ether possessing a methyl group at the α position gave only the γ product in high yield as a mixture of stereoisomers ($E/Z = 59:41$) (eq 2). The E/Z ratio remained constant throughout the reaction, indicating that the stereo mixture is not due to product isomerization, but due to the allylation step itself. Attempts to control the E/Z ratio using ligands with different electronic and steric properties resulted in little change of the ratio (Table 6, entries 1–5). Although t Bu-SciOPP showed higher E/Z ratio, the yield of the allylation product decreased dramatically (entry 6). Allyl phenyl ethers possessing a substituent at β or γ position did not participate in the reaction.

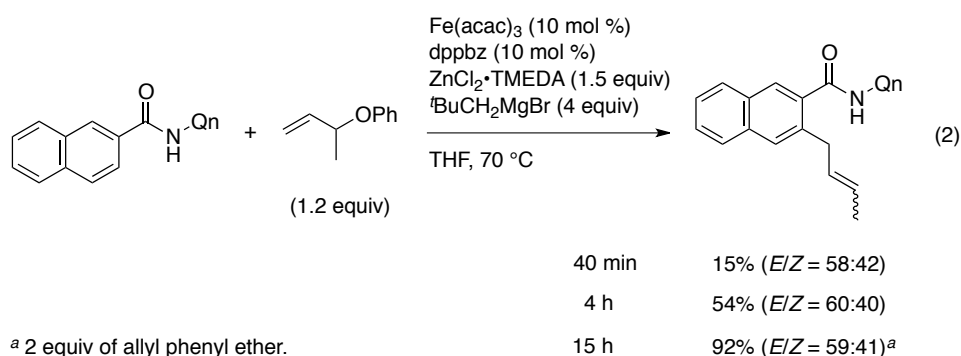


Table 6. Ligand Effect on Iron-Catalyzed Allylation of *N*-(quinolin-8-yl)-2-naphthamide with (*But-3-en-2-yl*oxy)benzene

entry	ligand	yield (<i>E/Z</i> ratio) ^a
1	F-dppbz	46% (<i>E/Z</i> = 62:38)
2 ^b	dppbz	92% (<i>E/Z</i> = 59:41)
3	OMe-dppbz	97% (<i>E/Z</i> = 41:59)
4	NMe ₂ -dppbz	98% (<i>E/Z</i> = 34:66)
5	dppen	98% (<i>E/Z</i> = 58:42)
6	^t Bu-SciOPP	18% (<i>E/Z</i> = 76:24)

dppbz: Ar = C₆H₅
F-dppbz: Ar = 4-F-C₆H₄
OMe-dppbz: Ar = 4-OMe-C₆H₄
NMe₂-dppbz: Ar = 4-NMe₂-C₆H₄
^tBu-SciOPP: Ar = 3,5-^tBu₂-C₆H₃

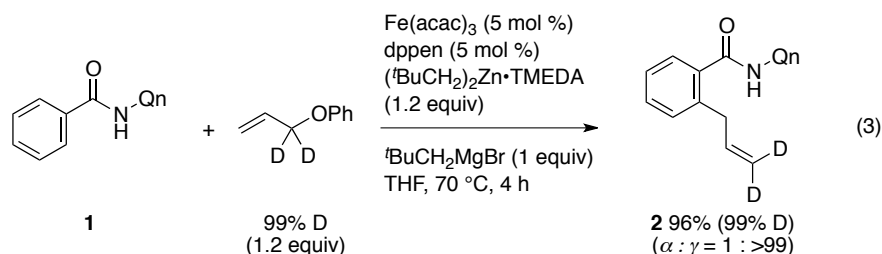
dppen

^a Determined by ¹H NMR.

^b 2 equiv of allyl phenyl ether.

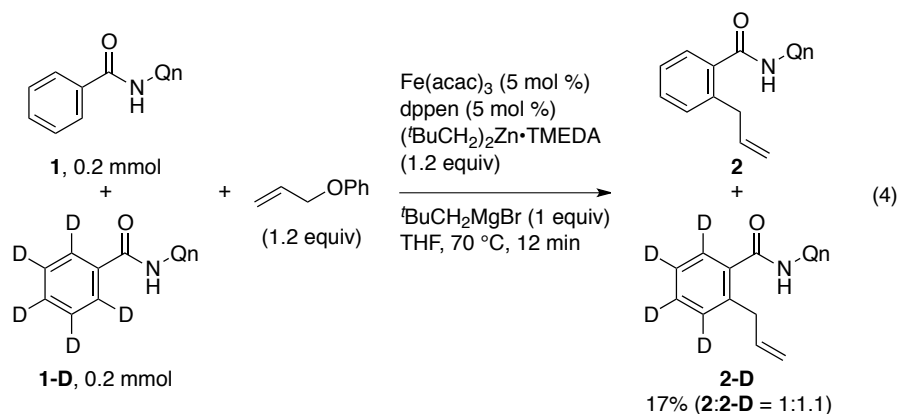
4.8. Mechanistic Insight

The reaction of ((1,1-dideuterioallyl)oxy)benzene selectively gave the γ product in 96% yield, which confirmed the preferred γ selective allylation (eq 3). The result also excludes the involvement of π -allyl iron intermediate.



An intermolecular competitive reaction using an equimolar amount of **1** and **1-D** was stopped at 17% conversion to give an intermolecular KIE value of 1.1 (eq 4).

The observed small KIE value suggests that the C–H bond cleavage step is not involved in the turnover-limiting step unlike the iron-catalyzed oxidative C–H bond arylation reaction, which showed a large KIE.^{2,4f}



The reactions with different amount of allyl phenyl ether were monitored to find nearly first order rate dependence on the concentration of allyl phenyl ether (Figure 1). Thus, when the amount of allyl phenyl ether was increased from 1.2 equiv to 2.4 equiv, the reaction rate became about 2 times higher. This result may suggest that the allylation step is the turnover-limiting step of the reaction.

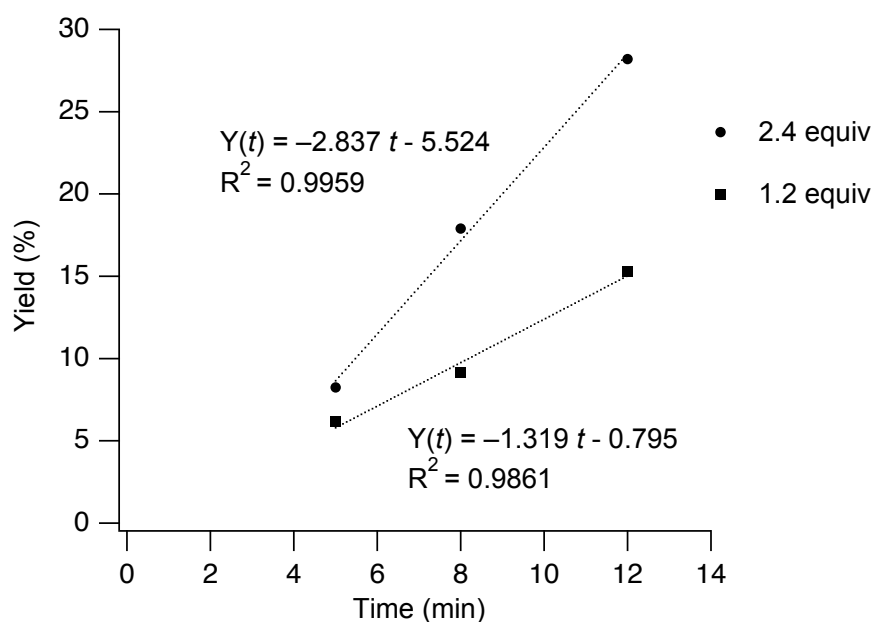
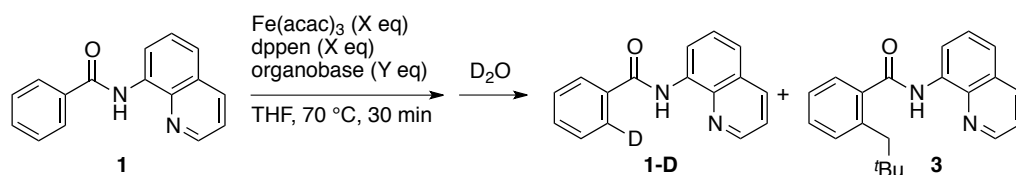


Figure 1. Rate Dependence on [allyl phenyl ether]

4.9. Metallacyclic Iron Intermediate

In order to obtain the information on the putative metallacyclic iron intermediate, the stoichiometric reaction was performed using 1 equiv of $\text{Fe}(\text{acac})_3$, 1 equiv of dppen, 2 equiv of $(t\text{-BuCH}_2)_2\text{Zn}\cdot\text{TMEDA}$, and 1 equiv of $t\text{-BuCH}_2\text{MgBr}$ (for deprotonation of the amide proton) (Table 7, entry 1). The addition of D_2O after stirring at 70 °C for 30 min afforded the recovered starting material with 88% D incorporation, suggesting the existence of a stable metallacyclic intermediate. A similar result was obtained with 3 equiv of $t\text{-BuCH}_2\text{MgBr}$ instead of the organozinc reagent (entry 2). No D incorporation was observed with $(t\text{-BuCH}_2)_2\text{Zn}\cdot\text{TMEDA}$ in the absence of $\text{Fe}(\text{acac})_3$, excluding the possibility of simple zincation for the C–H bond cleavage (entry 5). The D incorporation was found to be nearly proportional to the amount of $\text{Fe}(\text{acac})_3$ used, i.e., 89% D, 73% D, and 45% D for 1, 0.75, and 0.5 equiv of $\text{Fe}(\text{acac})_3$, respectively (entries 2–4). Therefore, it seems that the chelated metal is not zinc or magnesium but the chelated iron intermediate is formed after the C–H bond activation by an active iron species. The reaction of the stoichiometrically generated iron intermediate with 2 equiv of allyl phenyl ether at 70 °C for 10 min afforded the allylated product **2** in 54% yield.

Table 7. Stoichiometric Reaction of *N*-(quinolin-8-yl)benzamide

entry	X	organobase (Y)	NMR ratio		
				1	3
1	1	$(^t\text{BuCH}_2)_2\text{Zn}\cdot\text{TMEDA}$ (2 eq) + $^t\text{BuCH}_2\text{MgBr}$ (1 eq)	95%	88%D	5%
2	1	$^t\text{BuCH}_2\text{MgBr}$ (3 eq)	quant	89%D	trace
3	0.75	$^t\text{BuCH}_2\text{MgBr}$ (2.5 eq)	94%	73%D	6%
4	0.5	$^t\text{BuCH}_2\text{MgBr}$ (2 eq)	98%	45%D	2%
5	0	$(^t\text{BuCH}_2)_2\text{Zn}\cdot\text{TMEDA}$ (1.2 eq) + $^t\text{BuCH}_2\text{MgBr}$ (1 eq)	quant	0%D	0%

4.10. A Possible Catalytic Cycle

Figure 2 shows a possible catalytic cycle of the allylation reaction. First active iron species is generated from the catalyst precursor and organozinc reagent. The fast C–H bond cleavage takes place to form the iron metallacyclic intermediate along with elimination of neopentane, which was supported by the result of KIE experiment and the stoichiometric reaction. The turnover-limiting olefin insertion of allyl phenyl ether and β -phenoxy elimination afford the allylated product, as proposed for the *ortho*-allylation of 1-arylpyrazoles. The subsequent transmetallation completes the catalytic cycle.

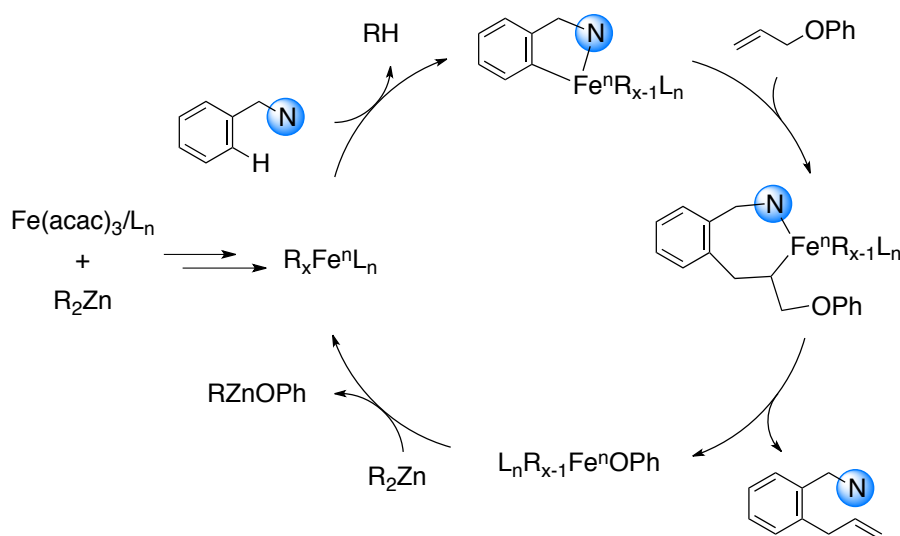


Figure 2. A Possible Catalytic Cycle

4.11. Summary

In conclusion, iron-catalyzed *ortho*-allylation of aromatic carboxamides via directed C–H bond activation was developed. The reaction proceeds smoothly under mild conditions to give allylbenzene derivatives with high γ selectivity and without isomerization of the double bond to styrene derivatives. The reaction exhibited a broad scope of the substrate and an excellent compatibility with functional groups in the presence of a catalytic amount of $\text{Fe}(\text{acac})_3$ and dppen using nearly stoichiometric amounts of allylic reagent and organozinc reagent. The reaction demonstrated another example of unprecedented iron-catalyzed directed C–H bond activation followed by the coupling with an electrophile.

4.12. Experimental Part

General. All reactions dealing with air- or moisture-sensitive compounds were carried out in a flame-dried, sealed Schlenk reaction tube under an atmosphere of nitrogen or argon. The water content of the solvent was confirmed with a Karl-Fischer Moisture Titrator (CA-21, Mitsubishi Chemical Analytech Company) to be less than 30 ppm. Analytical thin-layer chromatography was performed on glass plates coated with 0.25 mm 230–400 mesh silica gel containing a fluorescent indicator (Merck). Gas-liquid chromatographic (GLC) analysis was performed on a Shimadzu GC-14B or CG-2025 machine equipped with glass capillary column HR-1 (0.25-mm i.d. x 25 m). Flash silica gel column chromatography was performed on silica gel 60N (Kanto, spherical and neutral, 140–325 mesh) as described by Still.⁶ Gel permeation column chromatography was performed on a Japan Analytical Industry LC-908 (eluent: chloroform or toluene) with JAIGEL 1H and 2H polystyrene columns. ¹H NMR, ¹³C NMR, and ¹⁹F NMR spectra were measured on a JEOL ECA-500 or ECX-400 spectrometer and reported in parts per million from an internal standard, tetramethylsilane (0.0 ppm), CDCl₃ (77.0 ppm), and C₆F₆ (–164.9 ppm), respectively. Methyl, methylene, and methyne signals in ¹³C NMR spectra were assigned by DEPT spectra. Mass spectra were acquired by Shimadzu Parvum 2 gas chromatograph mass spectrometer (GC-MS) or by atmospheric pressure ionization (APCI) or electrospray ionization (ESI) using a time-of-flight mass analyzer on JEOL JMS-T100LC (AccuTOF) spectrometer with a calibration standard of polyethylene glycol (MW 400).

Materials. Unless otherwise noted, materials were purchased from Tokyo Kasei Co., Aldrich Inc., and other commercial suppliers and used as received. Anhydrous THF and

diethyl ether (stabilizer-free) were purchased from WAKO Pure Chemical and purified by a solvent purification system (GlassContour) equipped with columns of activated alumina and supported copper catalyst (Q-5) prior to use.⁷ Fe(acac)₃ (99.9% metal basis) and *cis*-1,2-bis(diphenylphosphino)ethylene were purchased from Aldrich Inc. and allyl phenyl ether was purchased from Tokyo Kasei Co., respectively, and used as received. Grignard reagents were purchased from Aldrich Inc. or prepared from the corresponding halides and magnesium turnings in anhydrous THF, and titrated prior to use. ZnCl₂•TMEDA was prepared according to the literature.⁸

Preparation of Substrates

The following compounds were prepared according to the literature procedures, and purified by column chromatography and recrystallization for the solid compounds.

N-(quinolin-8-yl)benzamide⁹

4-methyl-*N*-(quinolin-8-yl)benzamide⁹

4-methoxy-*N*-(quinolin-8-yl)benzamide⁹

4-fluoro-*N*-(quinolin-8-yl)benzamide⁹

4-chloro-*N*-(quinolin-8-yl)benzamide⁹

4-bromo-*N*-(quinolin-8-yl)benzamide⁹

4-trifluoromethyl-*N*-(quinolin-8-yl)benzamide⁹

methyl 4-(quinolin-8-ylcarbamoyl)benzoate⁹

3-methyl-*N*-(quinolin-8-yl)benzamide⁹

3-methoxyl-*N*-(quinolin-8-yl)benzamide⁹

2-methyl-*N*-(quinolin-8-yl)benzamide⁹

N-(quinolin-8-yl)-2-naphthamide⁹

N-(quinolin-8-yl)pyrene-1-carboxamide⁹

1-methyl-*N*-(quinolin-8-yl)-1*H*-indole-2-carboxamide¹⁰

N-(quinolin-8-yl)thiophene-2-carboxamide⁹

2,3,4,5,6-pentadeuterio-*N*-(quinolin-8-yl)benzamide was prepared according to the literature¹⁰ from benzoic acid-*d*₅ (99.1% deuterium incorporation) purchased from CDN Isotopes

(but-3-en-2-yloxy)benzene¹¹

((1,1-dideuterioallyl)oxy)benzene¹²

Spectral data for the following compounds showed good agreement with the literature data: *N*-(quinolin-8-yl)benzamide¹³

4-methyl-*N*-(quinolin-8-yl)benzamide¹³

4-methoxy-*N*-(quinolin-8-yl)benzamide⁹

4-fluoro-*N*-(quinolin-8-yl)benzamide⁹

4-chloro-*N*-(quinolin-8-yl)benzamide¹⁴

4-bromo-*N*-(quinolin-8-yl)benzamide⁹

4-trifluoromethyl-*N*-(quinolin-8-yl)benzamide¹⁵

methyl 4-(quinolin-8-ylcarbamoyl)benzoate⁹

3-methyl-*N*-(quinolin-8-yl)benzamide¹³

3-methoxyl-*N*-(quinolin-8-yl)benzamide⁹

2-methyl-*N*-(quinolin-8-yl)benzamide⁹

N-(quinolin-8-yl)-2-naphthamide¹⁶

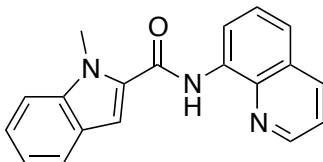
N-(quinolin-8-yl)pyrene-1-carboxamide¹⁷

N-(quinolin-8-yl)thiophene-2-carboxamide¹⁶

(but-3-en-2-yloxy)benzene¹⁸

((1,1-dideuterioallyl)oxy)benzene¹²

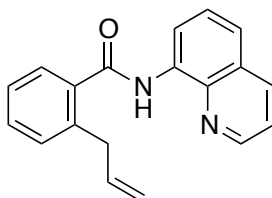
1-Methyl-*N*-(quinolin-8-yl)-1*H*-indole-2-carboxamide:



Colorless solid. ¹H NMR (500 MHz, CDCl₃): δ 10.72 (br s, 1H), 8.88–8.86 (m, 2H), 8.19 (dd, *J* = 8.3, 1.5 Hz, 1H), 7.74 (d, *J* = 8.0 Hz, 1H), 7.59 (d, *J* = 7.8 Hz, 1H), 7.54 (d, *J* = 8.6 Hz, 1H), 7.49 (dd, *J* = 8.0, 4.0 Hz, 1H), 7.44 (d, *J* = 8.0 Hz, 1H), 7.37 (t, *J* = 7.7 Hz, 1H), 7.31 (s, 1H), 7.19 (t, *J* = 7.5 Hz, 1H), 4.18 (s, 3H); ¹³C NMR (125 MHz, CDCl₃): δ 160.7, 148.4, 139.5, 138.6, 136.4, 134.7, 132.3, 128.0, 127.4, 126.1, 124.4, 122.1, 121.7, 121.6, 120.6, 116.2, 110.2, 105.0, 31.7; GC-MS (EI) *m/z* (relative intensity): 301 (M⁺, 24), 257 (20), 158 (93), 130 (26), 89 (100).

General Procedure for Iron-Catalyzed *ortho*-Allylation with Allyl Phenyl Ether

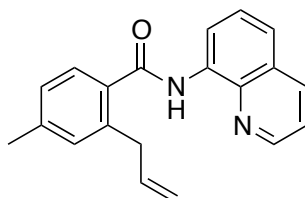
2-Allyl-*N*-(quinolin-8-yl)benzamide (Table 1, entry 1):



N-(Quinolin-8-yl)benzamide (1.00 g, 4.03 mmol) and ZnCl₂•TMEDA (1.22 g, 4.84 mmol) were placed in an oven-dried Schlenk flask under argon. A solution of *t*-BuCH₂MgBr in THF (1.10 M, 12.5 mL, 13.7 mmol) was added dropwise to this

mixture. After stirring for 5 min at rt, allyl phenyl ether (664 μL , 4.83 mmol) and a solution of $\text{Fe}(\text{acac})_3/\text{cis}$ -1,2-bis(diphenylphosphino)ethylene in THF (2.50 mL, 0.08 M, 200 μmol) were sequentially added. The reaction mixture was stirred at 70 $^\circ\text{C}$ for 4 h, and was diluted with Et_2O followed by the addition of a saturated aqueous solution of Rochelle's salt. After extraction with ethyl acetate, the combined organic layers were filtered through a pad of Florisil, and concentrated under reduced pressure. The crude product was purified by column chromatography on silica gel (hexane/AcOEt/ NEt_3 = 99/0.5/0.5) to afford the title compound as a colorless solid (1.12 g, 96%). Melting point: 88–89 $^\circ\text{C}$; ^1H NMR (500 MHz, CDCl_3): δ 10.18 (br s, 1H), 8.94 (d, J = 7.5 Hz, 1H), 8.76 (d, J = 4.0 Hz, 1H), 8.17 (d, J = 8.6 Hz, 1H), 7.67 (d, J = 7.5 Hz, 1H), 7.59 (t, J = 8.0 Hz, 1H), 7.54 (d, J = 8.0 Hz, 1H), 7.46–7.43 (m, 2H), 7.36–7.34 (m, 2H), 6.09–6.01 (m, 1H), 5.09–5.01 (m, 2H), 3.72 (d, J = 6.9 Hz, 2H); ^{13}C NMR (125 MHz, CDCl_3): δ 168.1, 148.2, 138.64, 138.55, 137.1, 136.6, 136.3, 134.7, 130.6, 130.4, 128.0, 127.4, 127.3, 126.5, 121.8, 121.6, 116.6, 116.1, 37.6; GC-MS (EI) m/z (relative intensity): 288 (M^+ , 10), 144 (100), 115 (43), 91 (15); HRMS (APCI) Calcd for $\text{C}_{19}\text{H}_{17}\text{N}_2\text{O}^+ [\text{M}+\text{H}]^+$ 289.1341, found, 289.1342.

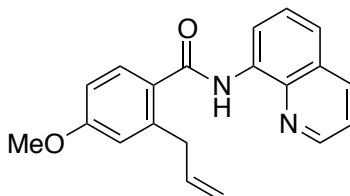
2-Allyl-4-methyl-*N*-(quinolin-8-yl)benzamide (Table 1, entry 2):



The general procedure was applied to 4-methyl-*N*-(quinolin-8-yl)benzamide (104.8 mg, 0.40 mmol) and the reaction mixture was stirred at 70 $^\circ\text{C}$ for 4 h. The crude product

was purified by column chromatography on silica gel (hexane/AcOEt/NEt₃ = 99/0.5/0.5) to afford the title compound as a colorless solid (117.3 mg, 97%). Melting point: 60–62 °C; ¹H NMR (500 MHz, CDCl₃): δ 10.19 (br s, 1H), 8.93 (d, *J* = 8.0 Hz, 1H), 8.74 (dd, *J* = 4.0, 1.2 Hz, 1H), 8.12 (d, *J* = 8.3 Hz, 1H), 7.59–7.55 (m, 2H), 7.50 (d, *J* = 8.0 Hz, 1H), 7.40 (dd, *J* = 8.3, 4.3 Hz, 1H), 7.14–7.13 (m, 2H), 6.09–6.01 (m, 1H), 5.09–5.02 (m, 2H), 3.71 (d, *J* = 6.3 Hz, 2H), 2.38 (s, 3H); ¹³C NMR (125 MHz, CDCl₃): δ 168.0, 148.1, 140.5, 138.7, 138.5, 137.3, 136.2, 134.7, 133.6, 131.3, 127.9, 127.34, 127.28, 127.0, 121.6, 121.5, 116.3, 115.9, 37.5, 21.3; GC-MS (EI) *m/z* (relative intensity): 302 (M⁺, 21), 158 (98), 144 (100), 131 (67), 115 (44), 91 (36); HRMS (APCI) Calcd for C₂₀H₁₉N₂O⁺ [M+H]⁺ 303.1497, found, 303.1501.

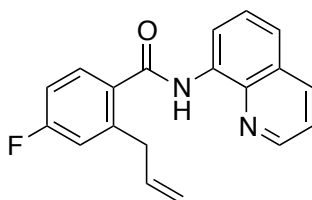
2-Allyl-4-methoxy-*N*-(quinolin-8-yl)benzamide (Table 1, entry 3):



The general procedure was applied to 4-methoxy-*N*-(quinolin-8-yl)benzamide (110.6 mg, 0.40 mmol) and the reaction mixture was stirred at 70 °C for 4 h. The crude product was purified by column chromatography on silica gel (hexane/AcOEt/NEt₃ = 97.5/2/0.5) to afford the title compound as a colorless solid (122.4 mg, 96%). Melting point: 134–135 °C; ¹H NMR (500 MHz, CDCl₃): δ 10.19 (br s, 1H), 8.91 (d, *J* = 7.4 Hz, 1H), 8.77 (dd, *J* = 4.3, 1.5 Hz, 1H), 8.16 (d, *J* = 8.1 Hz, 1H), 7.68 (d, *J* = 8.0 Hz, 1H), 7.58 (t, *J* = 8.0 Hz, 1H), 7.53 (d, *J* = 8.0 Hz, 1H), 7.44 (dd, *J* = 8.0, 4.0 Hz, 1H), 6.87–6.85 (m, 2H), 6.09–6.01 (m, 1H), 5.11–5.04 (m, 2H), 3.85 (s, 3H), 3.74 (d, *J* = 6.3 Hz,

2H); ^{13}C NMR (125 MHz, CDCl_3): δ 167.7, 161.1, 148.2, 141.3, 138.6, 137.0, 136.3, 134.9, 129.2, 129.0, 128.0, 127.4, 121.6, 121.5, 116.4, 116.2 (2C), 111.4, 55.3, 37.8; GC-MS (EI) m/z (relative intensity): 318 (M^+ , 17), 174 (85), 147 (100), 144 (64), 131 (23), 115 (33), 103 (26), 91 (42), 77 (19); HRMS (APCI) Calcd for $\text{C}_{20}\text{H}_{19}\text{N}_2\text{O}_2^+$ $[\text{M}+\text{H}]^+$ 319.1447, found, 319.1448.

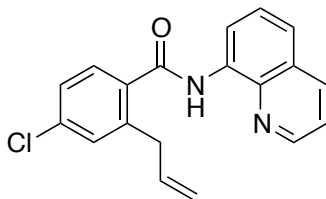
2-Allyl-4-fluoro-*N*-(quinolin-8-yl)benzamide (Table 1, entry 4):



The general procedure was applied to 4-fluoro-*N*-(quinolin-8-yl)benzamide (106.5 mg, 0.40 mmol) using $\text{Fe}(\text{acac})_3/\text{dppen}$ (10 mol %), $(t\text{-BuCH}_2)_2\text{Zn}$ (1.5 equiv), and allyl phenyl ether (1.5 equiv). The reaction mixture was stirred at 50 °C for 24 h. The crude product was purified by column chromatography on silica gel (hexane/AcOEt/ NEt_3 = 99/0.5/0.5) to afford the title compound as a colorless solid (114.0 mg, 93%). Melting point: 78–79 °C; ^1H NMR (500 MHz, CDCl_3): δ 10.17 (br s, 1H), 8.90 (d, J = 7.5 Hz, 1H), 8.78 (dd, J = 4.0, 1.8 Hz, 1H), 8.19 (dd, J = 8.3, 1.4 Hz, 1H), 7.69 (dd, J = 8.6, 5.7 Hz, 1H), 7.62–7.56 (m, 2H), 7.47 (dd, J = 8.3, 4.3 Hz, 1H), 7.08–7.02 (m, 2H), 6.06–5.98 (m, 1H), 5.12–5.08 (m, 2H), 3.72 (d, J = 6.3 Hz, 2H); ^{13}C NMR (125 MHz, CDCl_3): δ 167.1, 163.7 ($^1J_{\text{C-F}}$ = 248.0 Hz), 148.3, 142.0 ($^3J_{\text{C-F}}$ = 8.4 Hz), 138.5, 136.4, 136.2, 134.5, 132.7 ($^4J_{\text{C-F}}$ = 2.4 Hz), 129.4 ($^3J_{\text{C-F}}$ = 8.3 Hz), 128.0, 127.4, 121.9, 121.7, 117.4 ($^2J_{\text{C-F}}$ = 21.5 Hz), 116.9, 116.6, 113.4 ($^2J_{\text{C-F}}$ = 21.5 Hz), 37.4; ^{19}F NMR (470 MHz, CDCl_3): δ –113.0; GC-MS (EI) m/z (relative intensity): 306 (M^+ , 11), 162 (48), 144

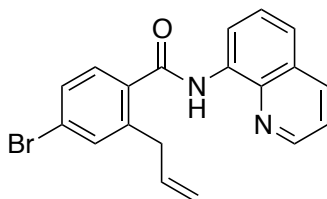
(100), 134 (75), 115 (46), 109 (32); HRMS (APCI) Calcd for $C_{19}H_{16}FN_2O^+$ $[M+H]^+$ 307.1247, found, 307.1254.

2-Allyl-4-chloro-*N*-(quinolin-8-yl)benzamide (Table 1, entry 5):



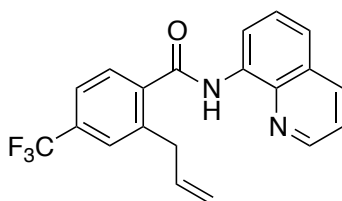
The general procedure was applied to 4-chloro-*N*-(quinolin-8-yl)benzamide (112.9 mg, 0.40 mmol) and the reaction mixture was stirred at 70 °C for 15 h. The crude product was purified by column chromatography on silica gel (hexane/AcOEt/ NEt_3 = 99/0.5/0.5) to afford the title compound as a colorless solid (119.3 mg, 93%). Melting point: 107–108 °C; 1H NMR (500 MHz, $CDCl_3$): δ 10.17 (br s, 1H), 8.90 (d, J = 6.9 Hz, 1H), 8.78 (dd, J = 4.0, 1.7 Hz, 1H), 8.19 (d, J = 8.3 Hz, 1H), 7.63–7.56 (m, 3H), 7.47 (dd, J = 8.1, 4.0 Hz, 1H), 7.35–7.33 (m, 2H), 6.05–5.97 (m, 1H), 5.11–5.07 (m, 2H), 3.70 (d, J = 6.3 Hz, 2H); ^{13}C NMR (125 MHz, $CDCl_3$): δ 167.1, 148.3, 140.9, 138.5, 136.4, 136.3, 136.2, 135.0, 134.5, 130.6, 128.7, 128.0, 127.4, 126.7, 122.0, 121.7, 116.9, 116.6, 37.3; GC-MS (EI) m/z (relative intensity): 324 (M^+ , 4), 322 (M^+ , 11), 180 (11), 178 (30), 144 (100), 115 (97), 89 (19); HRMS (APCI) Calcd for $C_{19}H_{16}^{35}ClN_2O^+$ $[M+H]^+$ 323.0951, found, 323.0947.

2-Allyl-4-bromo-*N*-(quinolin-8-yl)benzamide (Table 1, entry 6):



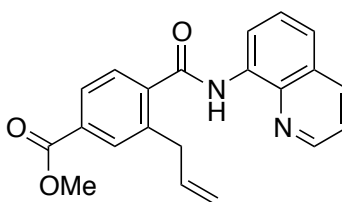
A solution of *t*-BuCH₂MgBr in THF (1.04 M, 1.54 mL, 1.60 mmol) was added dropwise to ZnCl₂•TMEDA (152 mg, 0.60 mmol) in an oven-dried Schlenk flask. After stirring for 5 min at 0 °C, 4-bromo-*N*-(quinolin-8-yl)benzamide (130.4 mg, 0.40 mmol), allyl phenyl ether (82 μL, 0.60 mmol), and a solution of Fe(acac)₃/*cis*-1,2-bis(diphenylphosphino)ethylene in THF (0.50 mL, 0.08 M, 40 μmol) were sequentially added. The reaction mixture was stirred at 50 °C for 24 h. The crude product was purified by column chromatography on silica gel (hexane/AcOEt/NEt₃ = 99/0.5/0.5) to afford the title compound as a colorless solid (135.2 mg, 92%). Melting point: 107–108 °C; ¹H NMR (500 MHz, CDCl₃): δ 10.17 (br s, 1H), 8.90 (d, *J* = 7.5 Hz, 1H), 8.78 (dd, *J* = 4.0, 1.7 Hz, 1H), 8.19 (d, *J* = 8.3 Hz, 1H), 7.61–7.54 (m, 3H), 7.51–7.46 (m, 3H), 6.05–5.97 (m, 1H), 5.11–5.07 (m, 2H), 3.69 (d, *J* = 6.9 Hz, 2H); ¹³C NMR (125 MHz, CDCl₃): δ 167.1, 148.3, 141.0, 138.5, 136.4, 136.2, 135.4, 134.4, 133.5, 129.6, 128.9, 128.0, 127.4, 124.7, 122.0, 121.7, 117.0, 116.6, 37.3; GC-MS (EI) *m/z* (relative intensity): 368 (M⁺, 8), 366 (M⁺, 9), 224 (11), 222 (10), 144 (100), 115 (84), 89 (15); HRMS (APCI) Calcd for C₁₉H₁₆⁷⁹BrN₂O⁺ [M+H]⁺ 367.0446, found, 367.0455.

2-Allyl-4-trifluoromethyl-*N*-(quinolin-8-yl)benzamide (Table 1, entry 7):



The general procedure was applied to 4-trifluoromethyl-*N*-(quinolin-8-yl)benzamide (126.6 mg, 0.40 mmol) and the reaction mixture was stirred at 70 °C for 36 h. The crude product was purified by column chromatography on silica gel (hexane/AcOEt/NEt₃ = 99/0.5/0.5) to afford the title compound as a colorless solid (128.8 mg, 90%). Melting point: 101–102 °C; ¹H NMR (500 MHz, CDCl₃): δ 10.19 (br s, 1H), 8.91 (dd, *J* = 6.9, 1.7 Hz, 1H), 8.78 (dd, *J* = 4.0, 1.7 Hz, 1H), 8.20 (dd, *J* = 8.3, 1.5 Hz, 1H), 7.78 (d, *J* = 7.4 Hz, 1H), 7.64–7.58 (m, 4H), 7.48 (dd, *J* = 8.3, 4.3 Hz, 1H), 6.06–5.98 (m, 1H), 5.12–5.08 (m, 2H), 3.75 (d, *J* = 6.9 Hz, 2H); ¹³C NMR (125 MHz, CDCl₃): δ 166.7, 148.3, 139.8, 139.6, 138.4, 136.4, 135.9, 134.2, 132.1 (q, ²*J*_{C-F} = 32.2 Hz), 127.9, 127.7, 127.3 (2C), 123.7 (q, ¹*J*_{C-F} = 271.0 Hz), 123.4 (q, ³*J*_{C-F} = 3.6 Hz), 122.2, 121.7, 117.2, 116.7, 37.3; ¹⁹F NMR (470 MHz, CDCl₃): δ –66.0; GC-MS (EI) *m/z* (relative intensity): 356 (M⁺, 15), 212 (15), 184 (22), 165 (16), 144 (100), 115 (40); HRMS (APCI) Calcd for C₂₀H₁₆F₃N₂O⁺ [M+H]⁺ 357.1215, found, 357.1208.

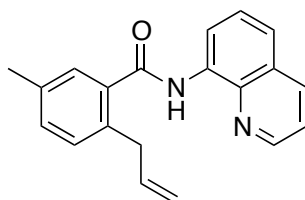
Methyl 3-allyl-4-(quinolin-8-ylcarbamoyl)benzoate (Table 1, entry 8):



The general procedure was applied to methyl 4-(quinolin-8-ylcarbamoyl)benzoate

(122.5 mg, 0.40 mmol) and the reaction mixture was stirred at 70 °C for 6 h. The crude product was purified by column chromatography on silica gel (hexane/AcOEt/NEt₃ = 97/2.5/0.5) to afford the title compound as a colorless solid (102.8 mg, 74%). Melting point: 121–122 °C; ¹H NMR (500 MHz, CDCl₃): δ 10.20 (br s, 1H), 8.92 (d, *J* = 7.2 Hz, 1H), 8.77 (dd, *J* = 4.0, 1.8 Hz, 1H), 8.18 (d, *J* = 8.0 Hz, 1H), 8.02–8.01 (m, 2H), 7.73 (d, *J* = 8.0 Hz, 1H), 7.61–7.56 (m, 2H), 7.46 (dd, *J* = 8.3, 4.3 Hz, 1H), 6.08–6.00 (m, 1H), 5.10–5.05 (m, 2H), 3.96 (s, 3H), 3.74 (d, *J* = 6.9 Hz, 2H); ¹³C NMR (125 MHz, CDCl₃): δ 167.1, 166.3, 148.3, 140.5, 138.8, 138.4, 136.3 (2C), 134.3, 131.6 (2C), 127.9, 127.7, 127.3, 127.2, 122.1, 121.7, 116.7, 116.6, 52.3, 37.4; GC-MS (EI) *m/z* (relative intensity): 346 (M⁺, 11), 202 (11), 171 (16), 144 (100), 129 (12), 115 (59), 91 (16); HRMS (APCI) Calcd for C₂₁H₁₉N₂O₃⁺ [M+H]⁺ 347.1396, found, 347.1396.

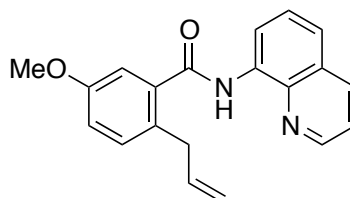
2-Allyl-5-methyl-*N*-(quinolin-8-yl)benzamide (Table 1, entry 9):



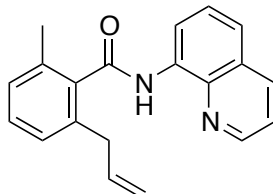
The general procedure was applied to 3-methyl-*N*-(quinolin-8-yl)benzamide (104.4 mg, 0.40 mmol) and the reaction mixture was stirred at 70 °C for 4 h. The crude product was purified by column chromatography on silica gel (hexane/AcOEt/NEt₃ = 99/0.5/0.5) to afford the title compound as a colorless solid (114.8 mg, 95%). Melting point: 78–79 °C; ¹H NMR (500 MHz, CDCl₃): δ 10.15 (br s, 1H), 8.93 (d, *J* = 7.5 Hz, 1H), 8.77 (d, *J* = 4.0 Hz, 1H), 8.17 (d, *J* = 8.1 Hz, 1H), 7.61–7.53 (m, 2H), 7.47–7.43 (m, 2H), 7.26–7.22 (m, 2H), 6.07–5.99 (m, 1H), 5.06–5.00 (m, 2H), 3.66 (d, *J* = 6.3 Hz,

2H), 2.40 (s, 3H); ^{13}C NMR (125 MHz, CDCl_3): δ 168.3, 148.2, 138.6, 137.4, 136.6, 136.3, 136.1, 135.4, 134.7, 131.1, 130.5, 128.0, 127.8, 127.4, 121.7, 121.6, 116.6, 115.9, 37.2, 21.0; GC-MS (EI) m/z (relative intensity): 302 (M^+ , 16), 287 (9), 158 (80), 144 (100), 131 (46), 115 (39), 91 (30); HRMS (APCI) Calcd for $\text{C}_{20}\text{H}_{19}\text{N}_2\text{O}^+$ $[\text{M}+\text{H}]^+$ 303.1497, found, 303.1499.

2-Allyl-5-methoxyl-*N*-(quinolin-8-yl)benzamide (Table 1, entry 10):

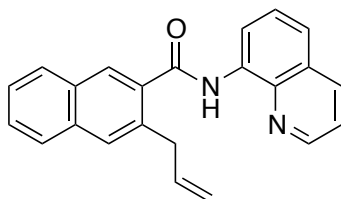


The general procedure was applied to 3-methoxyl-*N*-(quinolin-8-yl)benzamide (111.5 mg, 0.40 mmol) and the reaction mixture was stirred at 70 °C for 4 h. The crude product was purified by column chromatography on silica gel (hexane/AcOEt/ NEt_3 = 97.5/2/0.5) to afford the title compound as a colorless solid (124.9 mg, 98%). Melting point: 100–101 °C; ^1H NMR (500 MHz, CDCl_3): δ 10.17 (br s, 1H), 8.92 (d, J = 7.5 Hz, 1H), 8.77 (dd, J = 4.0, 1.8 Hz, 1H), 8.17 (dd, J = 8.0, 1.7 Hz, 1H), 7.61–7.54 (m, 2H), 7.45 (dd, J = 8.3, 4.3 Hz, 1H), 7.25 (d, J = 8.0 Hz, 1H), 7.20 (d, J = 2.3 Hz, 1H), 6.99 (dd, J = 8.6, 2.9 Hz, 1H), 6.06–5.98 (m, 1H), 5.05–4.99 (m, 2H), 3.85 (s, 3H), 3.63 (d, J = 6.3 Hz, 2H); ^{13}C NMR (125 MHz, CDCl_3): δ 167.9, 158.0, 148.2, 138.6, 137.6, 137.5, 136.3, 134.6, 131.7, 130.2, 128.0, 127.4, 121.8, 121.6, 116.6, 116.0, 115.8, 112.7, 55.5, 36.8; GC-MS (EI) m/z (relative intensity): 318 (M^+ , 9), 303 (18), 174 (44), 159 (20), 144 (100), 131 (30), 115 (21), 103 (26), 91 (25), 77 (16); HRMS (APCI) Calcd for $\text{C}_{20}\text{H}_{19}\text{N}_2\text{O}_2^+$ $[\text{M}+\text{H}]^+$ 319.1447, found, 319.1447.

2-Allyl-6-methyl-*N*-(quinolin-8-yl)benzamide (Table 1, entry 11):

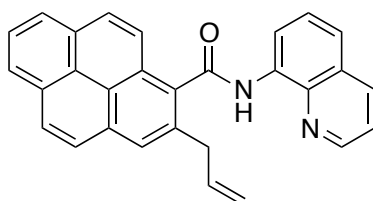
The general procedure was applied to 2-methyl-*N*-(quinolin-8-yl)benzamide (104.5 mg, 0.40 mmol) using $\text{Fe}(\text{acac})_3/\text{dppen}$ (20 mol %), $(t\text{-BuCH}_2)_2\text{Zn}$ (2.0 equiv), and allyl phenyl ether (1.5 equiv). The reaction mixture was stirred at 70 °C for 160 h. The crude product was purified by column chromatography on silica gel (hexane/AcOEt/ NEt_3 = 99/0.5/0.5) and GPC using CHCl_3 as an eluent to afford the title compound as a pale yellow oil (89.5 mg, 74%). ^1H NMR (500 MHz, CDCl_3): δ 9.94 (br s, 1H), 8.99 (dd, J = 7.5, 1.2 Hz, 1H), 8.72 (dd, J = 4.0, 1.7 Hz, 1H), 8.16 (dd, J = 8.6, 1.7 Hz, 1H), 7.60 (t, J = 8.0 Hz, 1H), 7.55 (dd, J = 8.3, 1.5 Hz, 1H), 7.43 (dd, J = 8.0, 4.0 Hz, 1H), 7.29 (t, J = 7.7 Hz, 1H), 7.15–7.13 (m, 2H), 6.02–5.94 (m, 1H), 5.03–4.96 (m, 2H), 3.51 (d, J = 6.3 Hz, 2H), 2.44 (s, 3H); ^{13}C NMR (125 MHz, CDCl_3): δ 168.5, 148.2, 138.4, 137.7, 136.8, 136.6, 136.3, 134.7, 134.3, 129.1, 128.2, 127.9, 127.3, 127.0, 121.9, 121.6, 116.7, 116.2, 37.7, 19.5; GC-MS (EI) m/z (relative intensity): 302 (M^+ , 16), 158 (100), 144 (65), 131 (84), 115 (57), 91 (62); HRMS (APCI) Calcd for $\text{C}_{20}\text{H}_{19}\text{N}_2\text{O}^+$ [$\text{M}+\text{H}$] $^+$ 303.1497, found, 303.1493.

3-Allyl-*N*-(quinolin-8-yl)-2-naphthamide (Table 1, entry 12):



The general procedure was applied to *N*-(quinolin-8-yl)-2-naphthamide (118.7 mg, 0.40 mmol) and the reaction mixture was stirred at 70 °C for 4 h. The crude product was purified by column chromatography on silica gel (hexane/AcOEt/NEt₃ = 99/0.5/0.5) to afford the title compound as a colorless solid (133.3 mg, 98%). Melting point: 111–113 °C; ¹H NMR (500 MHz, CDCl₃): δ 10.32 (br s, 1H), 8.97 (d, *J* = 7.5 Hz, 1H), 8.77 (d, *J* = 4.0 Hz, 1H), 8.18–8.17 (m, 2H), 7.91 (d, *J* = 7.5 Hz, 1H), 7.84 (d, *J* = 8.0 Hz, 1H), 7.77 (s, 1H), 7.62 (t, *J* = 8.0 Hz, 1H), 7.57–7.49 (m, 3H), 7.45 (dd, *J* = 8.0, 4.0 Hz, 1H), 6.15–6.07 (m, 1H), 5.13–5.05 (m, 2H), 3.88 (d, *J* = 6.3 Hz, 2H); ¹³C NMR (125 MHz, CDCl₃): δ 168.1, 148.3, 138.6, 137.1, 136.3, 135.6, 135.3, 134.8, 134.2, 131.4, 129.0, 128.2, 128.0, 127.42 (2C), 127.36, 127.3, 126.2, 121.8, 121.7, 116.6, 116.4, 37.6; GC-MS (EI) *m/z* (relative intensity): 338 (M⁺, 15), 194 (44), 165 (63), 152 (36), 144 (100); HRMS (APCI) Calcd for C₂₃H₁₉N₂O⁺ [M+H]⁺ 339.1497, found, 339.1501.

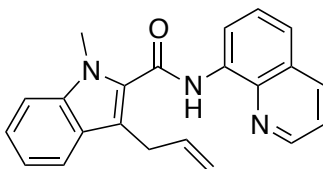
2-Allyl-*N*-(quinolin-8-yl)pyrene-1-carboxamide (Table 1, entry 13):



The general procedure was applied to *N*-(quinolin-8-yl)pyrene-1-carboxamide (148.5 mg, 0.40 mmol) using Fe(acac)₃/dppen (20 mol %), (*t*-BuCH₂)₂Zn (2.0 equiv), and allyl phenyl ether (2.0 equiv). The reaction mixture was stirred at 70 °C for 135 h. The crude

product was purified by column chromatography on silica gel (hexane/AcOEt/NEt₃ = 99/0.5/0.5) to afford the title compound as a colorless solid (112.2 mg, 68%). Melting point: 200–201 °C; ¹H NMR (400 MHz, CDCl₃): δ 10.28 (br s, 1H), 9.18 (dd, *J* = 7.5, 1.2 Hz, 1H), 8.56 (dd, *J* = 4.2, 1.4 Hz, 1H), 8.25 (d, *J* = 9.2 Hz, 1H), 8.16–8.03 (m, 6H), 8.00–7.94 (m, 2H), 7.65 (t, *J* = 7.7 Hz, 1H), 7.55 (d, *J* = 8.0 Hz, 1H), 7.31 (dd, *J* = 7.3, 4.3 Hz, 1H), 6.23–6.15 (m, 1H), 5.14 (dd, *J* = 17.2, 1.7 Hz, 1H), 5.08 (dd, *J* = 10.3, 1.2 Hz, 1H), 3.96 (d, *J* = 6.9 Hz, 2H); ¹³C NMR (125 MHz, CDCl₃): δ 168.4, 148.2, 138.4, 137.0, 136.2, 134.5, 134.4, 132.3, 131.8, 130.9, 130.5, 128.7, 128.4, 128.1, 127.9, 127.4, 126.9, 126.0, 125.8, 125.6, 125.4, 124.3, 124.2, 123.2, 122.1, 121.6, 116.9, 116.6, 38.3; HRMS (APCI) Calcd for C₂₉H₂₁N₂O⁺ [M+H]⁺ 413.1654, found, 413.1652.

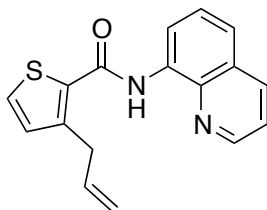
3-Allyl-1-methyl-*N*-(quinolin-8-yl)-1*H*-indole-2-carboxamide (Table 1, entry 14):



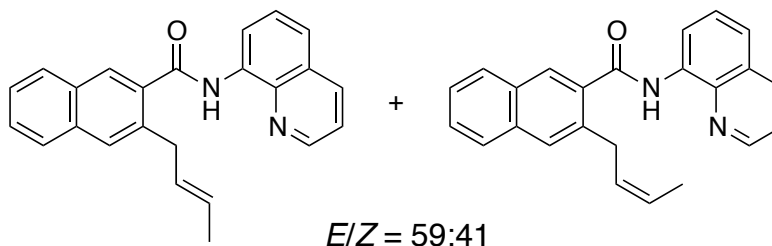
The general procedure was applied to 1-methyl-*N*-(quinolin-8-yl)-1*H*-indole-2-carboxamide (120.6 mg, 0.40 mmol) and the reaction mixture was stirred at 70 °C for 18 h. The crude product was purified by column chromatography on silica gel (hexane/AcOEt/NEt₃ = 98.5/1/0.5) to afford the title compound as a colorless solid (123.9 mg, 91%). Melting point: 119–120 °C; ¹H NMR (500 MHz, CDCl₃): δ 10.40 (br s, 1H), 8.91 (d, *J* = 7.5 Hz, 1H), 8.77 (dd, *J* = 4.3, 1.5 Hz, 1H), 8.14 (dd, *J* = 8.3, 1.5 Hz, 1H), 7.68 (d, *J* = 8.0, 1H), 7.58 (t, *J* = 7.7 Hz, 1H), 7.53 (d, *J* = 8.1 Hz, 1H), 7.42 (dd, *J* = 8.6, 4.0 Hz, 1H), 7.38–7.33 (m, 2H), 7.16 (t, *J* = 8.0 Hz, 1H), 6.24–6.17 (m, 1H), 5.12–5.08 (m, 2H), 4.00 (s, 3H), 3.91 (d, *J* = 5.8

Hz, 2H); ^{13}C NMR (125 MHz, CDCl_3): δ 161.0, 148.2, 138.6, 138.3, 136.7, 136.2, 134.6, 131.0, 128.0, 127.3, 126.9, 124.3, 121.9, 121.7, 120.5, 119.9, 116.8, 115.6, 115.2, 109.9, 31.5, 29.3; GC-MS (EI) m/z (relative intensity): 341 (M^+ , 12), 326 (35), 212 (20), 197 (50), 171 (73), 170 (100), 154 (28), 144 (68), 128 (42), 115 (32), 102 (17), 89 (18), 77 (25); HRMS (APCI) Calcd for $\text{C}_{22}\text{H}_{20}\text{N}_3\text{O}^+$ [$\text{M}+\text{H}$] $^+$ 342.1606, found, 342.1594.

3-Allyl-*N*-(quinolin-8-yl)thiophene-2-carboxamide (Table 1, entry 15):

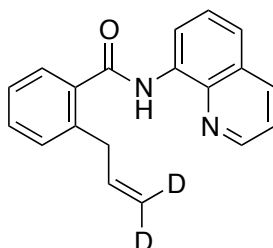


The general procedure was applied to *N*-(quinolin-8-yl)thiophene-2-carboxamide (100.6 mg, 0.40 mmol) and the reaction mixture was stirred at 50 °C for 40 h. The crude product was purified by column chromatography on silica gel (hexane/AcOEt/ NEt_3 = 99/0.5/0.5) and GPC using CHCl_3 as an eluent to afford the title compound as a colorless solid (70.7 mg, 61%). Melting point: 62–63 °C; ^1H NMR (500 MHz, CDCl_3): δ 10.43 (br s, 1H), 8.85–8.83 (m, 2H), 8.18 (d, J = 7.5 Hz, 1H), 7.59–7.53 (m, 2H), 7.47 (dd, J = 8.3, 4.3 Hz, 1H), 7.42 (d, J = 5.2 Hz, 1H), 7.03 (d, J = 5.2 Hz, 1H), 6.16–6.09 (m, 1H), 5.16–5.12 (m, 2H), 3.91 (d, J = 6.9 Hz, 2H); ^{13}C NMR (125 MHz, CDCl_3): δ 161.0, 148.3, 143.8, 138.6, 136.3, 136.1, 134.7, 132.4, 131.3, 128.0, 127.6, 127.4, 121.6 (2C), 116.6, 116.3, 33.9; GC-MS (EI) m/z (relative intensity): 294 (M^+ , 29), 279 (17), 150 (88), 144 (97), 123 (100), 79 (41); HRMS (APCI) Calcd for $\text{C}_{17}\text{H}_{15}\text{FN}_2\text{OS}^+$ [$\text{M}+\text{H}$] $^+$ 295.0905, found, 295.0904.

(E)-3-(But-2-en-1-yl)-N-(quinolin-8-yl)-2-naphthamide**and****(Z)-3-(but-2-en-1-yl)-N-(quinolin-8-yl)-2-naphthamide (Eq 2):**

The general procedure was applied to *N*-(quinolin-8-yl)-2-naphthamide (119.6 mg, 0.40 mmol) using $\text{Fe}(\text{acac})_3/\text{dppen}$ (10 mol %) and the reaction mixture was stirred at 70 °C for 6 h. The crude product was purified by column chromatography on silica gel (hexane/AcOEt/ NEt_3 = 98.5/1/0.5) and GPC using toluene as an eluent to afford a mixture of the title compounds as a colorless solid (126.6 mg, 90% (E/Z = 59:41)). ^1H NMR (500 MHz, CDCl_3): δ 10.32 (Z: br s, 0.41H), 10.28 (*E*: br s, 0.57H), 8.99–8.97 (m, 1H), 8.76–8.74 (m, 1H), 8.16–8.15 (m, 2H), 7.88 (d, J = 8.0 Hz, 1H), 7.82 (d, J = 8.0 Hz, 1H), 7.76 (d, J = 8.6 Hz, 1H), 7.62–7.59 (m, 1H), 7.56–7.51 (m, 2H), 7.50–7.46 (m, 1H), 7.43 (ddd, J = 8.0, 4.0, 1.7 Hz, 1H), 5.72–5.67 (m, 1H), 5.60–5.50 (m, 1H), 3.89 (Z: d, J = 7.5 Hz, 0.83H), 3.78 (*E*: d, J = 6.3 Hz, 1.19H), 1.68 (Z: d, J = 6.9 Hz, 1.29H), 1.55 (*E*: d, J = 6.3 Hz, 1.79H); ^{13}C NMR (125 MHz, CDCl_3): δ 168.3 (*E*), 168.2 (*Z*), 148.23 (*E*), 148.21 (*Z*), 138.5 (*E* + *Z*), 136.5 (*Z*), 136.4 (*E*), 136.3 (*E* + *Z*), 135.5 (*E*), 135.4 (*Z*), 134.8 (*Z*), 134.7 (*E*), 134.19 (*Z*), 134.15 (*E*), 131.3 (*E*), 131.2 (*Z*), 129.5 (*Z*), 128.7 (*E*), 128.44 (*Z*), 128.37 (*E*), 128.1 (*E* + *Z*), 127.9 (*E* + *Z*), 127.4 (*E* + *Z*), 127.32 (*E* + *Z*), 127.31 (*Z*), 127.29 (*E*), 127.14 (*E*), 127.12 (*Z*), 127.0 (*E*), 126.0 (*E* + *Z*), 125.6 (*Z*), 121.8 (*E* + *Z*), 121.63 (*Z*), 121.61 (*E*), 116.62 (*E*), 116.56 (*Z*), 36.5 (*E*), 30.9 (*Z*), 17.9 (*E*), 12.9 (*Z*); GC-MS (EI) m/z (relative intensity): 352 (M^+ , 7), 208 (51), 181 (25), 165 (66), 144 (100); HRMS (APCI) Calcd for $\text{C}_{24}\text{H}_{21}\text{N}_2\text{O}^+$ [$\text{M}+\text{H}$] $^+$ 353.1654, found,

353.1659.

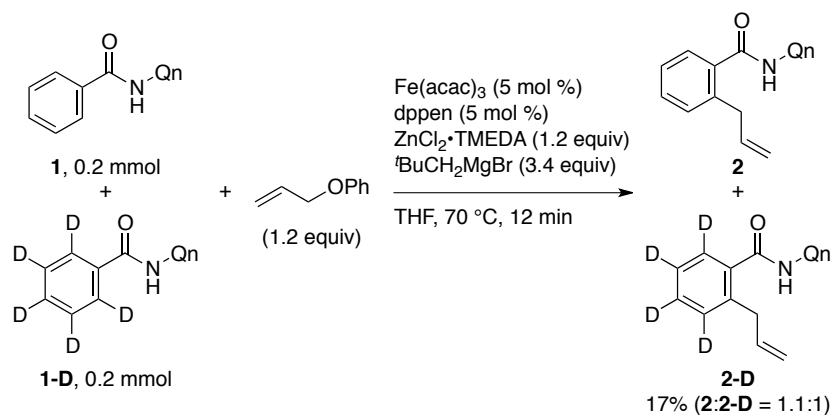
2-(3,3-Dideuterioallyl)-*N*-(quinolin-8-yl)benzamide (Eq 3):

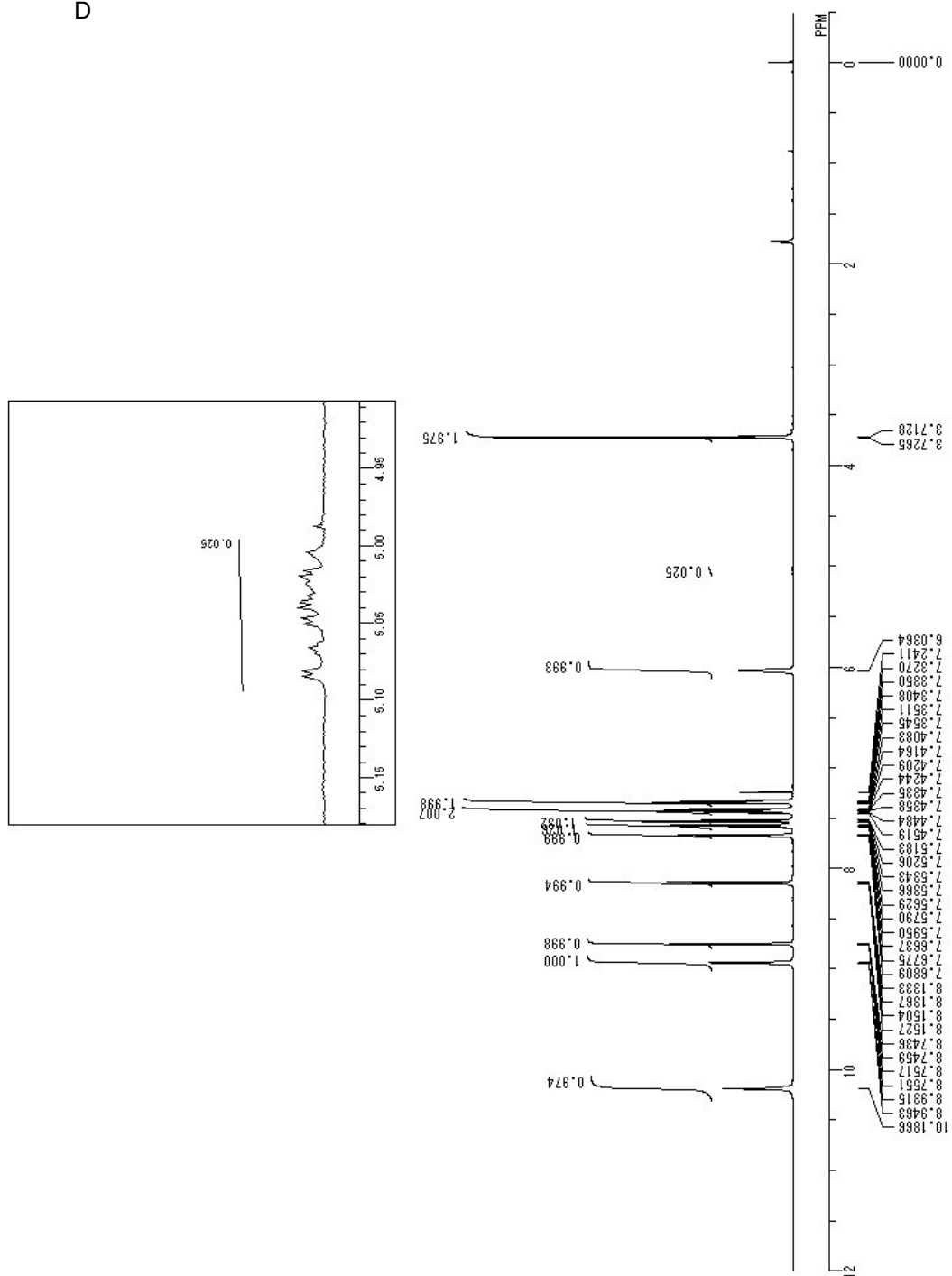
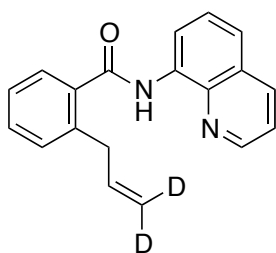
The general procedure was applied to *N*-(quinolin-8-yl)benzamide (99.7 mg, 0.40 mmol) and ((1,1-dideuterioallyl)oxy)benzene (1.2 equiv), and the reaction mixture was stirred at 70 °C for 4 h. The crude product was purified by column chromatography on silica gel (hexane/AcOEt/NEt₃ = 99/0.5/0.5) to afford the title compound as a colorless solid (112.4 mg, 96%). ¹H NMR (500 MHz, CDCl₃): δ 10.19 (br s, 1H), 8.94 (d, *J* = 7.4 Hz, 1H), 8.75 (dd, *J* = 4.3, 1.4 Hz, 1H), 8.14 (dd, *J* = 8.3, 1.4 Hz, 1H), 7.67 (d, *J* = 7.8 Hz, 1H), 7.58 (t, *J* = 8.0 Hz, 1H), 7.53 (dd, *J* = 8.0, 1.2 Hz, 1H), 7.45–7.41 (m, 2H), 7.35–7.33 (m, 2H), 6.07–6.00 (m, 1H), 5.09–5.00 (m, 0.025H), 3.72 (d, *J* = 6.9 Hz, 2H); ¹³C NMR (125 MHz, CDCl₃): δ 168.0, 148.2, 138.6, 138.5, 136.9, 136.6, 136.3, 134.6, 130.6, 130.4, 127.9, 127.3, 127.2, 126.4, 121.8, 121.6, 116.5, 37.4; GC-MS (EI) *m/z* (relative intensity): 290 (M⁺, 13), 144 (100), 117 (71), 93 (21); HRMS (APCI) Calcd for C₁₉H₁₅D₂N₂O⁺ [M+H]⁺ 291.1466, found, 291.1457.

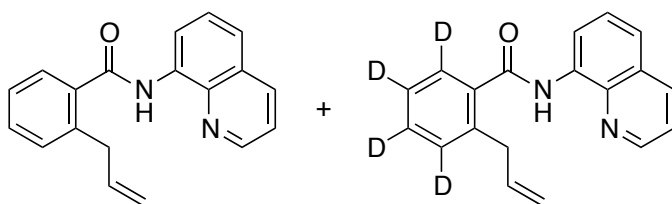
Intermolecular KIE

N-(quinolin-8-yl)benzamide (49.6 mg, 0.20 mmol), 2,3,4,5,6-pentadeuterio-*N*-(quinolin-8-yl)benzamide (50.7 mg, 0.20 mmol), and ZnCl₂•TMEDA (121 mg, 0.48 mmol) were placed in an oven-dried Schlenk flask under

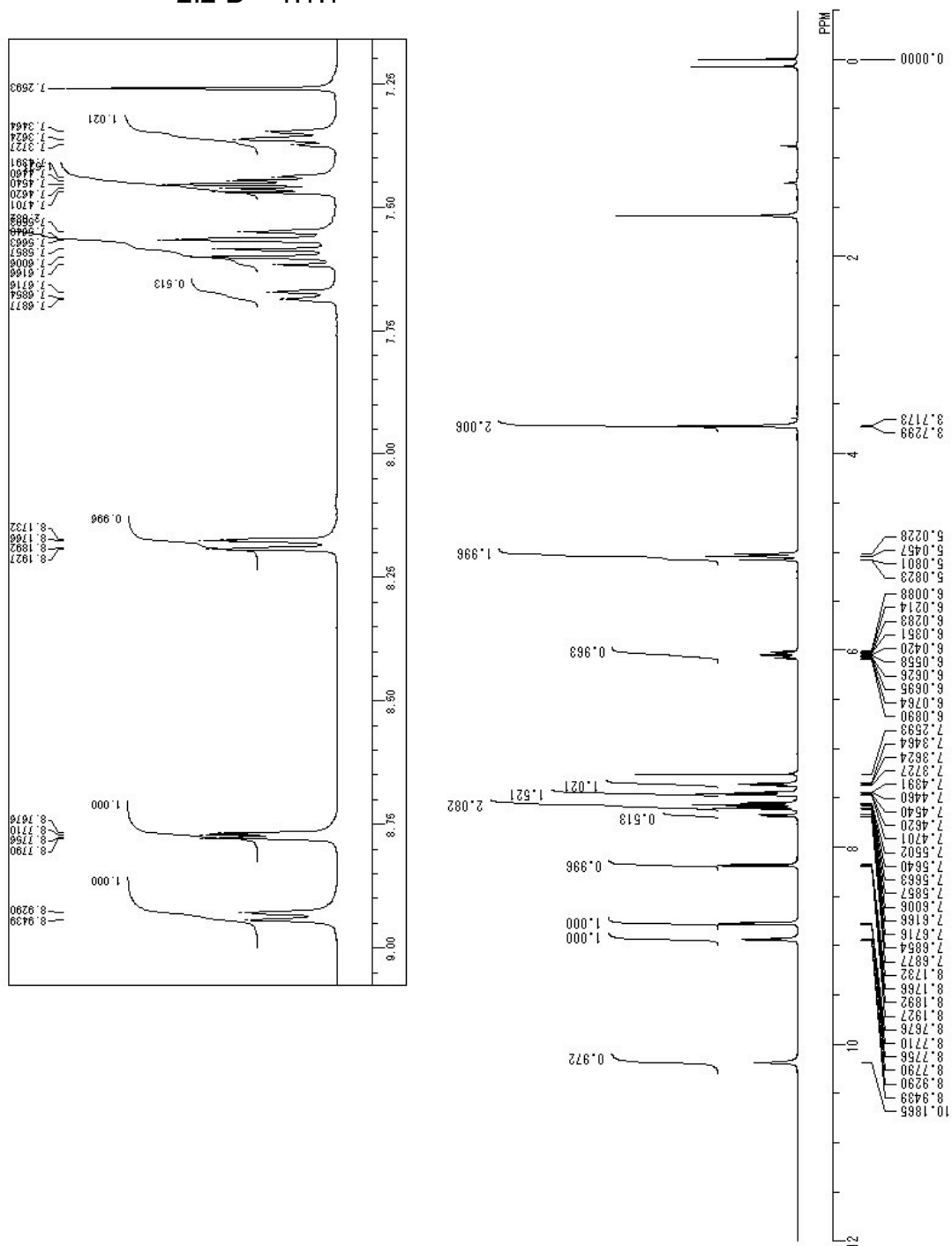
argon. A solution of *t*-BuCH₂MgBr in THF (1.16 M, 1.17 mL, 1.36 mmol) was added dropwise to the mixture. After stirring for 5 min at rt, allyl phenyl ether (66 μ L, 0.48 mmol) and a solution of Fe(acac)₃/*cis*-1,2-bis(diphenylphosphino)ethylene in THF (0.25 mL, 0.08 M, 20 μ mol) were sequentially added. The reaction mixture was stirred at 70 °C for 12 min, and was diluted with Et₂O followed by the addition of a saturated aqueous solution of Rochelle's salt. After extraction with ethyl acetate, the combined organic layers were filtered through a pad of Florisil, and concentrated under reduced pressure. The crude product was analyzed by ¹H NMR using 1,1,2,2-tetrachloroethane as an internal standard and the yield of the allylated products was determined to be 17%. After purification by GPC using CHCl₃ as an eluent, the isolated allylated products were analyzed by ¹H NMR to determine the ratio of **2** and **2-D**.







2:2-D = 1.1:1



References

- ¹ (a) Klein, H.-F.; Camadanli, S.; Beck, R.; Leukel, D.; Flörke, U. *Angew. Chem. Int. Ed.* **2005**, *44*, 975–977. (b) Beck, R.; Sun, H.; Li, X.; Camadanli, S.; Klien, H.-F. *Eur. J. Inorg. Chem.* **2008**, 3253–3257. (c) Beck, R.; Zheng, T.; Sun, H.; Li, X.; Flörke, U.; Klien, H.-F. *J. Organomet. Chem.* **2008**, *693*, 3471–3478. (d) Camadanli, S.; Beck, R.; Flörke, U.; Klein, H.-F. *Organometallics* **2009**, *28*, 2300–2310.
- ² Yoshikai, N.; Asako, S.; Yamakawa, T.; Ilies, L.; Nakamura, E. *Chem. Asian J.* **2011**, *6*, 3059–3065.
- ³ (a) Yanagisawa, A.; Nomura, N.; Yamamoto, H. *Synlett* **1991**, 513–514. (b) Stephen, A.; Hashmi, K.; Szeimies, G. *Chem. Ber.* **1994**, *127*, 1075–1089. (c) Nakamura, M.; Matsuo, K.; Inoue, T.; Nakamura, E. *Org. Lett.* **2003**, *5*, 1373–1375. (d) Martin, R.; Fürstner, A. *Angew. Chem. Int. Ed.* **2004**, *43*, 3955–3957. (e) Volla, C. M. R.; Marković, D.; Dubbaka, S. R.; Vogel, P. *Eur. J. Org. Chem.* **2009**, 6281–6288.
- ⁴ (a) Zaitsev, V.; Shabashov, D.; Daugulis, O. *J. Am. Chem. Soc.* **2005**, *127*, 13154–13155. (b) Shabashov, D.; Daugulis, O. *J. Am. Chem. Soc.* **2010**, *132*, 3965–3972. (c) Ano, Y.; Tobisu, M.; Chatani, N. *Org. Lett.* **2012**, *14*, 354–357. (d) Tran, L. D.; Popov, I.; Daugulis, O. *J. Am. Chem. Soc.* **2012**, *134*, 18237–18240. (e) Aihara, Y.; Chatani, N. *J. Am. Chem. Soc.* **2013**, *135*, 5308–5311. (f) Rouquet, G.; Chatani, N. *Angew. Chem. Int. Ed.* **2013**, *52*, 11726–11743. (g) Shang, R.; Ilies, L.; Matsumoto, A.; Nakamura, E. *J. Am. Chem. Soc.* **2013**, *135*, 6030–6032.
- ⁵ Mayer, M.; Welther, A.; Jacobi von Wangelin, A. *ChemCatChem* **2011**, *3*, 1567–1571.

- ⁶ Still, W. C.; Kahn, M.; Mitra, A. *J. Org. Chem.* **1978**, *43*, 2923–2925.
- ⁷ Pangborn, A. B.; Giardello, M. A.; Grubbs, R. H.; Rosen, R. K.; Timmers, F. J. *Organometallics* **1996**, *15*, 1518–1520.
- ⁸ Isobe, M.; Kondo, S.; Nagasawa, N.; Goto, T. *Chem. Lett.* **1977**, 679–682.
- ⁹ Tran, L. D.; Popov, I.; Daugulis, L. *J. Am. Chem. Soc.* **2012**, *134*, 18237–18240.
- ¹⁰ Nishino, M.; Hirano, K.; Satoh, T.; Miura, M. *Angew. Chem. Int. Ed.* **2013**, *52*, 4457–4461.
- ¹¹ Wolter, M.; Nordmann, G.; Job, G. E.; Buchwald, S. L. *Org. Lett.* **2002**, *6*, 973–976.
- ¹² (a) Tsang, D. S.; Yang, S.; Alphonse, F.-A.; Yudin, A. K. *Chem. Eur. J.* **2008**, *14*, 886–894. (b) Dimmel, D. R.; Gharpure, S. B. *J. Am. Chem. Soc.* **1971**, *93*, 3991–3996.
- ¹³ Gou, F.-R.; Wang, X.-C.; Huo, P.-F.; Bi, H.-P.; Guan, Z.-H.; Liang, Y.-M. *Org. Lett.* **2009**, *11*, 5726–5729.
- ¹⁴ Yang, Y.; Shi, L.; Zhou, Y.; Li, H.-Q.; Zhu, Z.-W.; Zhu, H.-L. *Bioorg. Med. Chem. Lett.* **2010**, *20*, 6653–6656.
- ¹⁵ Rouffet, M.; de Oliveira, C. A. F.; Udi, Y.; Agrawal, A.; Sagi, I.; McCammon, J. A.; Cohen, S. M. *J. Am. Chem. Soc.* **2010**, *132*, 8232–8233.
- ¹⁶ Ano, Y.; Tobisu, M.; Chatani, N. *Org. Lett.* **2012**, *14*, 354–357.
- ¹⁷ Jung, H. S.; Park, M.; Han, D. Y.; Kim, E.; Lee, C.; Ham, S.; Kim, J. S. *Org. Lett.* **2009**, *11*, 3378–3381.
- ¹⁸ Quach, T. D.; Batey, R. A. *Org. Lett.* **2003**, *5*, 1381–1384.

CHAPTER 5

インターネット公表に関する共著者全員の同意が得られていないため、

本章については、非公開

Chapter 5

CHAPTER 6

Summary and Outlook

The transition metal-catalyzed functionalization of a C–H bond has been rapidly emerging as a straightforward and efficient method to construct organic frameworks and replacing the conventional transition metal-catalyzed cross-coupling reaction. However, most of these reactions require rare and toxic transition metal catalysts and typically harsh reaction conditions, which is incompatible with the concept of sustainability. Throughout my Ph.D. studies, I focused on the development of C–H bond functionalization reactions using iron as a sustainable catalyst, and achieved an unprecedented iron-based directed aromatic C–H bond functionalization using electrophilic coupling partners.

In Chapter 2, iron-catalyzed C–H functionalization using electrophiles as the coupling partner instead of an organometallic reagent was attempted using 2-phenylpyridine as a substrate. Unfortunately, most of the electrophiles could not be successfully introduced to a C–H bond due to the competitive coupling with a Ph group used to generate a chelated iron intermediate.

In Chapter 3, a combination of 1-arylpdrazoles as substrate and allyl phenyl ether as electrophile was found to effect the unprecedented iron-catalyzed C–H bond functionalization with electrophile. Thus, *ortho*-allylation of arylpdrazoles with allyl phenyl ether took place smoothly at 0 °C to afford derivatives of allylbenzene, a part structure of natural products and bioactive compounds, and versatile intermediates in synthesis, in the presence of a catalytic amount of an iron salt, 4,4'-di-*tert*-butyl-2,2'-bipyridyl, and diphenylzinc reagent as an organometallic base.

In Chapter 4, *N*-(quinlin-8-yl)benzamide possessing a bidentate directing group and neopentyl reagent were used to stabilize the metallacyclic iron intermediate and suppress the competing side reactions. The new reaction design was effective for

the iron-catalyzed aromatic C–H bond allylation with allyl ether and greatly improved the reactivity and selectivity of the reaction. Thus, the reaction of *N*-(quinolin-8-yl)benzamide and congeners with allyl phenyl ether proceeded smoothly under mild conditions in the presence of a catalytic amount of iron salt, *cis*-1,2-bis(diphenylphosphino)ethylene, and dineopentylzinc reagent as an organometallic base. The reaction exhibited a broad scope of the substrate and an excellent compatibility with functional groups. A stoichiometric reaction suggested an intermediacy of the stable metallacyclic iron intermediate.

In Chapter 5, iron-mediated C–H bond functionalization with electrophiles was further demonstrated using the stoichiometrically generated iron intermediate derived from *N*-(quinolin-8-yl)benzamide. The results demonstrated that the iron intermediate is an excellent and general tool for C–H bond functionalization with electrophiles.

In this study, a novel concept of iron-catalyzed directed aromatic C–H bond activation followed by reaction with an electrophile was demonstrated for the first time. The factors governing the reactivity and selectivity of organoiron species in the aromatic C–H bond activation were revealed and *N*-(quinolin-8-yl)benzamide was found to be a particularly efficient directing group. The newly established concept will provide a basis for novel iron-catalyzed aromatic C–H bond functionalization with various electrophiles.

Further elucidation of the structure and reactivity of the iron intermediates will be necessary for developing more efficient and practical catalytic systems in more rational ways. Combined experimental and theoretical studies on the mechanism of iron-catalyzed C–H bond activation will contribute to the future development of sustainable C–H bond functionalization reactions using iron as a catalyst.

